Republic of Iraq
Ministry of Higher Education
and Scientific Research

NONLINEAR FINITE ELEMENT ANALYSIS OF REINFORCED CONCRETE BEAMS FLEXURALLY STRENGTHENED WITH CARBON FIBER REINFORCED POLYMER PLATES

A Thesis
Submitted to the College of Engineering of the University of Babylon in Partial Fulfillment of the Requirements for the Degree of Master of Science
in
Civil Engineering (Structural Engineering)

By
Hassaniene Mohammad Theiab Al-Shmmary

B.Sc. Civil Engineering (٢٠٠٣)

December ٢٠٠٦ ***Thu al Qidah*** ١٤٢٧

جمهورية العراق

وزارة التعليم العالي والبحث العلمي

التحليل غير الخطي باستخدام طريقة العناصر المحددة للعتبات الخرسانية المسلحة المقواة انحنائيا بألواح البوليمر المسلحة بالألياف الكاربونية

رسالة

مقدمة إلى كلية الهندسة في جامعة بابل

كجزء من متطلبات نيل درجة الماجستير

في علوم الهندسة المدنية

(إنشاءات)

من قبل

حسنين محمد ذياب الشمري

بكالوريوس علوم في الهندسة المدنية (٢٠٠٣)

كانون الأول ٢٠٠٦ جماد

الثاني ١٤٢٧

قالوا سبحانك لا علم لنا إلا ما علمتنا إنك أنت العليم الحكيم

صدق الله العلي العظيم

سورة البقرة (الآية ٣٢)

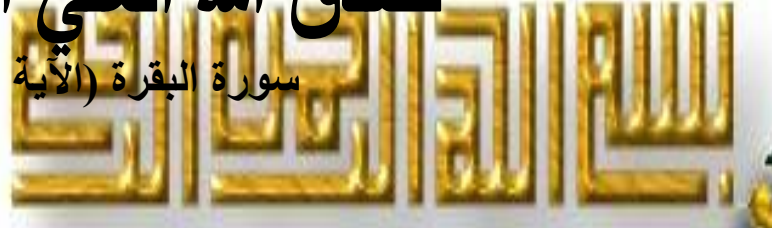

الخلاصة

تتضمن هذه الدراسة أنموذجاً لاخطياً ثلاثي الأبعاد للعناصر المحددة ملائماً لتحليل العتبات الخرسانية المسلحة المقواة أنحنائياً بألواح البوليمر المسلحة بالألياف الكاربونية تحت تأثير أحمال ساكنة باستخدام برامج الحاسوب (ANSYS). وهو عبارة عن مجموعة برامج خاصة بطريقة العناصر المحددة قادرة على تحليل أي نوع من المنشآت في حالة السكون والحركة بتصرف خطي أو لا خطي تحت مختلف حالات التحميل.

تم استخدام العنصر الطابوقي ذو ثمانية عقد لتمثيل اللب الخرساني وتم تمثيل حديد التسليح الداخلي بمحدد أضافي منتشر موزع خلال العنصر الخرساني حسب الاتجاه المحدد. وكذلك تم تمثيل ألواح البوليمر المسلحة بالألياف الكاربونية بعنصر قشري أو صدفي ذو أربعة عقد ولكل عقدة ثلاث درجات حرية للحركة. تم افتراض وجود ترابط تام بين العناصر. لقد أخذ بنظر الاعتبار التصرف اللاخطي للمواد والتي تشمل التشقق والتهشم للخرسانة والخضوع للحديد. اعتبر تصرف الخرسانة تحت تأثير اجهادات الانضغاط تصرفاً مرن ثم مرن- لدن يتبعه تصرف لدن تام ينتهي بتهشم الخرسانة. أما تصرف الخرسانة تحت اجهادات الشد تمثل مع الأخذ بنظر (Fixed Smeared Crack Model) باستخدام أنموذج التشقق المنتشر الثابت الاعتبار انتقال قوى القص بعد التشقق.

تم حل معادلات التوازن اللاخطية باستخدام طريقة-تزايدية-تكرارية (Incremental-Iterative-Method) تعمل تحت أحمال مسيطرة واستخدمت في الحل طريقة نيوتن-رافسن المعدّلة, أجريت التكاملات العددية باستخدام قواعد كاوس للتكامل ذات ثمن نقاط للعنصر الطابوقي وأربع نقاط للعنصر القشري أو الصدفي.

تم استخدام برنامج ANSYS في تحليل أنواع مختلفة من العتبات المكبة من ألواح البوليمر المسلحة بالألياف الكاربونية والخرسانة وتمت مقارنة النتائج المستحصلة لمنحنيات الحمل-الهطول على طول العتبة المفحوصة مع النتائج المختبرية المتوفرة. بشكل عام تم الحصول على توافق بين النتائج المستحصلة من طريقة العناصر المحددة والنتائج المختبرية المتوفرة بنسبة اختلاف (٢%).

كذلك تم تقصي تأثير مجموعة من المتغيرات الخاصة بالمادة على تصرف منحنيات الحمل-الهطول. تضمنت هذه المتغيرات دراسة تأثير فعالية طريقة التقوية، تأثير سمك، عرض وموقع ألواح البوليمر المسلحة بالألياف الكاربونية، تأثير كمية حديد التسليح الطولية، تأثير كمية حديد التسليح العرضية، تأثير طول مسافة القص، تأثير حالة الإسناد ونمط التشقق لحالات مختلفة من التحميل. وقد وجد فعالية طريقة التقوية الانحنائية بألواح البوليمر المسلحة بالألياف الكاربونية للعتب الخرساني المسلح حيث تتراوح الزيادة في مقدار التحمل الأقصى بين (٣٠%-٤٥%).

ذو تأثير واضح على تصرف منحني (CFRP)من خلال دراسة التغيرات وجد أن سمك الحمل-الهطول للعتب الخرساني المركب حيث بزيادة السمك ٥٠%، ١٠٠%، ٢٠٠% سوف يزداد التحمل الأقصى للعتب المركب بنسبة ٩%، ١٣%، ١٧.٢% على التوالي. وكذلك وجد يؤثر على التصرف الكلي لمنحني الحمل-الهطول للعتب المركب حيث وجد (CFRP)أن عرض أن زيادة العرض من ١٠٠% إلى ٣٠٠% سوف يزداد التحمل الأقصى من ١٧% إلى ٢٦%. وكذلك نلاحظ زيادة جيدة بالتحمل الأقصى للعتب المركب بزيادة كمية التسليح الطولي إلى (١.٥-٢) مرة من كمية حديد التسليح الطولية المتوفرة في الدراسة العملية. أن الزيادة تتراوح من (٩% ألي ٣٠%).

Abstract

This thesis presents a three-dimensional nonlinear finite element model suitable for the analysis of reinforced concrete beams flexurally strengthened with CFRP (Carbon Fiber Reinforced Polymer) plates under static load using the ANSYS (**An**alysis **SYS**tem) computer package. This package is a finite element program capable of analyzing different types of structure for static, dynamic, thermal and conductively. The load is using linear or nonlinear analysis under general one, two, or three-dimensional state of loading.

The eight-noded isoparametric brick elements are used to represent the concrete and the internal reinforcement may be modeled as an additional smeared stiffness distributed through concrete element in a specified orientation. Also, a membrane shell element which has four nodes with three translation degrees of freedom at each node has been used to model the CFRP plate. A Perfect bond is assumed between the elements. Material nonlinearities due to cracking, crushing of the concrete and yielding of the steel reinforcement are taken into consideration during the analysis. The behavior of concrete in compression is simulated by an elasto-plastic work hardening model followed by a perfect plastic response plateau which is terminated at the onset of crushing has been used .In tension, the crack is represented by a fixed smeared crack with post-cracking shear transfer model to simulate the aggregate interlock and dowel actions.

The nonlinear equations of equilibrium have been solved by using an incremental-iterative technique operating under load control. The solution algorithms are applied utilizing the modified Newton-Raphson method. The numerical integration has been conducted by using (٢x٢x٢) Gaussian rule for the brick elements and (٢x٢) Gaussian quadrate rule for shell elements.

The ANSYS computer program has been used to investigate the behavior of the different composite CFRP-reinforced concrete beams. The analytical results of load-deflection response along the examined beams have been compared with available experimental tests. In general, a good agreement between the finite element solutions and experimental results has been obtained with difference about (٢ %).

Parametric studies have been carried out to investigate the effect of some important material parameters. These parameters include the effect flexural strengthening method, thickness of CFRP, width of CFRP, location of CFRP, longitudinal reinforcement, shear reinforcement, shear span length, boundary condition and crack pattern at different load. It was found that the flexural strengthening of R.C. beams with CFRP is effective with an increment in the ultimate load about (٣٠- ٤٥) %. The parametric study with respect to the thickness of the CFRP plate shows that this effect has a significant effect on the load–deflection behavior of CFRP-reinforced concrete beam. A ٥٠٪, ١٠٠٪ and ٢٠٠٪ increase in the thickness of CFRP plate caused an increase of ٩٪, ١٣٪ and ١٧.٢٪ in the ultimate load capacity of the CFRP-reinforced concrete beam respectively.

The width of the CFRP plate affects the overall load-deflection behavior of the CFRP-concrete beams. A ١٠٠٪ and ٣٠٠٪ an increase in the CFRP plate width caused an increase of ١٧ % and ٢٦ % in the ultimate load capacity of the

CFRP-reinforced concrete beam respectively. A good increase in the ultimate load is obtained from increasing the longitudinal reinforcement of the CFRP-concrete beam to (١.٥-٢) times the amount of reinforcement provided in the experimental work. The increase varied from (٩ to ٣٠ %).

Acknowledgments

In the name of Allah, the most gracious, the most merciful, before anything, thank Allah who enables me to achieve this research.

I would like to express my sincere thanks and deep gratitude to my supervisors **Dr. Ammar Y. Ali** and **Dr. Haitham H. Al-Daami** for their advice, kindness, guidance and encouragement throughout this work.

Thanks are to be given to the Dean of the College of Engineering and to the Head and Staff of the Department of Civil Engineering in the University of Babylon for their support to finish this work.

Great thanks to my family for their support to finish this work.

Also, I thank **Mr.Laith Shaker** for his help in this work.

Finally, I am indebted to all my friends, especially for **Amir**, **Haider** and **Munaf** for their support and encouragement.

Appendix (A)

Derivation of the stiffness matrix for smeared reinforcement bar

The reinforcement has uniaxial stiffness only and is assumed to be smeared throughout the element. Directional orientation is accomplished through user specified angles. The stress-strain matrix [D]used for this element (Solid ٦٥) is defined as:

$$[D]=\left[1-\sum_{j=1}^{Nr} V_j^R\right]\left[D^c\right]+\sum_{j=1}^{Nr} V_j^R\left[D^r\right]_j \quad \text{..... (A.١)}$$

Where:

Nr= number of reinforcing materials (maximum of three, al reinforcement is ignored if MAT١ (explained below) equals zero. Also, if MAT١, MAT٢ or MAT٣ equals the concrete material number, the reinforcement with that material number is ignored)

$\mathbf{V_j^R}$**=** ratio of the volume of reinforcing material to the total volume of the element

$\mathbf{[D^c]}$**=** stress-strain matrix for concrete

$\mathbf{[D^r]j}$**=** stress-strain matrix for reinforcement j, defined by equation (A.٤)

MAT١, MAT٢, MAT٣= material numbers associated with material behaviour of reinforcement

The orientation of the reinforcement j within an element is depicted in Fig. (A-١). The element coordinate system is denoted by (X, Y, Z) and (x_j^r, y_j^r, z_j^r) describes the coordinate system for reinforcement type j. The stress strain matrix with respect to each coordinate system (x_j^r, y_j^r, z_j^r) has the form

$$\begin{Bmatrix} \sigma^r_{xx} \\ \sigma^r_{yy} \\ \sigma^r_{zz} \\ \sigma^r_{xy} \\ \sigma^r_{yz} \\ \sigma^r_{xz} \end{Bmatrix} = \begin{bmatrix} E^r_j & 0 & 0 & 0 & 0 & 0 \\ 0 & 0 & 0 & 0 & 0 & 0 \\ 0 & 0 & 0 & 0 & 0 & 0 \\ 0 & 0 & 0 & 0 & 0 & 0 \\ 0 & 0 & 0 & 0 & 0 & 0 \\ 0 & 0 & 0 & 0 & 0 & 0 \end{bmatrix} \begin{Bmatrix} \varepsilon^r_{xx} \\ \varepsilon^r_{yy} \\ \varepsilon^r_{zz} \\ \varepsilon^r_{xy} \\ \varepsilon^r_{yz} \\ \varepsilon^r_{xz} \end{Bmatrix} = \left[D^r\right]_j \begin{Bmatrix} \varepsilon^r_{xx} \\ \varepsilon^r_{yy} \\ \varepsilon^r_{zz} \\ \varepsilon^r_{xy} \\ \varepsilon^r_{yz} \\ \varepsilon^r_{xz} \end{Bmatrix} \quad \text{..... (A.٢)}$$

Where: $\mathbf{E_j^r}$**=** Young modulus of reinforcement type j

It may be seen that the only nonzero stress component is σ^r_{xx}, the axial stress in the direction of reinforcement type j. The reinforcement direction X_j^r is related to element coordinates X, Y, Z through

$$\begin{Bmatrix} X \\ Y \\ Z \end{Bmatrix} = \begin{Bmatrix} \cos\theta_i & \cos\phi_i \\ \sin\theta_i & \cos\phi_i \\ \sin\phi_i & \end{Bmatrix} X_j^r = \begin{Bmatrix} \ell_1^r \\ \ell_2^r \\ \ell_3^r \end{Bmatrix} X_j^r \quad \text{..... (A.٣)}$$

Where:

$\theta_i =$ Angle between the projection of the X_j axis on XY plane and the X axis

$\phi_i =$ Angle between the X_j axis and the XY plane

$\ell_i^r =$

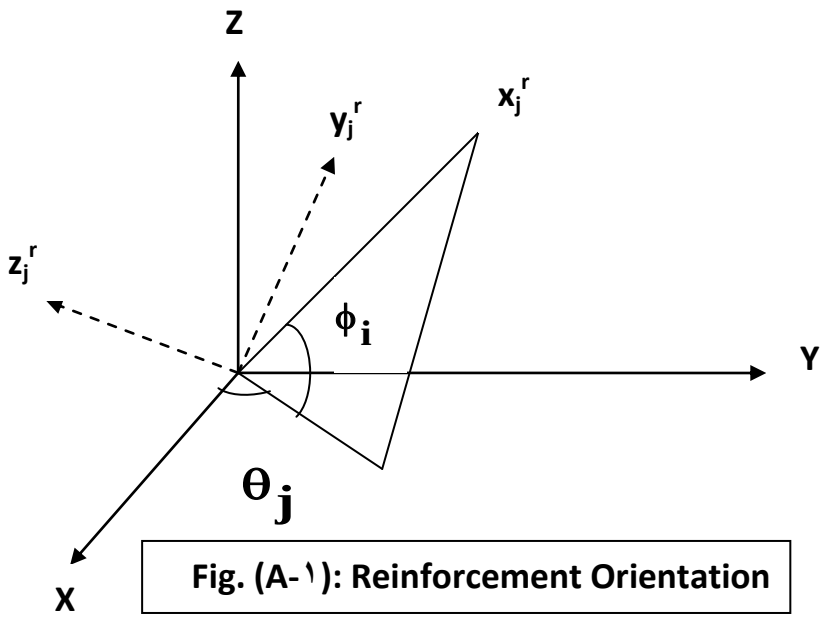

Fig. (A-١): Reinforcement Orientation

Since the reinforcement material matrix is defined in coordinates aligned in the direction of reinforcement orientation, it is necessary to construct a transformation of the form

$$\left[D^R\right]_j = \left[T^r\right]^T \left[D^r\right]_j \left[T^r\right] \quad \text{..... (A.٤)}$$

In order to express the material behavior of the reinforcement in global coordinates. The transformation by (**ANSYS, ١٩٩٨**) is

$$\left[T^{r}\right]=\begin{bmatrix} a_{11}^{2} & a_{12}^{2} & a_{13}^{2} & a_{11}a_{12} & a_{12}a_{13} & a_{11}a_{13} \\ a_{21}^{2} & a_{22}^{2} & a_{23}^{2} & a_{21}a_{22} & a_{22}a_{23} & a_{21}a_{23} \\ a_{31}^{2} & a_{32}^{2} & a_{33}^{2} & a_{31}a_{32} & a_{32}a_{33} & a_{31}a_{33} \\ 2a_{11}a_{21} & 2a_{12}a_{22} & 2a_{13}a_{23} & a_{11}a_{22}+a_{12}a_{21} & a_{12}a_{23}+a_{13}a_{32} & a_{11}a_{23}+a_{13}a_{21} \\ 2a_{21}a_{31} & 2a_{22}a_{32} & 2a_{23}a_{33} & a_{21}a_{32}+a_{22}a_{32} & a_{22}a_{33}+a_{23}a_{32} & a_{21}a_{33}+a_{13}a_{21} \\ 2a_{11}a_{31} & 2a_{12}a_{32} & 2a_{13}a_{33} & a_{11}a_{32}+a_{12}a_{31} & a_{12}a_{33}+a_{13}a_{32} & a_{11}a_{33}+a_{13}a_{31} \end{bmatrix}$$

. ..... (A.٥)

$$\begin{bmatrix} a_{11} & a_{12} & a_{13} \\ a_{21} & a_{22} & a_{23} \\ a_{31} & a_{32} & a_{33} \end{bmatrix}=\begin{bmatrix} \ell_{1}^{r} & \ell_{2}^{r} & \ell_{3}^{r} \\ m_{1}^{r} & m_{2}^{r} & m_{3}^{r} \\ n_{1}^{r} & n_{2}^{r} & n_{3}^{r} \end{bmatrix} \qquad \text{..... (A.٦)}$$

The vector $\begin{bmatrix} \ell_{1}^{r} & \ell_{2}^{r} & \ell_{3}^{r} \end{bmatrix}^{T}$ is defined by equation **(A.٦)** while $\begin{bmatrix} m_{1}^{r} & m_{2}^{r} & m_{3}^{r} \end{bmatrix}^{T}$ **and** $\begin{bmatrix} n_{1}^{r} & n_{2}^{r} & n_{3}^{r} \end{bmatrix}^{T}$ are unit vectors mutually orthogonal to $\begin{bmatrix} \ell_{1}^{r} & \ell_{2}^{r} & \ell_{3}^{r} \end{bmatrix}^{T}$ thus defining a Cartesian coordinate referring to reinforcement directions. If the operations presented by equation (A.٤) are performed substituting equation (A.٢) and equation (A.٥), the resulting reinforcement material matrix in element coordinates takes the form

$$\left[D^{r}\right]_{j}=E_{j}^{r}\left\{A_{d}\right\}\left\{A_{d}\right\}^{T} \qquad \text{..... (A.٧)}$$

Where:

$$\left\{A_{d}\right\}=\begin{bmatrix} a_{11}^{2} & a_{21}^{2} & \cdots & a_{11} & a_{13} \end{bmatrix}^{T}$$

Therefore the only direction cosines used in $[D^R]_j$ involve the uniquely defined unit vector $\left\lfloor \ell_{\mathbf{1}}^{\mathbf{r}} \quad \ell_{\mathbf{2}}^{\mathbf{r}} \quad \ell_{\mathbf{3}}^{\mathbf{r}} \right\rfloor^{\mathbf{T}}$.

CERTIFICATION

We certify that this thesis titled "***Nonlinear Finite Element Analysis of reinforced concrete beams flexurally strengthened with carbon fiber reinforced polymer plates***", was prepared by "**Hassaniene Mohammad Theiab Al-Shmmary** " under our supervision as partial requirement for the degree of Master of Science in Civil Engineering (structures).

Signature:

Name: Asst. Prof. Dr. Ammar Y. Ali

Date: / /٢٠٠٦

Signature:

Name: Asst. Prof. Dr. Haitham H. Al-Daami

Date: / /٢٠٠٦

Republic of Iraq
Ministry of Higher Education
and Scientific Research

NONLINEAR FINITE ELEMENT ANALYSIS OF REINFORCED CONCRETE BEAMS FLEXURALLY STRENGTHENED WITH CARBON FIBER REINFORCED POLYMER PLATES

A Thesis
Submitted to the College of Engineering of the University of Babylon in Partial Fulfillment of the Requirements for the Degree of Master of Science
in
Civil Engineering (Structural Engineering)

By

Hassaniene Mohammad Theiab Al-Shmmary

B.Sc. Civil Engineering (٢٠٠٣)

Supervised By

Dr. Ammar Y. Ali **Dr. Haitham H. Al-Daami**

July ٢٠٠٦ ***Jamada Al Thani*** ١٤٢٦

جمهورية العراق

وزارة التعليم العالي والبحث العلمي

التحليل غير الخطي باستخدام طريقة العناصر المحددة للعتبات الخرسانية المسلحة المقواة انحنائيا بألواح البوليمر المسلحة بالألياف الكاربونية

رسالة

مقدمة إلى كلية الهندسة في جامعة بابل

كجزء من متطلبات نيل درجة الماجستير

في علوم الهندسة المدنية

(إنشاءات)

من قبل

حسنين محمد ذياب الشمري

بكالوريوس علوم في الهندسة المدنية (٢٠٠٣)

إشراف

الدكتور عمار ياسر علي الدكتور هيثم حسن الدعمي

تموز ٢٠٠٦ جماد الثاني ١٤٢٦

CERTIFICATION

We certify that we have read this thesis, titled "***Nonlinear Finite Element Analysis of reinforced concrete beams flexurally strengthened with carbon fiber reinforced polymer plates*** ", and as examining committee examined the student **Hassaniene Mohammad Theiab** in contents and in what is connected with it, and that in our opinion it meets the standard of thesis for the Degree of Master of Science in Civil Engineering (Structures).

Signature:

Name:Asst.Prof.Dr. Mustafa B. Dawood

(Member)

Signature:

Name: Asst. Prof. Mr. Abdul Ridah Saleh

(Member)

Date: / /

Signature:

Name: Prof. Dr. Hisham M. Al-Hassani

(Chairman)

Signature:

Name: Asst. Prof. Dr. Ammar Y. Ali

(Supervisor)

Signature:

Name: Asst. Prof. Dr. Haitham H. Al-Daami

(Supervisor)

Approval of the Civil Engineering Department

Head of the Civil Engineering Department

Signature:

Name: Asst. Prof. Dr. Ammar Y. Ali

Approval of the Deanery of the College of Engineering

Signature:

Name: Prof. Dr. Abd AL-Wahid K. Rajih

Date: / /

Dean of the College of Engi

Notations

The major part of the symbols used in the text is listed below. Others are defined they first appear

General Symbols

$\mathbf{[B]^T, \{a\}^T}$	:	Transpose of matrix [B] and vector {a}
$\mathbf{[B]^{-1}}$	:	Inverse of matrix [B]
$\mathbf{d}$, ∂	:	Differential symbols
$\mid \mid$, **det.**	:	Determinant of a matrix or absolute value
{ }	:	Vector
[ ]	:	Matrix

Scalar

$\mathbf{A_s}$	:	Area of tension reinforcing steel
$\mathbf{B_o}$, $\boldsymbol{\beta_c}$	:	Shear transfer coefficients
E	:	Modulus of elasticity
$\mathbf{E_c}$	:	Modulus of elasticity of concrete
$\mathbf{E_s}$	:	Modulus of elasticity of steel

f	:	Functions
f_c'	:	Uniaxial compressive strength of concrete
f_u	:	Ultimate strength of steel
f_y	:	Yield strength of steel at specified yield strain
f_t	:	Uniaxial tensile strength of concrete
f_r	:	Modulus of rupture of concrete
f_1	:	Ultimate compressive strength for a state of biaxial compression
f_2	:	Ultimate compressive strength for a state of uniaxial compression
h	:	Depth of concrete beam
I_1	:	First stress invariant
I_1'	:	First strain invariant
J	:	Jacobian
J_2	:	Second deviator stress invariant
P	:	Applied concentrated load
$\overline{S}$	:	Failure surface function
T_n	:	Convergence tolerance
u, v, w	:	Displacement components, in X , Y and Z Cartesian coordinates
V	:	Volume

W	:	Weight of a sampling point
X , Y , Z	:	Cartesian coordinates
ε	:	Strain
ε_{cu}	:	Ultimate strain of concrete
ν	:	Poisson's ratio
σ	:	Stress
σ_h	:	Hydrostatic stresses
σ^a_h	:	Ambient hydrostatic pressure
ξ, η, ζ	:	Local coordinate

Matrix

[A]	:	Displacement gradient matrix
[B]	:	Strain displacement matrix
[D]	:	Constitutive matrix
[J]	:	Jacobean matrix
[K]	:	Stiffness matrix
[N]	:	Shape function matrix
[T]	:	Transformation matrix

Vector

{a} : Nodal displacement or flow vector

{f} : External load vector

{P} : Internal load

{r} : Residual load vector

{u} : Displacement vector

{ε} : Strain vector

{σ} : Stress vector

LIST OF FIGURES

LIST OF TABLES

CHAPTER ONE

INTRODUCTION

١.١ General

Concrete is a construction material with a high compressive strength and a poor tensile strength. A concrete structure without any form of reinforcement will crack and fail when subjected to a relatively small load. The failure occurs in most cases suddenly and in a brittle manner. To increase the structural load carrying capacity and ductility it needs to be reinforced. This is mostly done by reinforcing with steel bars that are placed in the structure before concrete is cast. The reinforcement then interacts with the hardened

concrete so that the concrete and the steel together carry the load on the structure. Since a concrete structure usually has a long life the demands on the structure will normally change over time.

In the extreme cases, a structure may be adverse and need to be repaired due to accidents (earthquake, explosions), change in loading, change in use and change in configuration. Another reason includes errors occur during the design or construction phase so that the structure needs to be strengthened before using it.

To keep a structure at the same performance level it needs to be maintained at predestined time intervals. If the lack of maintenance has lowered the performance level of the structure, then the need for repairing it up to the original performance level may be required. In cases when higher performance levels are needed, upgrading is necessary. Where performance level means load carrying capacity, durability, function or aesthetic appearance. While upgrading refers to strengthening, increased durability,

and change of function or improved aesthetic appearance. In this thesis, mainly strengthening is discussed.

Maintenance, repair and strengthening of old concrete structures are becoming increasingly common. If one considers the capital that has been invested in existing infrastructures, then it is not always economically viable to replace an existing structure with a new one. The challenge must be taken to develop relatively simple measures to keep or increase a structure performance level through its life. This places a great demand on both consultants and contractors. There are difficulties in identifying the most

suitable method for an actual subject; for example, two identical columns within the same structure can have totally different life spans depending on their individual microclimate. Because of this, it is important to analyse the problem thoroughly to be able to select the most suitable method. The choice of an inappropriate repair or strengthening method can even worsen the structure's function. In comparison to building a new structure, strengthening an existing one is often more complicated since the structure conditions are already set. In addition, it is not always easy to reach the areas that need to be strengthened; often there is also limited space.

Today it exists many methods for strengthening a concrete structure, for example ; hand applied repairs with concrete mortar, shot concrete, injection techniques, different kind of concrete castings, *(Carolin, ١٩٩٩)*. However, an interesting strengthening method developed during the mid ٧٠-ties was steel plate bonding.

Even this method technically performs quite well, but it has some drawbacks. One is that the steel plates sometimes are quite heavy to mount at the work site. Another is the risk of corrosion at the joint between the steel and the adhesive. A third is that the joints between the steel plates must

beform properly, which is based of the limited delivery lengths of the steel plates *(Täljsten and Carolin, ١٩٩٨).*

In recent years the development of the plate bonding repair technique has been shown to be applicable to many existing strengthening problems in the building industry. This technique may be defined as one in which composite sheets or plates of relatively small thickness are bonded with an epoxy adhesive to, in most cases, a concrete structure to improve its structure behaviour and strength. The sheets or plates do not require much space and give a composite action between the adherents. The adhesive that is used to bond the fabric or the laminate to the concrete surface is a two-component epoxy adhesive, see Fig.(١-١).

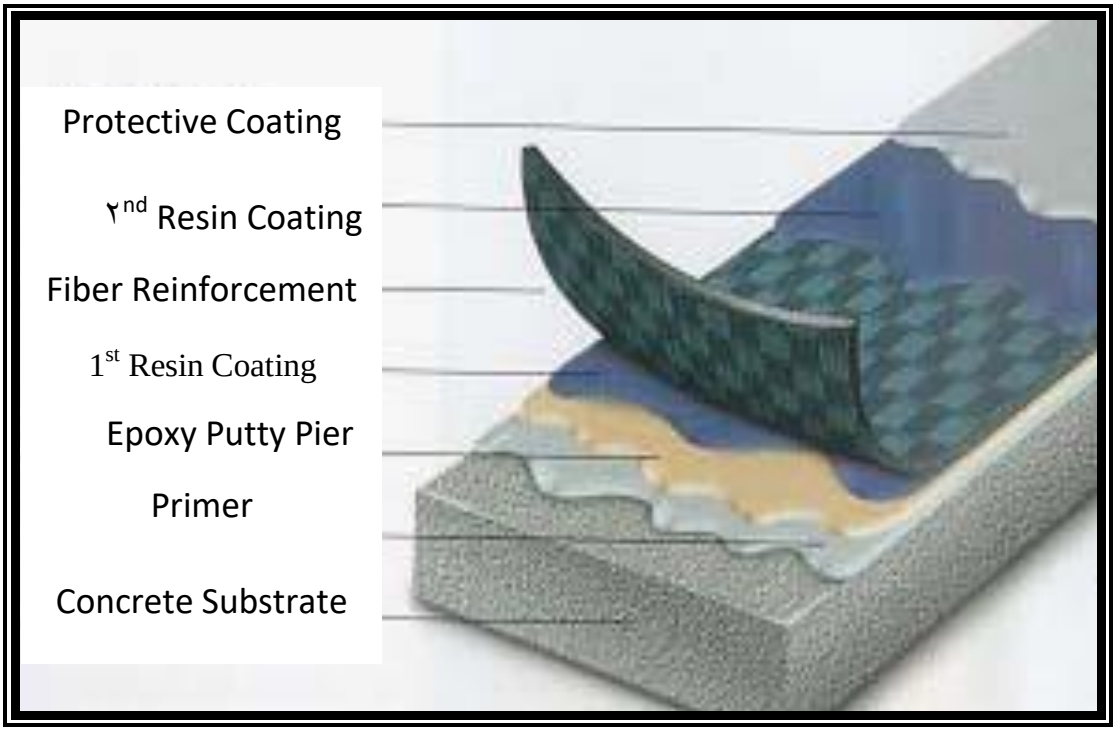

Fig.(١-١): Composite Strengthening System (Mbrace, ٢٠٠١).

The old structure and the new bonded-on material create a new structure element that has a higher strength and stiffness than the original. The basic ideas related to the use of FRP (Fibre Reinforced Polymers) for structural strengthening, along with examples of application, have been presented by (Triantafillou, ١٩٩٨). The past and potential future use of FRP

strengthening and rehabilitation have also recently been documented in many conference proceedings (Meier and Bette, ١٩٩٧; Benmokrane and Rahman, ١٩٩٨; keynote lectures (Maruyama, ١٩٩٧; Neale and Labossiere, ١٩٩٧) and journal articles (Täljsten, ١٩٩٧; Thomas, ١٩٩٨) *(Carolin, ٢٠٠٣).*

١.٢ Types and Engineering Specifications for

The strengthening or repairing of concrete structure by using externally bonded fibre reinforced polymer (FRP) provides an alternative solution to the tradition methods of strengthening such as externally bonded steel plate. FRP materials are currently being used for upgrading existing structures because of their resistance to corrosion, their lightweight, good strength, good stiffness and then comes the long lengths. Different types of fibre can be used, such as, glass, carbon, aramid, and carbon fibre which is considered in this thesis. Fig.(١-٢) and Table (١-١) present a comparison of mechanical behaviour of materials that are available for strengthening of structures. It can be seen that the non-metallic fibre have tensile strengths that are ١٠ times more than that of steel plate. The ultimate strain of these fibres is also very high but there is no ductile behavior.

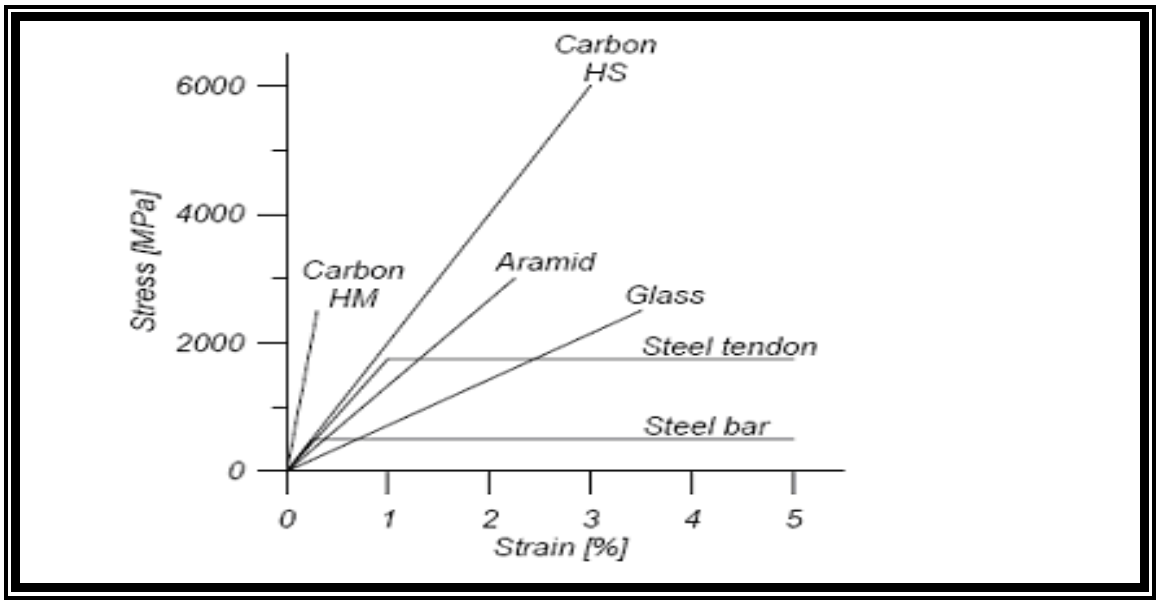

Fig. (١-٢): Properties of Different Fibres and Typical Steel

(ACI Committee ٤٤٠. ١٩٩٦)

Table (١-١): Mechanical Properties of Common Strengthening Material

(ACI Committee ٤٤٠, ١٩٩٦)

MATERIAL	MODULUS OF ELASTICITY [GPA]	COMPRESSIVE STRENGTH [MPA]	TENSILE STRENGTH [MPA]	DENSITY [KG/M³]
Concrete	٢٠-٤٠	٥-٦٠	١-٣	٢٤٠٠
Steel	٢٠٠-٢١٠	٢٤٠-٦٩٠	٢٤٠-٦٩٠	٧٨٠٠
Carbon fibre*	٢٠٠-٨٠٠	NA**	٢٥٠٠-٦٠٠٠	١٧٥٠-١٩٥٠

*) Given values are for plain carbon fibre. The characteristics of the composite will vary with amount and property of the used matrix.

**) Not applicable. Plain fibre buckle.

١.٣ Applications of FRP in Structures

The FRP is applied to different reinforced concrete elements such as beams, columns, and slabs, to provide substantial increase in strength and durability. Typical FRP applications are**:**

- **Flexural strengthening** of slabs or beams: The FRP is bonded to the tension zones with the fibres parallel to the principal stress direction.
- **Shear strengthening** of beams and columns: The FRP is bonded to the sides of the concrete elements with the fibres parallel to the principal tensile stresses, to act as external shear reinforcement. The FRP is most effective when it fully wraps the element, but partial wrapping can also be used where full wraps is not possible.
- **Column wrapping:** The capacity of columns can be increased by wrapping them with FRP materials though the confinement effect provided by the FRP.

The typical and scenario of the application of composites are shown in Fig. (١-٣) and (١-٤).

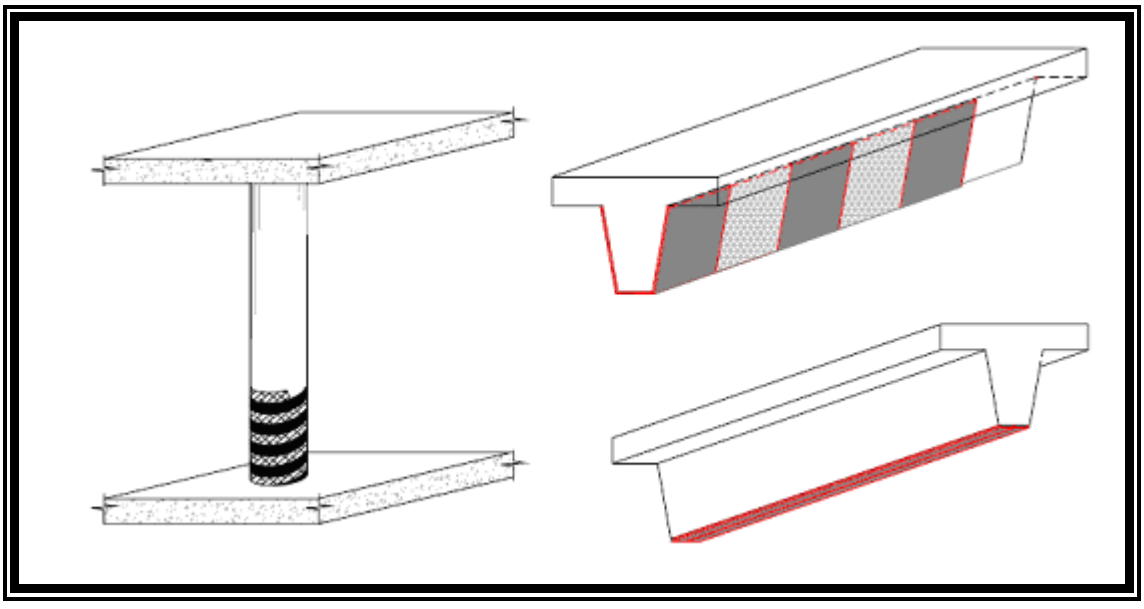

Fig. (١-٣): Typical Applications of Bonded FRP Strengthening Systems (Annex, J., ٢٠٠٠)

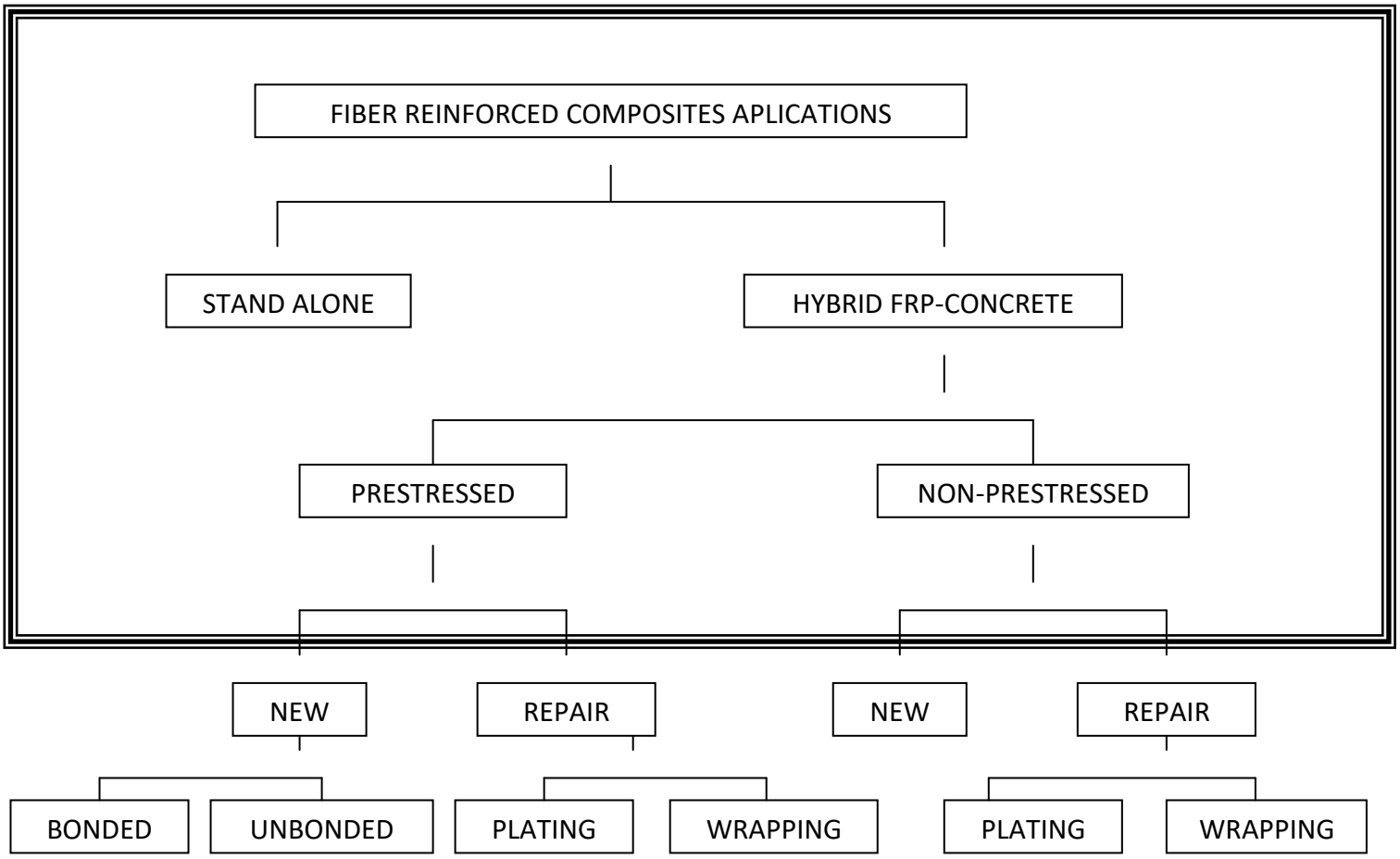

Fig. (١-٤): Applications of FRP in Structures *(Mukherjee and Joshi, ٢٠٠١).*

١.٥ Objective and Scope of Study

The main objective of this thesis is to develop a computer models utilizing finite element to predict the overall behaviour of flexural

strengthened reinforced concrete beams with CFRP and then to trace the effectiveness of CFRP plate or sheet supplied by Fibre Reinforced System (FRS) in enhancement the flexural strength of concrete beams.

Finite element method (FEM) models were to simulate the behaviour of reinforced concrete beam with CFRP laminates through nonlinear response and up to failure, using the ANSYS program *(ANSYS, ١٩٩٨).*

The ANSYS programme allows only three reinforcement bars distributed in the concrete element. The beams cross sections in this study are divided into elements, each element contains a real constant and each real constant allows containing three-bar reinforcement distributed in the concrete element.

Different types of beams flexural strengthened with CFRP plate have been chosen for the analysis by using the three-dimensional finite element model adopted in this study. The examples were chosen in order to demonstrate the applicability of the models by comparing the predicted behaviour with that observed in the laboratory.

Parametric studies have been carried out to investigate the effect of, thickness and width of CFRP plate, depth of the concrete beam, amount of flexural reinforcement, amount of shear reinforcement, shear span length, distribution the stress and strain along the span of the composite beam and crack pattern at different load levels on the overall behaviour.

١.٦ Layout of Thesis

The thesis consists of seven chapters. A general description of the significance of reinforced concrete structures strengthened with FRP in construction and numerical analysis is described in *chapter one****. This chapter***

also describes FRP (types, specifications, applications) and the objectives and scope of the thesis.

Chapter two ***reviews the experimental work of reinforced concrete beams flexural strengthened with FRP, the analytical methods and FRP strengthened reinforced concrete beams.***

Chapter three deals with the basic concepts of the finite element method, ٨-node isoperimetric brick elements are used to model the concrete together with the smeared representations of reinforcement and membrane shell element, which has four nodes to represent the CFRP plate. The numerical integration rules to determine the element stiffness matrices are described together with the nonlinear solution techniques adopted to solve the nonlinear equations of equilibrium are also described. An outline of the computer program ANSYS (Non-linear Finite Element Analysis of Composite Beams) is also presented.

Material modelling and properties of composite CFRP-concrete (CFRP, concrete and steel reinforcement) are presented in **chapter four**.

Chapter five deals with analysis of composite CFRP-concrete beams, in this chapter, the applicability of the model is checked through three examples. The analytical and experimental results are compared.

Chapter six ***includes parametric studies to investigate some material and numerical parameters on the behaviour of reinforced concrete beam strengthened with CFRP such as the effect of thickness, width and configuration of CFRP plate, depth of the concrete beam, amount of flexural reinforcement, amount of shear reinforcement, shear span length,***

distribution the stress and strain along the span of the composite beam, crack pattern at different load levels and effect of the boundary condition.

Finally, the conclusions drawn from the current work and suggestions for future works are summarized in *chapter seven.*

CHAPTER TWO

REVIEW OF LITERATURE

٢.١ INTRODUCTION

There is a wide range of research pertaining to the use of FRP in bridge repair. Rebar, grating into concrete, and wrapping around columns and piers are just a few examples of the broad applications of these composites *(Norris and Saadatmanesh, ١٩٩٤).* This literature review will be limited to research of FRP material externally bonded to the tensile face of concrete beams. In particular, research studying the effect of externally applied FRP materials on the flexural performance of reinforced concrete beams will be reported.

٢.٢ EXPERIMENTAL STUDIES

Experimental studies involving bonded CFRP to reinforced concrete beams has been performed by Meier et al. since ١٩٨٥ at the Swiss

Laboratories for Materials Testing and Research. This program envisions the replacement of steel plates with FRP laminates for repairing and strengthening reinforced concrete beams. Examining the strength and stiffness of beams with unidirectional CFRP plates is a primary focus of their past research.

An earlier study ***(Meier et al.,*** *١٩٩١)* encompassed externally bonding CFRP sheets to twenty-six concrete beams. Each beam (١٥٠mm x٢٥٠mm x٢٠٠٠mm) was minimally reinforced with steel (two ٨ mm diameter bars) on top and bottom and included shear reinforcement (٦.٣٥ mm spaced every ٢١٦ mm). The test set-up consisted of a two point loading on simple supports.

The maximum load increased over ١٠٠٪ compared to the control beam (unstrengthened) by applying a unidirectional CFRP laminate sheet (٠.٣ mm x٢٠٣ mm x٢٠٠٧ mm) to the tensile side of the specimens. Also, the deflection of the strengthened beam was ٥٠٪ less than the control beam. The cracks in the repaired beams were small and closely spaced along the length of the member. This differed from the control beam, which showed a classic reinforced concrete crack pattern of fewer and larger cracks. This study presented the first evidence that FRP laminates could help in the repair of deteriorated concrete beams.

Meier et al. *(١٩٩١)* also studied the failure modes related to FRP repaired beams. A preliminary study dealt with three different failures:

١. Tensile failure of the CFRP sheets.

٢. Classical concrete failure in the compressive zone.

٣. Continuous peeling-off of the CFRP sheets due to an uneven concrete surface Tensile failure of the CFRP is described as very sudden and explosive,

but is easily predicted due to cracking sounds. Peeling-off of the laminate is caused by vertical displacement across shear cracks in the concrete.

Within the next year, ***Meier et al.*** *(١٩٩٢)* expanded the possible failure modes to nine. The additional six failures are as follows:

١. Shearing of the concrete in the tensile zone.

٢. Interlaminar shear within the CFRP sheet.

٣. Failure of the reinforcing steel in the tensile zone.

٤. Cohesive failure within the adhesive.

٥. Adhesive failure at the interface CFRP sheet/adhesive.

٦. Adhesive failure at the interface CFRP concrete/adhesive.

The latter three were not observed but described as “theoretically possible”.

The first full-scale FRP repaired beam test conducted in the United States was at the University of Arizona (***Saadatmanesh and Ehsani,*** ١٩٩١). The tests consisted of six large concrete beams; five rectangle cross-sections (٢٠٣ mm x ٤٥٧ mm) and one T-beam (٧٦.٢ mm x ٦٠٩.٦ mm flange, ٢٠٣ mm x ٤٥٧ mm web). All the specimens were ٤٨٧٦.٨ mm long and tested as a simple span in two points loading. Steel reinforcement ratios, shear reinforcement, and cambering were varied in the six beams. However, the externally applied GFRP was identical for each beam (٦.٣٥ mm x ٢٥٠ mm x ٤٢٦٧.٢ mm).

The research concluded that adding GFRP (Glass Fibre Reinforced Polymer) plates improved the strength and stiffness of the specimens. The tests showed that the GFRP sheets carried a portion of the tensile force, which

decreased the stress in the steel reinforcement. This was particularly evident with the smaller steel reinforcement ratios.

One of the first studies in this area was by (***Triantafillou et al.***, ١٩٩٢). This study consisted of bonding CFRP plates to the bottom of prestressed concrete beams. Five specimens were prepared with steel reinforcing bars on the bottom and steel shear stirrups. Four beams had prestressing applied at varying widths and thicknesses. The fifth beam was a control beam. The beams where tested in one points bending and results are shown in Fig.(٢-١). As can be seen, both the ultimate strength and stiffness were improved substantially over the control beam 'E' by the prestressing. The beams failed by localised diagonal cracks causing peeling off of the reinforcement. This peeling off was stopped at the supports because the CFRP went over the supports resulting in a clamping effect. The authors stated that the CFRP's placement over the supports was important to the performance of the beams. While this may work well in a new construction this would be difficult to achieve in rehabilitation projects. Despite this, prestressing of plates is a promising technique.

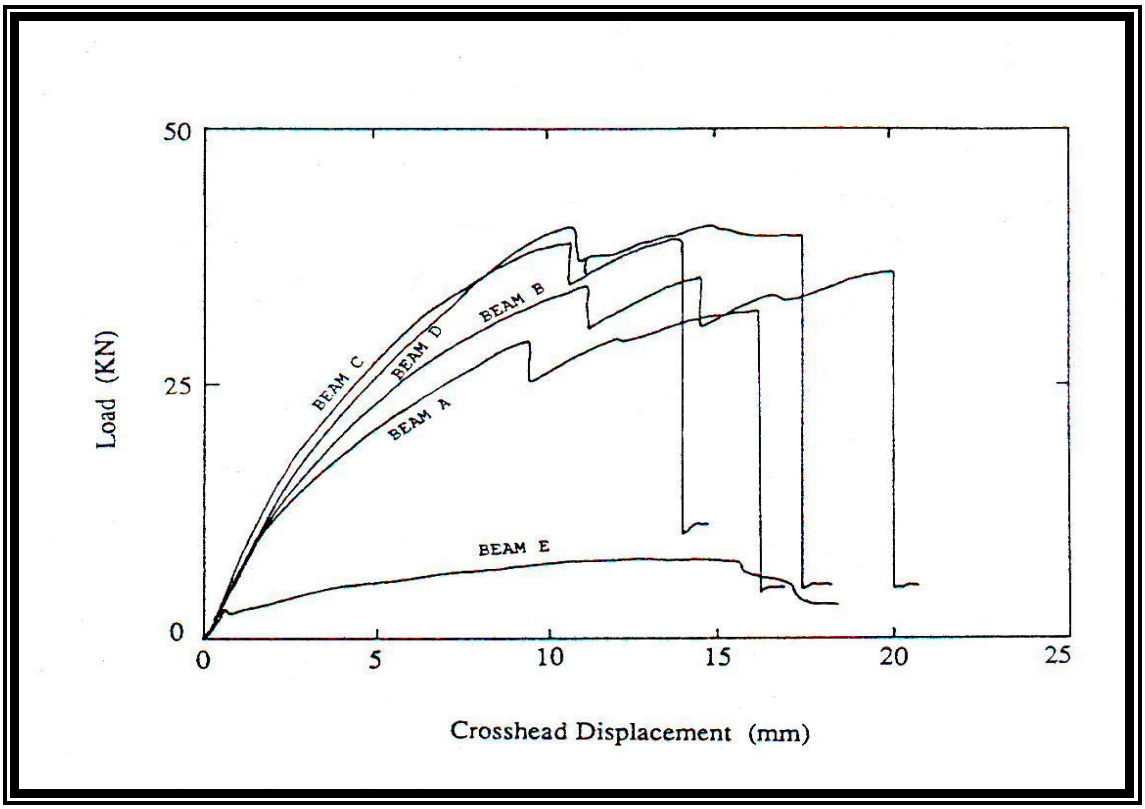

Fig.(٢-١): Load Versus Displacement for CFRP Prestressed Concrete Beams (*Triantafillou et al.,* ١٩٩٢)

Norris *and* ***Saadatmanesh***, (١٩٩٤) cast thirteen concrete beams for flexural tests to compare three different fiber/epoxy systems and several orientations of fiber. The beams (١٢٧ mm x٢٠٣.٢ mm x ٢٤٣٨.٤ mm) contained close to the minimal amount of steel reinforcement (two ٩.٥ mm diameter bars) and were over-designed against shear. Some beams were pre-cracked before the application of the CFRP to see if pre-cracking caused any substantial differences in behavior. Two types of fiber were tested with ٠°, ٩٠°, and ±٤٥° orientations, and the third fiber was used with orientations of ٠°/٩٠° and ±٤٥° with respect to the longitudinal axis. The same fiber weight was applied to every beam.

The research showed little difference in the behavior between the types of fiber of pre-cracked and uncracked beams, but the different fiber

orientations provided amiable results. The unidirectional fibers (٠°) yielded the largest strength and stiffness increase and deflection decrease with respect to the control beam. These beams failed very abruptly due to the peeling-off of the CFRP. The ٠°/٩٠° fibers had a maximum strength, which was ٢٠٪ less than the unidirectional, but they showed much more ductility and deflection (٤٠٪ greater than ٠°). They also failed less explosively than the unidirectional fibers. A ٤٥٪ decrease in the strength and stiffness occurred with the ±٤٥° laminate compared to the ٠° orientation. However, the ±٤٥° laminate experienced is much more ductility than the other lay-ups. Failure of the beam applied with ±٤٥° laminate acted in such a slow, ductile manner that loading had to be stopped.

Norris et al. concluded that off-axis CFRP laminates need to be studied at length. The use of different orientations could increase the strength and stiffness of concrete beams without causing catastrophic, brittle failures associated with unidirectional laminates. Also, they may provide ductile yielding properties that are very important in the civil engineering field.

Shahawy et al., (١٩٩٥) assessed the effectiveness of external reinforcement in terms of the cracking moment, maximum moment, deflection, and crack patterns. Four beams (٢٠٣.٢ mm x٣٠٤.٨ mm x ٢٧٤٣.٢ mm) were tested by using minimum steel reinforcement (two ١٢.٧ mm diameter bars) and varying the layers of unidirectional CFRP. Also, non-linear finite element computer model was used to compare the results of the experiment.

The cracking moment of the CFRP repaired beams was much larger than that of the control beam. For one, two, and three layers of CFRP, the cracking moment increased ١٢٪, ٦١٪, and ١٠٥٪, respectively. The maximum moment

also became larger and corresponded well to the theoretical data. A ١٣٪, ٦٦٪, and ١٠٥٪ increase was observed for the three different layers. This showed the CFRP behaved similarly before and after cracking of the beam.

The deflection and cracking patterns showed results similar to experiments previously discussed. The deflection decreased inversely with the number of CFRP layers on each beam. This, alternatively, caused the stiffness to increase. The cracking patterns between the control and the CFRP repaired beams exhibited different patterns. The control had wider cracks while the repaired beams showed smaller cracks at relatively close spacing. This shows an enhanced concrete refinement due to the CFRP sheets.

The research by ***Bazaa et al****. (١٩٩٦)* was based on optimizing the length and orientation of the CFRP to increase beam strength and ductility. Eight beams (٢٠٣.٢ mm x ٣٠٤.٨ mm x ٣٠٤٨ mm) were minimally reinforced with steel (two ١١.١ mm diameter bars) and overdesigned for shear to cause a flexural failure. One beam was used as a control while the others were bonded with three layers of CFRP (٠.٣ mm x ١٦٧.٦ mm). The sheets varied in length and orientation of the fibers. Four had unidirectional fibers with different lengths, and the other three had various fiber directions with regard to the longitudinal direction (±٦°, ±٩°, ±١٢°).

The results of the experiment showed an increase in strength and stiffness and a decrease in deflection as compared to the control beam. All failures occurred at a load at least ٥٧٪ higher than the control beam. The stiffness was similar until the cracking moment. At this point, less deflection was observed in the repaired beams. The load versus deflection plots exhibit three different section modulus; the start of the experiment to first crack, first

crack to yielding of the steel began, and yielding of the steel to failure of the member.

The use of small angle, off-axis laminates and different CFRP sheet lengths had no effect on strength or stiffness of the repaired beams. However, the off-axis CFRP provided improved warning of failure due to a cracking sound.

Chan et al., *(١٩٩٧)* presented the behaviour of full-scale reinforced concrete beams strengthened with CFRP plate. The beams of dimensions ٢٥٠x٤٧٠x٥٠٠٠mm were reinforced with different steel ratios, and tested under ٢-point static loading.

The objective of the tests was to investigate the delamination of the plate within the plate length as these beams were designed to prevent failures caused by the termination of the bonded plate before the supports.

The research concluded that flexural bond stress between the CFRP plate and concrete caused by the cracks located in constant moment region was believed to be a main reason for the delamination failure; the delamination failure mode may be prevented by a limit on the maximum strain in the plate.

Nguyen et al., *(١٩٩٧)* tested five reinforced concrete beams of length ١.٥ m and strengthened with CFRP plates bonded to their soffits. Failure modes, the increase in strength and stiffness of the strengthened beams as compared to unplated beams, were investigated with particular emphasis on the effect of the plate curtailment. The distribution of strain along the plate was studied. The effect of the plate length on the overall behaviour of the beams was discussed.

Two modes of failure, which were ripping-off of concrete layer between the plate and the longitudinal steel at the plate end region and flexural failures, were observed. It was found that just before concrete ripping-off occurred the distance from the plate end to where the strengthened beam was considered to have fully composite behaviour was almost the same despite that the beams were bonded with different plate length. The strains in the plate reduced linearly to zero within the bond development zone.

Emmanuelle et al., *(١٩٩٨)* had tested several FRP (Fibre Reinforced Plastic) materials. The experimental study was divided into two parts: on one hand initially preloaded beams and then repaired them with epoxy-bonded glass fibre plates, on the other hand beams were simply strengthened with several composite materials. Ten rectangular beams were tested in order to evaluate the effect of externally bonded composite-material reinforcement on the flexural capacity of RC beams. All ten beams had span length of ٢.٨ m (beams were ٣ m long) and cross-sectional dimensions of ١٥x٣٠ cm. These beams had internal reinforcement provided by two ١٤ mm diameter rebar's (yield strength: ٥٠٠ MPa). Twenty-one ٦ mm diameter stirrups were also used. The average compressive strength of the concrete at the day of the test was ٤٠ MPa. Descriptions of the ten beams are listed in Table (٢-١).

Table (٢-١): Description of the Ten Beams *(Emmanuelle et al., ١٩٩٨)*

P_1	Control beam
P_2	Precracked beam repaired using a 3 mm Delmat plate
P_3	Precracked beam repaired using a 3 mm Delmat plate
P_4	Precracked beam repaired using a 6 mm Delmat plate
P_5	Reinforced beam using a single layer of 7.4 mm diameter Jitec rods
P_6	Reinforced beam using a 6 mm Delmat plate
P_7	Reinforced beam using a single layer of two Sikadur sheets
P_8	Reinforced beam using a single layer of two Sikadur sheets
P_9	Reinforced beam using two layers of two Sikadur sheets
P_{10}	Reinforced beam using two layers of two Sikadur sheets

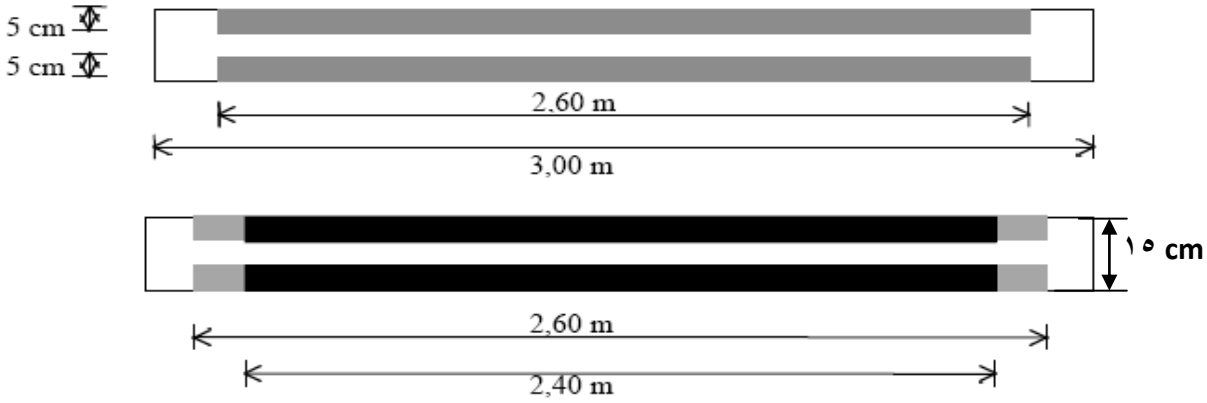

Fig. (٢-٢): Bonding of the Three Composite Material *(Emmanuelle et al., ١٩٩٨)*

Table (٢-٢): Experimental Results of the Ten Beams *(Emmanuelle et al., ١٩٩٨)*

Beam	Ultimate load [kN]	Ultimate strain in the external reinforcement	Failure mode
P_1	90		Concrete crushing
P_2	101	8 ‰	Failure of the plate
P_3	101	8 ‰	Failure of the plate
P_4	115	6 ‰	Local debonding of the 6 mm Delmat plate and shear failure of a concrete layer between the rebars and the external plate
P_5	100	2 ‰	Failure of a concrete layer along the internal reinforcement
P_6	132	10 ‰	Idem
P_7	136	4 ‰	Idem
P_8	143	4 ‰	Idem
P_9	156	2.8 ‰	Idem
P_{10}	159	2.8 ‰	Idem

Spadea et al., (١٩٩٨) tested four beams. Three with bonded CFRP plates on the tension face, and two of which were provided with carefully designed external anchorages at the ends of the plates and along the span, were tested under four-point bending over a span of ٤.٨ m. The tests were carried out under displacement control. The beams were extensively instrumented to monitor strains, deflection, and curvature over the entire spectrum of loading to total failure, and to determine the structural response to load of the composite beams.

The results showed that bonding a CFRP plate on the tension face of a RC beam, without consideration of the end-anchorage stresses and the bond slip between the plate and the concrete substrate, can lead to significant degradation in the structural response of the plated beam. Carefully designed external anchorages, on the other hand, can lead to preservation of composite action to almost the failure load, increases in load capacity of up to ٧٠٪, substantial regain of structural ductility, and the transformation of a brittle failure to a more ductile failure.

Shahawy and Beitelman, *(١٩٩٩)* presented the results of a study involving the static and fatigue performance of reinforced concrete beams strengthened with externally bonded carbon-fiber-reinforced plastic (CFRP) sheets. The main parameters in the static test study were the concrete compressive strength, the number of CFRP laminates, and the placement of CFRP reinforcement. The static test program showed that the application of CFRP to reinforced concrete beams results in increased strength and enhanced performance. Accelerated fatigue testing was performed on several specimens receiving various amounts of the CFRP lamination system, including one member that was fatigued for over half the expected fatigue life, then rehabilitated with the CFRP, and fatigued again until failure.

Comparisons were made for the standard section and equivalent sections with two and three layers of CFRP involving the improvements in fatigue behavior, stiffness, and capacity. The results from the fatigue study indicate that fatigue life of reinforced concrete beams can be significantly extended through the use of externally bonded CFRP laminates.

Kachlakev and David (٢٠٠٠), studied four full-size beams were constructed to match the dimensions and strength capacity of the Horsetail Creek Bridge crossbeams as closely as possible. One of these beams was used as the control, while the other three beams were strengthened with various composite configurations including the same configuration used on the bridge crossbeams. The beams were loaded in one point bending to determine their capacity. The beam strengthened with the same composite design used on the bridge could not be broken with loading equipment used.

Based on the maximum loads applied, the Bridge beams had at least a ٥٠٪ increase in shear and a ٩٩٪ increase in moment capacity over the unstrengthened condition.

Timothy et al., *(٢٠٠١)* carried out an experimental programme to investigate the effects of strain rate on the behaviour reinforced concrete beams strengthened with carbon fibre- reinforced polymer (CFRP) laminates. Nine ٣-m RC beams, one unstrengthened, four strengthened with S-type CFRP laminates, four strengthened with R-type laminates, were loaded under four different loading schedules. Some beams were subjected to their ١ or ١٢ cycles of loading prior to a fast rate of loading to failure. The rapidly loaded beams showed an increase of approximately ٥٪ in capacity, stiffness, and energy absorption. Ductility and the mode of failure were not directly affected by the change in loading rate. Pre cycled beams performed similarly to the beams loaded monotonically to failure but showed a ١٠٪ increase in service stiffness and ١٠٪ loss in energy absorption.

The research concluded strengthening with CFRP will increase capacity and stiffness but will reduce the energy absorption and ductility. These magnitudes of these changes are dependent on the amount of CFRP reinforcement, steel reinforcement, and the mode of failure.

Chan et al., *(٢٠٠١)* presented full-scale reinforced concrete beams strengthened with CFRP plate. A total of ٨ beams having dimensions of ٢٥٠mm x ٤٧٠mm x ٥٠٠٠mm were tested under ٢-point bending with a clear span of ٤.٦m. All beams were nominally reinforced in compression by ٢T١٦ bars. Details of the beams are shown in Table (٢-٣) and Fig (٢-٣). All the beams were reinforced in shear with R١٠ spaced at ٢٠٠mm (centre to centre) to investigate

the effect of the conventional shear strength on the strength and failure mode of the beam.

The objective of the tests was to investigate the delamination of the plate within the plate length as these beams were designed to prevent failures caused by the termination of the bonded plate before the supports.

Their study concluded that strengthened beams failed in delamination of the plate and the classical shear failure. The delamination initiated from the flexural region and immediately extended towards the ends of the plates.

Table (٢-٣): Summary of the Test Results *(Chan et al., ٢٠٠١)*

Beam	Tension reinfor-cing steel	CFRP plate length l_p (mm)	Maximum strain in the plate (10^{-6})	Strength of unplated beam P_0(kN)[1]	Shear capacity of unplated beam (kN)[1]	Failure load P_u (kN)	Increase in the strength ΔP (%)[2]	Ductility index	Mode of failure
(1)	(2)	(3)	(4)	(5)	(6)	(7)	(8)	(9)	(10)
Group 1									
B1	2T20	-	-	160	360	165	-	4.62	flexural
B2	2T20	4500	7486	160	360	285	78	2.41	delamination
B3	3T20	4500	6843	241	389	352	46	2.13	delamination
B4	4T20	4500	7279	316	403	442	39	1.99	shear
Group 2									
B5	2T20	3700	6040	160	461	235	47	2.31	delamination
B6	2T20	3700	6944	160	360	258	61	2.27	delamination
B7	4T20	3700	8556	316	504	452	43	2.07	delamination
B8	4T20	3700	7763	316	403	440	39	1.93	delamination

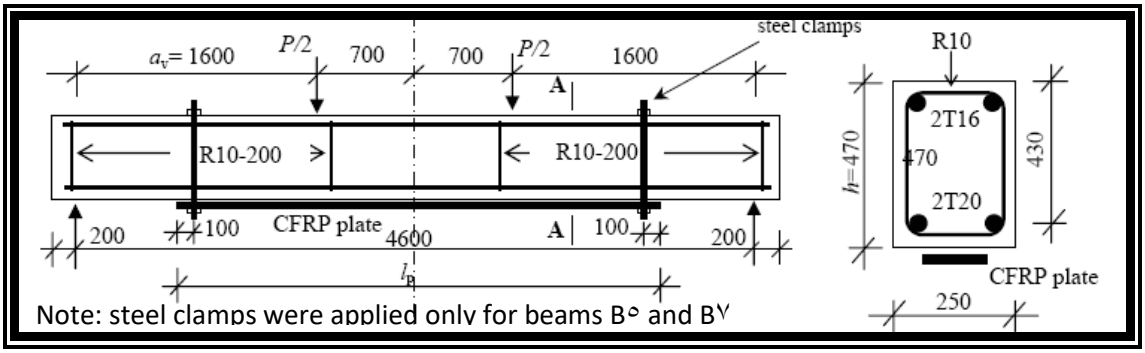

Fig.(٢-٣) : Details of the Beams *(Chan et al., ٢٠٠١)*

***Dat and Starnes**, (٢٠٠١)* tested seven concrete beams reinforced internally with varying amounts of steel and externally with carbon fiber-reinforced polymer (CFRP) laminates applied after the concrete had cracked under service loads. The beams were tested under two-point bending.

Results showed that FRP is very effective for flexural strengthening. As the amount of steel increases, the additional strength provided by the carbon FRP laminates decreases. Compared to a beam reinforced heavily with steel only, beams reinforced with both steel and carbon have adequate deformation capacity, in spite of their brittle mode of failure.

***Alagusundaramoorthy et al.**, (٢٠٠٢)* tested two control beams and twelve concrete beams strengthened with externally bonded CFRP sheet or fabric on the tension face(five beams strengthened with different layouts of CFRP sheets and three beams strengthened with different layers of anchored CFRP sheets and four beams strengthened with different layouts of CFRP fabric). The length, breadth and depth (L x B x D) of all concrete beams was kept as ٤٨٨٠mm x ٢٣٠mm x ٣٨٠mm. Each concrete beam was reinforced with two bars of diameter ٢٥mm for tension and two bars of diameter ٩mm at spacing of ١٥٠mm center-to-center for shear. The flexural span of all beams was kept as ٤٥٧٦mm.

Results of the testing showed that the flexural strength was increased up to ٤٠٪ for beams strengthened with two layers of CFRP fabric, ٤٩٪ for beams strengthened with two ١.٤٢ mm thick CFRP sheets, ٥٨٪ for beams strengthened with two anchored ٤.٧٨ mm CFRP sheets.

***Wobbe et al.,** (٢٠٠٣)* used of externally bonded Steel-Reinforced Polymer (SRP) and Steel Reinforced Grout (SRG) composites was a promising new

technology for increasing the flexural and shear capacities of reinforced concrete (RC) members. The reinforcement system in these composites was a sheet made up of unidirectional cords consisting of tightly wound ultra high strength steel wires. The reinforcement could be molded into resin systems (SRP) or cementations grout (SRG).The research aimed for investigating the flexural strength improvement and performance of RC beams with externally bonded SRP and SRG. Three specimens were tested under two-point bending with variables considered including the number of reinforcement plies and types of bonding agents. Based on their study, it was concluded that this new technology had potential for the repair and strengthening of concrete structures.

Test results indicated that up to ١٠٠٪ increase in the flexural capacity could be achieved using these strengthening systems.

***Carolin Anders**, (٢٠٠٣)* tested ٤ m long beams, showed that a structure should be strengthened against live loads during the strengthening process. Their holds both for Near Surface Mounted Reinforcement (NSMR) and traditional laminate bonding. Normally, in strengthening applications CFRPs were used as additional tensile reinforcement, also their study showed how CFRP plate bonding may be used for strengthening of increase buckling load-bearing capacity for steel members subjected to compression.

A testing program including ١٨ rectangular reinforced concrete beams was carried out by ***Pham and Al-Mahaidi**, (٢٠٠٤)* to investigate the failure mechanisms and the influence of several parameters on these debond modes. Testing showed that end cover separation starts from FRP ends and failed in the form of shear failure at steel reinforcement level at the root of the concrete teeth between shear cracks. Shear crack debond failure was due to

the opening of one of those inclined cracks. Several debond prediction models were then verified with the experiment proving to work relatively well.

The research concluded the following: Mid-span and end debond are the result of the high shear stress level in concrete (around ١MPa), concrete cover and amount of shear reinforcement have insignificant influence on debonding and steel clamps provide good method to avoid end debond. It does not prevent mid-span debond but it helps the beam ductility by holding the delaminated fabrics to concrete by friction, After debonding of FRP, RC beams still have their original strength as without bonding FRP.

Michael et al., (٢٠٠٥) described a laboratory study of the effects of traffic loads applied during and after strengthening on the performance of a reinforced concrete (RC) bridge strengthened with externally bonded fiber-reinforced polymer (FRP) reinforcement. Eight beams were tested to failure. Seven of the beams were strengthened with a procured, unidirectional, carbon-fiber laminate strip representative of the material used on the actual bridge.

Test variables included the intensity and frequency of load cycles applied during the epoxy-curing period, the thickness of the epoxy layer, and the thickness of the FRP strip. Failure of all strengthened specimens initiated with FRP debonding in the maximum moment region. For the entire traffic load regimens applied during and after installation, no reduction in the effectiveness of the strengthening was observed.

٢.٣ THEORETICAL

٢.٣.١ ANALYTICAL METHODS

An et al., *(١٩٩١)* developed a model to predict the stresses and forces of a reinforced concrete beam with externally applied glass fiber reinforced plastics (GFRP). Their study was based on five assumptions: ١) linear strain distribution throughout the beam; ٢) small deformations; ٣) tensile strength of concrete was ignored; ٤) shear deformation was ignored; ٥) perfect bond between concrete and GFRP. Using classical flexural theory and strain compatibility, effects of variables such as material strength, modulus of elasticity, and reinforcement ratios of the steel and GFRP were compared with experimental results of a previous test (*Saadatmanesh and Ehsani, ١٩٩١).*The behavior of the beams was predicted with reasonable accuracy using the model.

Triantifillou and Plevris, *(١٩٩١)* used strain compatibility and fracture mechanics to analyze reinforced concrete beams applied with externally bonded carbon fiber reinforced plastics (CFRP). The same assumptions as ***An et al.,*** *(١٩٩١)* were used with the inclusion of an equivalent rectangular compression stress distribution in the concrete at failure. The applied moments that would cause each of the three failure modes were predicted. The failures were yielding of the steel reinforcement followed by CFRP rupture; yielding of the steel reinforcement followed by the crushing of the concrete compression zone; and concrete crushing before either tensile component fails. These models were compared with experimental studies and deemed creditable.

Nguyen et al., *(١٩٩٧)* studied a new closed analytical formulation which represents the full interaction between the plate and the strains in the plate is assumed to increase linearly in the bond development zone (Fig.(٢-٤)). Results

obtained using the developed formulation showed good agreement with published data. Debonding of the plate can be assessed by the strength of plate-adhesive-concrete interfaces. However, with the application of high strength adhesive, the beam commonly failed by ripping of the concrete layer between the adhesive and the longitudinal steel. A simple approximate formulation based on the full composite beam theory to predict the concrete ripping failure load was developed. Results obtained based on this analysis were well compared with those of tests on ١.٥m length CFRP strengthened beams.

From Table (٢.٤), it could be said that theoretical predicted failure loads compared well with the experimental results.

Table (٢-٤): Theoretical Predicted and Experimental Failure Loads

Beam	f_{cu} (f_t) (MPa)	l_p (mm)	Δ_p (mm)	T_p (kN)	Flexural cap. (kN)	Shear cap. (kN)	P_u (kN) theo.	P_u (kN) exper.	error (%)	Failure mode
B1150	33 (3)	1150	340	32.40	82	114	68.61	58.9	16	ripping.-off
B1100	33 (3)	1100	365	32.40	82	114	63.91	57.3	12	ripping.-off
B950	33 (3)	950	440	32.40	82	114	53.0	56.2	-6	ripping.-off

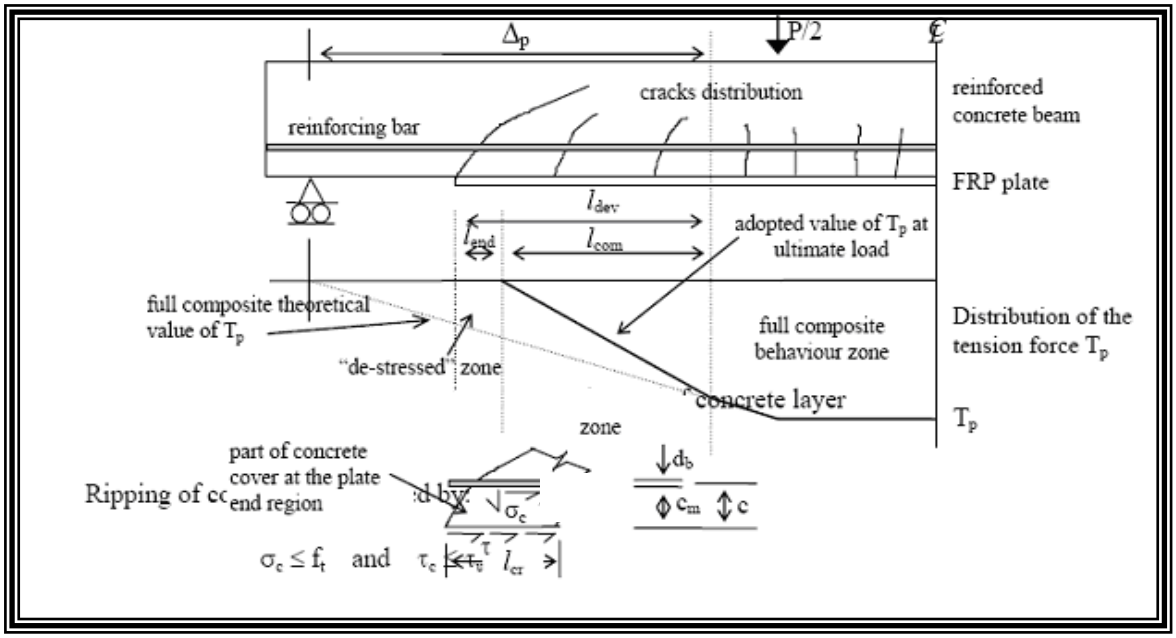

Fig.(٢-٤): Ripping-off of Concrete Layer Zone (*Nguyen et al., ١٩٩٧*)

Saadatmanesh and Malek, *(١٩٩٨)* developed design guidelines for strengthening reinforced concrete beams using fiber composite plates. The effect of multistep loading of the beam, before and after upgrading, had been included in their guidelines. Their study was assumed that the strain in the plate and the concrete at the interface are equal, full composite action exist between the plate and the beam (no slip at the interface), ignored the thickness of the plate, linear variation of strains in the cross section, the effect of the stresses that a concrete beam undergoes before upgrading, Rupture of the plate and crushing of concrete are the major modes of failure that are considered in calculating the ultimate strength of the plated beam.

The research concluded that the design guidelines presented of this study provide a relatively simple approach for designing concrete beams strengthened with epoxy bonded composite plates, Based on the above modes of failure, the stress level in the tension and compression steel reinforcement at the ultimate state. Local failure of concrete beam at the plate end, and debonding of the plate due to sheer stress concentration at flexural cracks were also considered in developing these guidelines. An additional experimental work could be conducted to verify and refine these equations and modes of failure.

An interesting paper on the analysis of concrete beams strengthened using FRP sheets was written by ***(El-Mihilmy and Tedesco,*** *٢٠٠٠).* In this paper they develop equations for the flexural analysis of rectangular and T-section RC beams. The intent of the analysis was to develop the equations to prevent failure in three primary ways: crushing of concrete, FRP rupture, and yielding of steel followed by concrete crushing. The equations were developed assuming that other potential failure modes (debonding, anchorage and shear)

would not occur because of proper detailing of the beams. Once the equations had been developed they were compared to experimental beams tested by other researchers. The analysis was developed by using American design procedures; thus, they have some differences to what would be developed for Canada. Despite this the analysis was quite clear and could easily be converted to Canadian design procedures. The procedures were developed from equilibrium equations and compatibility of strains, and it can be used on both singly and doubly reinforced sections. The intent was to avoid concrete compression failure and FRP rupture due to their non-ductile behaviour of this type of RC failure. This was achieved by setting minimum and maximum FRP cross-sectional areas.

Figure (٢-٥) is reproduced from this paper and shows a schematic of failure modes for strengthened FRP beams. The area above line EF represents compression failure zone where the steel has not yielded. The area below line AB represents the zone where FRP ruptures and above is tension failure. In developing the equation for maximum FRP area they took the balance condition and then backed off by ٧٥٪ to ensure ductile failures. The number of equations that were developed is numerous and can be viewed in the paper.

For the purposes of this paper they have been omitted, since they are developed for American design procedures and they would take up a lot of space. In the second part of the paper the authors took the analysis and applied it to fellow researcher's experimental results. Table (٢-٥) is reproduced from the paper and shows the comparison between the actual loads (col. ١٢) and calculated loads (col. ١٣). The correlation between experiment and theory was quite good.

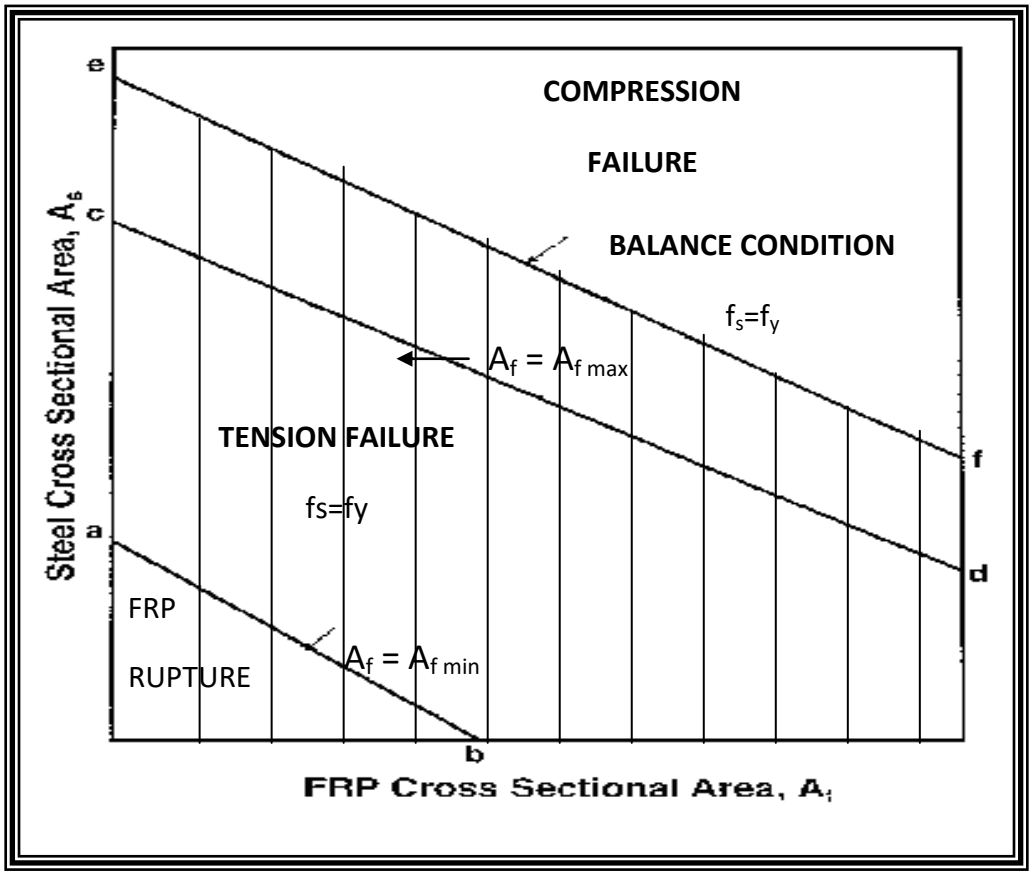

Fig.(٢-٥): Schematic of Failure Modes *(El-Mihilmy and Tedesco, ٢٠٠٠)*

Table (٢-٥): Comparison of Experimental and Calculated Loads *(El-Mihilmy & Tedesco, ٢٠٠٠)*

Reference (١)	Beam desination (٢)	b mm (٣)	d mm (٤)	As mm^2 (٥)	f_y MPa (٦)	f'_c MPa (٧)	A_f mm^2 (٨)	E_f GPa (٩)	d_f MPa (١٠)	f_{tu} MPa (١١)	Experimental ultimate Load kN (١٢)	Calculated ultimate Load kN (١٣)	Mode of failure (١٤)	**% difference (١٥)**
Chajes(١٩٩٤)	A٢	١٢٧	٥٠.٨	٧١	٤١٣	٤٢.٥	١٣٢	١١	٧٧	٢٢٣	١٤.٧٥	١٣.٤٨	(*)	-٨.٦
	E١	١٢٧	٥٠.٨	٧١	٤١٣	٣٣.٦	١٨٠	١٣.١	٧٧	١٣٨	١٥.٢٨	١٤.٠٩	(**)	-٧.٨
	E٢	١٢٧	٥٠.٨	٧١	٤١٣	٤٢.١	١٨٠	١٣.١	٧٧	١٣٨	١٥.٢٨	١٥.٠٢	(**)	-١.٧
	E٣	١٢٧	٥٠.٨	٧١	٤١٣	٤٢.٥	١٨٠	١٣.١	٧٧	١٣٨	١٥.٣٨	١٥.٠٤	(**)	-٢.٢
	G١	١٢٧	٥٠.٨	٧١	٤١٣	٤٢.٥	١٥٥	٢٢.١	٧٧	١٩٠	١٥.٠٦	١٦.٤٦	(**)	٩.٣
	G٢	١٢٧	٥٠.٨	٧١	٤١٣	٤٢.١	١٥٥	٢٢.١	٧٧	١٩٠	١٧.٠٣	١٦.٤٤	(**)	-٣.٥
	G٣	١٢٧	٥٠.٨	٧١	٤١٣	٣٦	١٥٥	٢٢.١	٧٧	١٩٠	١٤.٤٩	١٦.١٥	(**)	١١.٥
Triantafillou (١٩٩٢)	٢	٧٦	١١١	٣٣	٥١٧	٤٤.٧	٨.٥٢	١٨٦	١٢٧	١٤٥٠	١٣.١٦	١٤.٣٠	(**)	٨.٧
	٣	٧٦	١١١	٣٣	٥١٧	٤٤.٧	١٢.١	١٨٦	١٢٧	١٤٥٠	١٧.٢٧	١٦.٩١	(*)	-٢.١
Ross (١٩٩٩)	٦	٢٠٣	١٥٢	٥٦٦	٤١٤	٥٥	٩١	١٣٨	٢٠٤	٢٢١٠	١٠٧.٦٠	١١٠.٩٠	(*)	٣.١
	٧	٢٠٣	١٥٢	٧٧٤	٤١٤	٥٥	٩١	١٣٨	٢٠٤	٢٢١٠	١٤٦.٠٧	١٢٧.٧٣	(*)	-١٢.٦

	٨	٢٠٣	١٥٢	١٠٨١	٤١٤	٥٥	٩١	١٣٨	٢٠٤	٢٢١٠	١٥٢.٧٤	١٤٣.٣	(*)	-٦.٢
Saadat mansh (١٩٩٠)	C	٨٩	١٢٧	٧١	٤١٤	٣٦.٤	٤٥٠	٣٧.٢	١٥٥	٤٠٠	٥٧.٧٢	٤٥.٧	(*)	-٢٠.٨
Saadat mansh (١٩٩١)	A	٢٠٥	٤٠٠	١٥٢٠	٤٥٦	٣٥	٩١٢	٣٧.٢	٤٥٥	٤٠٠	٣٢٠.٠٠	٣١٧.٨٣	(*)	-٠.٧
	B	٢٠٥	٤٠٠	١٠١٣	٤٥٦	٣٥	٩١٢	٣٧.٢	٤٥٥	٤٠٠	٢٥٥.٠٠	٢٧٦.٠٠	(*)	٨.٢
	F	٦١٠	٤٠٠	١٠١٣	٤٥٦	٣٥	٩١٢	٣٧.٢	٤٥٥	٤٠٠	٣١٠.٠٠	٣٤٢.١٠	(**)	١٠.٤
Ritchie (١٩٨٨)	٥	١٥١	٢٥١	٢٥٨	٤١٤	٤٨.٨	٧٣١	١١.٧	٣١٠	١٦١	١٢٤.٣٢	١٢٨.٥١	(**)	**٣.٤**
	٩	١٥٦	٢٥٠	٢٥٨	٤١٩	٤٦.٣	١٩٣	٥٤.٤	٣٠٥	٦١٤	١١٩.٤٠	١٢٣.٩٤	(**)	**٣.٨**
Absolute value aver-age														**٦.٩**

(*): Concrete crushing

El-Tawil et al., *(٢٠٠١)* described an analytical model for simulating the static response and accelerated fatigue behaviour of reinforced concrete beams strengthened with CFRP laminates. Static and fatigue calculations are carried out using a fibre section model that accounts for the nonlinear time-dependent behaviour of concrete, steel yielding, and rupture of CFRP laminates. The main assumptions employed in the fibre section method are:

- Plane sections were considered to remain plane after bending.
- Perfect bond was assumed between concrete and other materials (steel reinforcement and CFRP laminates).
- Shear stresses were not accounted for. The fibre section method, as presented in this study, was therefore limited to long thin members whose behaviour was dominated by flexure.

In their discretized form, the cross-sectional forces were determined as stress resultants according to the following equations:

$$P = \sum_{i=1}^{n} S_i A_i \qquad \text{.....(٢-١)}$$

$$M_Z = \sum_{i=1}^{n} S_i A_i d_i \qquad \text{.....(٢-٢)}$$

Where P= axial load; M_Z= major bending moment; S_i= longitudinal stress at centroid of fiber I; A_i= area of fiber I; d_i= distance between centroid of fiber i and top of section; and n= total number of section fibers

The assumed constitutive properties for the component materials are shown in Fig. (٢-٦). The stress- strain response of CFRP was assumed to be elastic-perfectly brittle, whereas the stress-strain curve for steel was elastic-plastic with a post yield strain hardening of ١٪. A non linear stress- strain relationship was assumed for concrete fibres.

The research concluded many results which were compared with experimental data from two sets of accelerated fatigue tests on CFRP strengthened beams and showed good agreement.

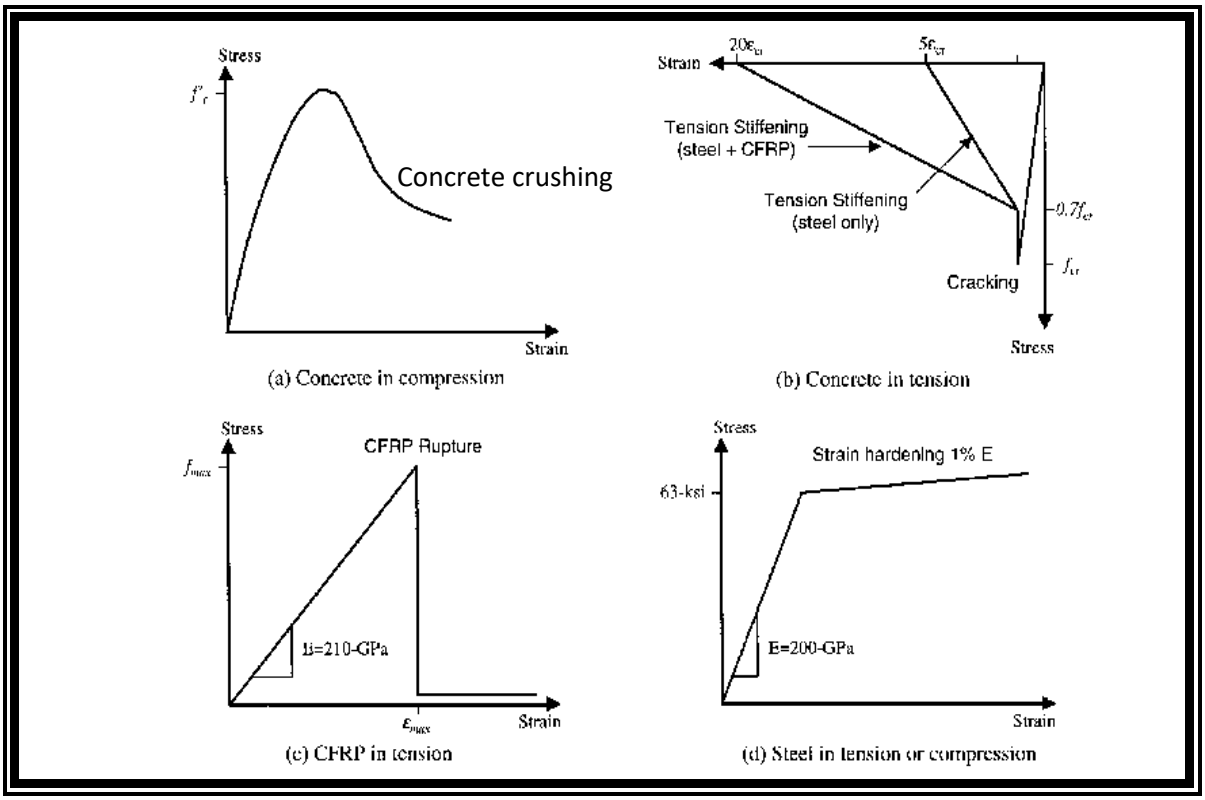

Fig.(٢-٦): Monotonic Constitutive Models for Component Material (Timothy et al., ٢٠٠١)

***NG** and **LEE**, (٢٠٠٢)* presented an analytical study on the flexural behavior of reinforced concrete beams strengthened with externally bonded carbon fiber-reinforced plastic (CFRP) laminates. Different failure modes of their strengthened reinforced beams had been reported and their failure modes are generally referred to as brittle failure or ductile failure involving the compression crushing of the concrete, debonding or rupture of the composite laminate and yielding of the steel reinforcement. For the analysis, the stresses and strains of all the components of the beam were related by the material properties, including the stress-strain curves for the concrete, steel and CFRP laminate. The strain distribution is assumed to be compatible within the distorted shape of the cross-section of the concrete beam. The resultant forces

on the cross section were balanced with the applied loads for static equilibrium.

The analytical solution was derived from the equilibrium equations and the compatibility of the strains, and it was applicable to both singly and doubly reinforced concrete beams strengthened with multi-layers of CFRP laminates. In their study, a simple and direct analytical procedure had been developed to evaluate the flexural capacity of concrete beams strengthened with CFRP and to predict their failure modes. A comparison between the analytical results and the data obtained from the literature had been made and the agreement is very good.

Alagusundaramoorthy et al., (٢٠٠٢) presented an analytical procedure, based on the compatibility of deformations and equilibrium of forces was developed to predict the flexural behavior of concrete beams strengthened with FRP composites. The following assumptions were made in the formulations: (١) Strain distribution was linear throughout the beam section; (٢) shear deformation was small; (٣) perfect bond between concrete surface and FRP sheets/fabric; and (٤) failure of the beam occur when either the compressive strain in concrete reaches ٠.٠٠٣ or the tensile strain in FRP composites reaches its ultimate strain. The reinforced steel was assumed to be elastic-plastic, and linear stress and strain relationship was assumed for CFRP sheets/ fabric.

The comparison of analytical calculations with experimental results indicated that the analytical procedure overestimated the centreline deflections at service load and underestimated the failure load. But the predictions on centreline deflection and maximum strain in CFRP sheets/fabric at failure were in good agreement with experimental results.

٢.٣.٢ FINITE ELEMENT METHOD

Arduini, et al., *(١٩٩٧)* used finite element method to simulate the behavior and failure mechanisms of RC beams strengthened with FRP plates. The FRP plates were modelled with two dimensional plate elements. However the crack patterns were not predicted in that study.

Shahawy and Beitelman, *(١٩٩٩)* used a two-dimensional finite-element program to calculate the response of the beams tested statically. The program considers the nonlinear response of the component materials and the geometric configuration of the cross section. Stress-strain curves for concrete were obtained from cylinder specimens tested in compression, while stress-strain curves for the steel were obtained from tensile testing of the grade ٦٠ rebar. The average test values of stress and strain at ultimate were used in modelling the CFRP system. Typical stress-strain plots for the three materials are shown in Fig. (٢-٧).

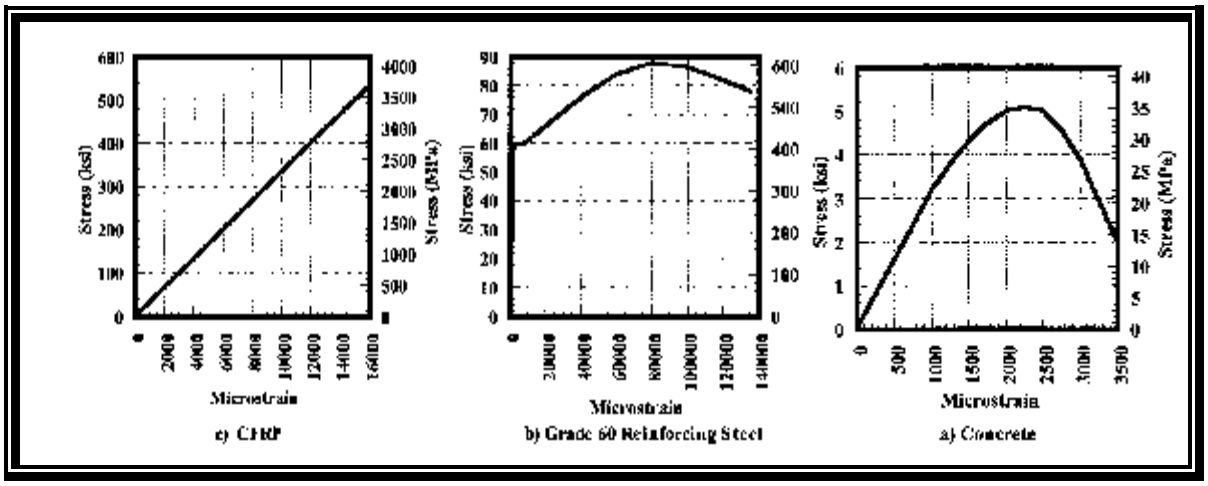

Fig.(٢-٧): Stress Versus Strain for Various Materials (Shahawy and Beitelman, ١٩٩٩)

Typically, the computer model predicts a higher capacity and slightly higher ductility than those observed in the tests. This disparity might be due to two factors. First, the computer model assumes a linear stress-strain relation for the CFRP fabric up to failure. A second factor controlling the prediction was at the level of control varies widely in the preparation of the strengthened beams. The effectiveness of bonding between fabric and concrete is probably affected by these factors. The research concluded that elementary finite-element provisions can be used to predict closely the behavior of beams reinforced with CFRP fabric up to failure.

Aprile et al., ٢٠٠١, The two-node displacement-based RC beam model for fiber is presented in this study, slip is considered between the concrete beam and the strengthening plate. The fiber section model in their study is used to compute the response of the RC beam section. The tension response of the concrete was assumed linear elastic up to the cracking stress. The elements were implemented in the program FEAP in two dimension, documented in *(Taylor,* ١٩٩٩*)*. This paper studies the role of bond slip and of bond failure in RC shallow beams strengthened with thin either steel or thin CFRP plates. The study relies on a simple and accurate displacement-based fiber frame element with bond slip between the RC beam and the strengthening plate. Numerical simulations of a series of experimental tests by Zarnic et al. (١٩٩٩) confirmed that the bond forces and the bond failure between the RC beam and the strengthening plates are fundamental issues in strengthening of shallow beams and must be taken into account to assess the effective stiffness and loading capacity of the strengthened member. In particular, implementation of an elastic-brittle bond-slip law yields detailed information on the evolution of the beam response under increasing applied loads. In particular, the following results were observed:

• Failure of the strengthened RC beams was always initiated by plate debonding.

• Beams strengthened by steel plates show a ductile response, mainly due to yielding of the strengthening plate, whereas beams strengthened by CFRP plates show a brittle response, because the response is dominated by the

elastic behavior of the plate.

• Debonding starts somewhere between the point of load application and the plate end. In CFRP-strengthened beams, debonding tends to start under the point of load application, corresponding to a peak in the bond force distribution. In steel-strengthened beams, debonding starts either at the plate end or somewhere in the cracked concrete zone, depending on the beam depth.

Timothy et al., (٢٠٠١) analyzed reinforced concrete beams strengthened with CFRP laminates by a finite element. Layered analysis is presented to predict the moment–curvature response of CFRP strengthened RC beams. Fig.(٢-٨) illustrate the procedure in which the internal forces of a strengthened RC rectangular or T-section might been calculated.

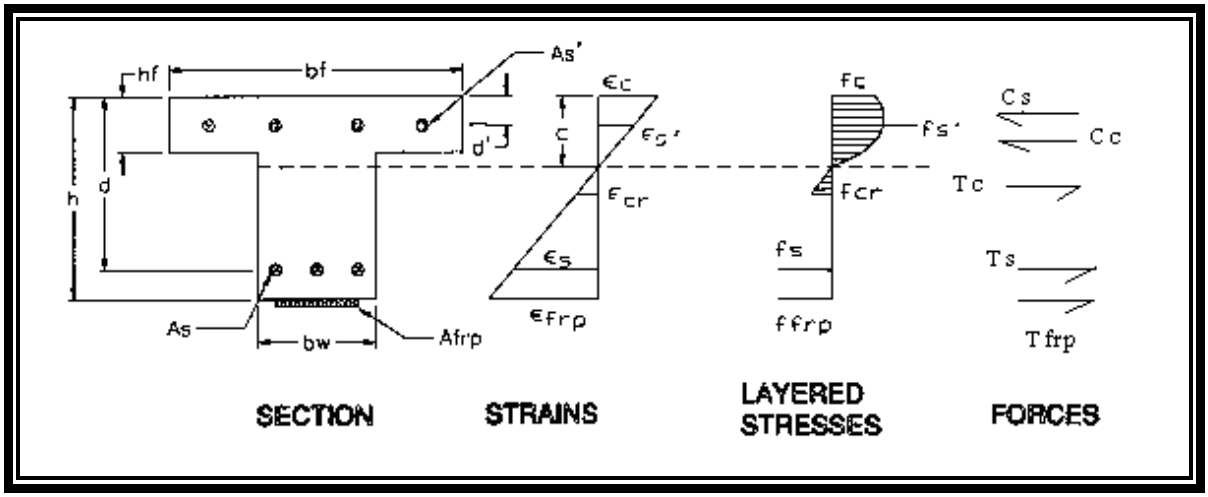

Fig.(٢-٨): Layered Analysis Resolution of Forces (Timothy et al., ٢٠٠١)

The compression steel, tension steel, and CFRP laminate are represented by one element each. The concrete is divided into several layers. Each of these layers or elements has its own area, centroied, strain, and stress. The stress is determined by using the appropriate material model and the strain. The value of the strain is based on the location of the neutral axis and the curvature (the independent variable). The location of the neutral axis is found through iteration, and the location is correct when the internal forces balance. The model includes several assumptions to simplify the calculations:

- The bond is perfect between the elements.
- The strain distribution is linear.
- All deformations are small.
- The section has no mass or inertia.

The model induced the effects of strain rate and correlated well with the experimental data.

Kachlakev *and* ***Thomas****, (٢٠٠١)* described a linear and nonlinear finite element method models for a reinforced concrete bridge that had been strengthened with fibre reinforced polymer composites. ANSYS and Sap٢٠٠٠ modelling software were used; however, most the development effort used ANSYS. In their study, Perfect bond between materials was assumed, An eight-node solid brick element was used to model the concrete and link element was used to model the steel reinforcement. Two nodes were required for this element. A layered solid brick element was used model the FPR composites.

The model results agreed well with measurements from full-size laboratory beams. Guidelines for developing finite element models for reinforced concrete bridges were discussed.

***Rahimi** and **Hutchiuson** (٢٠٠١)* presented theoretical analysis included ٢D nonlinear finite element modelling in corporating a (damage) material model for reinforced concrete beams strengthened with CFRP, GFRP and steel plate.

For ٢D analysis, concrete beams were modelled mostly with four- or eight-noded quadrilateral isoparametric elements. The internal rebars were modelled with two- or three-noded bar elements that were smeared onto the concrete elements, although shear reinforcement (vertical links) was not incorporated into the models. For beams with an adhesive layer, three- or six-noded triangular elements were used in the transition zones to reduce the size of elements toward the bond-line area (Fig.٢-٩). The adhesive layer and external reinforcement were modelled with a single row of four- or eight-noded elements.

In general there were reasonably good correlations between the experimental results and nonlinear finite element models. A typical FE model developed for analysis of RC beams in shown in Fig. (٢-٩).Although ***Rahimi** and **Hutchiuson*** used a much finer mesh discrimination to estimate the plate-end stress concentrations.

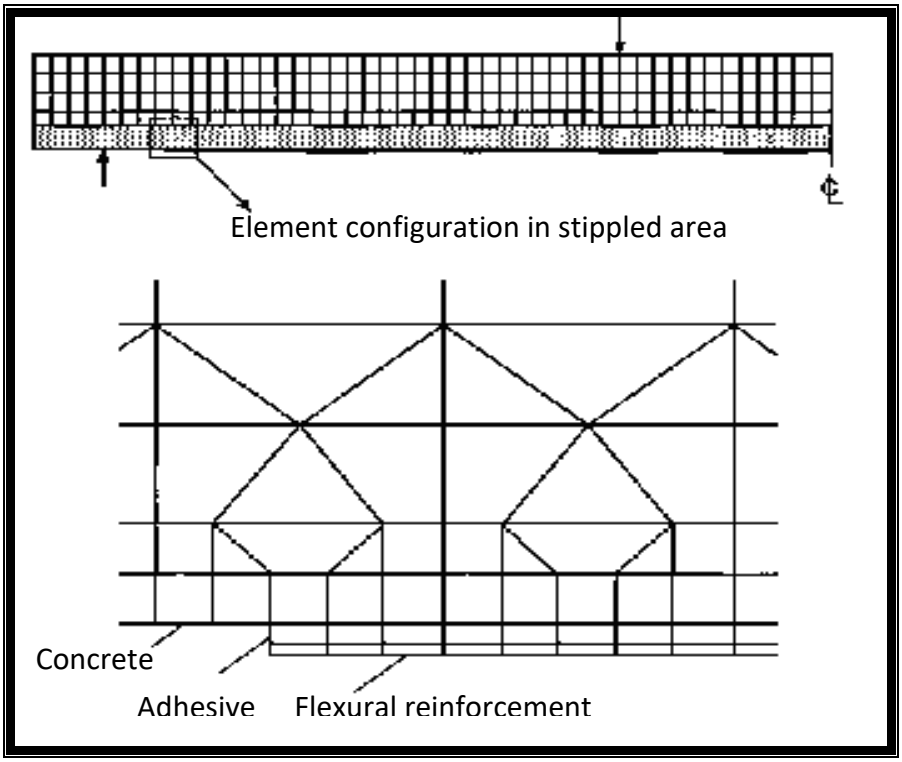

Fig.(٢-٩): Typical ٢D FE Model of RC Beam with Bonded External Reinforcement *(Rahimi and Hutchiuson , ٢٠٠١)*

Santhakumar et al., (٢٠٠٤) presented the numerical study to simulate the behaviour of both uncracked and precracked RC shear beams retrofitted using CFRP composites. The software package ANSYS was used for their study. For purpose of comparison, the study was carried out for the following beams that were experimentally tested and reported by Tom Norris. Solid brick elements were used to model the concrete. The rebar capability of their model was not considered. All reinforcements were modeled using Link element. Solid brick elements were used for the steel plate at the support and under the load. A layered brick element was used to model the CFRP composites.

When comparing with the experimental values, the numerical models show ٨٪ increase in ultimate load for control beam and uncracked retrofitted beam and ٨٪ decrease in ultimate load for precracked retrofitted beam. At the

ultimate stage all the numerical models show less deflection, especially the precracked retrofitted beam shows ٣١٪ less deflection.

CHAPTER THREE

FINITE ELEMENT FORMULATION

٣.١ Introduction:

The finite element method is now firmly established as an engineering tool of wide applicability. No longer is it regarded as the sole province of the searcher or academic but, it is now employed for design purposes in many branches of technology.

During its early development for stress analysis problems the method relied heavily on a physical interpretation in which the structure was assumed to be composed of elements physically connected only at a number of discrete nodal points. Later, the application of the finite element method to structural mechanics problems was developed through the use of the principle of virtual work and energy methods *(Hinton, ١٩٧٩)*.

With the finite element method, complex structures are divided into a large number of elements for which the behavior of each element is well defined. The response of a system is then computed by simply summing the effects of all the elements that comprise the model. Because the behavior of each element is known, the resulting system of equations, while perhaps very large, is readily solved.

The nonlinear finite element analysis of reinforced concrete structure has been extensively used in recent years. It is a powerful analytical tool which can be used to predict the structural response in the entire load range up to failure and study the effects of different parameters on the structure behavior. A suitable modelling of reinforced concrete material is often one of the major factors in limiting the capability of the analysis procedures.

In this chapter, three dimensional nonlinear finite element formulations suitable for the analysis of reinforced concrete beams flexural strengthened with CFRP (Carbon Fibre Reinforced Polymer) are described. The special numerical integration, nonlinear solution techniques, convergence criteria and outline of ANSYS program are also described.

٣.٢ Finite element formulation:

By considering a general three-dimensional body, subjected to a set of external forces, which consist of surface tractions and body forces, the individual element stiffness matrix can be determined easily by using the principle of virtual displacements (***Zienkiweicz,*** *١٩٧٧).*

The displacement vector at any point within the element $\{u\}_e$, can be interpolated as

$$\{u\}_e = [N] \cdot \{a\}_e \qquad \text{..... (٣-١)}$$

Where $[N]$ is a matrix containing the interpolation functions which relates the displacement, $\{u\}_e$, to the nodal displacements, $\{a\}_e$. where, $\{u\}_e$, is given by .

$$\{u\}_e = [u.v.w]_e \qquad \text{..... (٣-٢)}$$

By taking suitable derivatives of equation (٣- ١), the strain-displacement relationships can be written as.

$$\{\varepsilon\}_e = [A] \,.\, \{u\}_e \qquad \text{.....(٣-٣)}$$

Where: **[*A*]** is a matrix that contains the differential operators. Substitution of equation (٣-١) into (٣-٣) yields

$$\{\varepsilon\}_e = [B] \,.\, \{a\}_e \qquad \text{.....(٣-٤)}$$

Where: **[*B*]** is the strain-displacement matrix given by

$$[B] = [A] \,.\, [N] \qquad \text{..... (٣-٥)}$$

The constitutive matrix **[*D*]** is used to relate the vectors of stresses and strains as:

$$\{\sigma\}_e = [D] \,.\, \{\varepsilon\}_e \qquad \text{.....(٣-٦)}$$

Where: the corresponding vector of stresses is given by

$$\{\sigma\}_e^T = \{\sigma_x \ \sigma_y \ \sigma_z \ \tau_{xy} \ \tau_{yz} \ \tau_{zx}\} \qquad \text{..... (٣-٧)}$$

and the vector of strains , $\{\varepsilon\}_e$ is given by

$$\{\varepsilon\} = \begin{Bmatrix} \varepsilon_x \\ \varepsilon_y \\ \varepsilon_z \\ \gamma_{xy} \\ \gamma_{yz} \\ \gamma_{zx} \end{Bmatrix} = \begin{Bmatrix} \dfrac{\partial u}{\partial x} \\ \dfrac{\partial v}{\partial y} \\ \dfrac{\partial w}{\partial z} \\ \dfrac{\partial u}{\partial x} + \dfrac{\partial v}{\partial y} \\ \dfrac{\partial v}{\partial y} + \dfrac{\partial w}{\partial z} \\ \dfrac{\partial w}{\partial z} + \dfrac{\partial u}{\partial x} \end{Bmatrix} \qquad \text{..... (٣-٨)}$$

Substitution of equation (٣- ٤) into equation (٣- ٦) gives the stress-displacement relationship,

$$\{\sigma\}_e = [D] \,.\, [B] \,.\, \{a\}_e \qquad \text{..... (٣-٩)}$$

The principle of virtual displacements of a deformable body is used to establish the governing equations of static equilibrium. It states that "If a general structure in equilibrium is subjected to a system of small virtual displacements with a compatible state of deformation, the virtual work due to the external action, δW_{ext} , is equal to virtual strain energy due to the internal stress, δW_{int}"(**Zienkiweicz,** ١٩٧٧ and ***Dawe,*** ١٩٨٤) thus

$$\delta W_{int} - \delta W_{ext} = 0 \qquad \text{.....(٣-١٠)}$$

By considering a system of volume **v** and surface area ***s*** subjected to body forces $\boldsymbol{b_i}$ and surface tractions $\boldsymbol{t_i}$, the external work done in moving these forces through the virtual displacement **{*u*}** can be expressed as:

$$\delta W_{ext} = \int_v \partial\{u\}^T .\{b\}.dv + \int_v \partial\{u\}^T .\{t\}.ds \qquad \text{..... (٣-١١)}$$

The internal virtual work is given by

$$\delta W_{int} = \int_v \partial\{\varepsilon\}^T .\{\sigma\}.dv \qquad \text{..... (٣-١٢)}$$

Substitution of equation (٣-٦) into equation (٣-١٢) yields:

$$\delta W_{int} = \int_v \partial\{\varepsilon\}^T .\{D\}.\{\varepsilon\}.dv \qquad \text{..... (٣-١٣)}$$

By making use of equations (٣-١١) and (٣-١٣), equation (٣-١٠) may be expressed as:

$$\int_v \partial\{\varepsilon\}^T .\{D\}.\{\varepsilon\}.dv - \int_v \partial\{u\}^T .\{b\}.\, dv - \int_v \partial\{u\}^T .\{t\}.\, ds = \{0\}.. \text{ (٣-١٤)}$$

The above expression represents the equation of static equilibrium for a general body. Therefore, by making use of equations (٣-١) and (٣-٤), the discretized form of equation (٣-١٤) can be written as

$$\partial\{a\}^T\left[\sum_n \int_{v_e}[B]^T\{D\}.[B].dv_e\{a\}_e - \sum_n \int_{v_e}[N]^T\{b\}_e dv_e - \sum_n \int_{s_e}[N]^T\{t\}_e ds_e\right] = \{0\}$$

..... (٣-١٥)

Where: ***n*** is the total number of the elements of the discrete system.

Since the vector of the virtual nodal displacements, $\partial\{a\}^T$, is arbitrary, the following set of algebraic equations may be obtained

$$\{f\} = [K].\{a\} \qquad \text{..... (٣-١٦)}$$

Where: **[*K*]** is the stiffness matrix of the element assemblage and is given by

$$[K] = \sum_n [k] = \sum_n \int_{ve}[B]^T.[D].[B].dv_e \qquad \text{..... (٣-١٧)}$$

Where: **[*k*]** is the element stiffness matrix.

While, ***{f}*** is the element assemblage of external nodal forces vector given by:

$$\{f\} = \sum_n \int_{v_e}[N]^T.\{b\}_e dv_e + \sum_n \int_{s_e}[N]^T\{t\}_e ds_e \qquad \text{..... (٣-١٨)}$$

٣.٣ Concrete representation:

In the field of solid mechanics, the finite element is usually used to find approximate solutions for structures having complicated shapes and loading arrangement. In this study the concrete is represented by a hexahedron brick element having ٨-nodes.

The٨-node isoparametric linear element shown in Fig. (٣-١) is used in this study *(DYANA, ١٩٩٨)*. The element has eight corner nodes with three degrees of freedom u, v and w in the X, Y and Z direction respectively at each node.

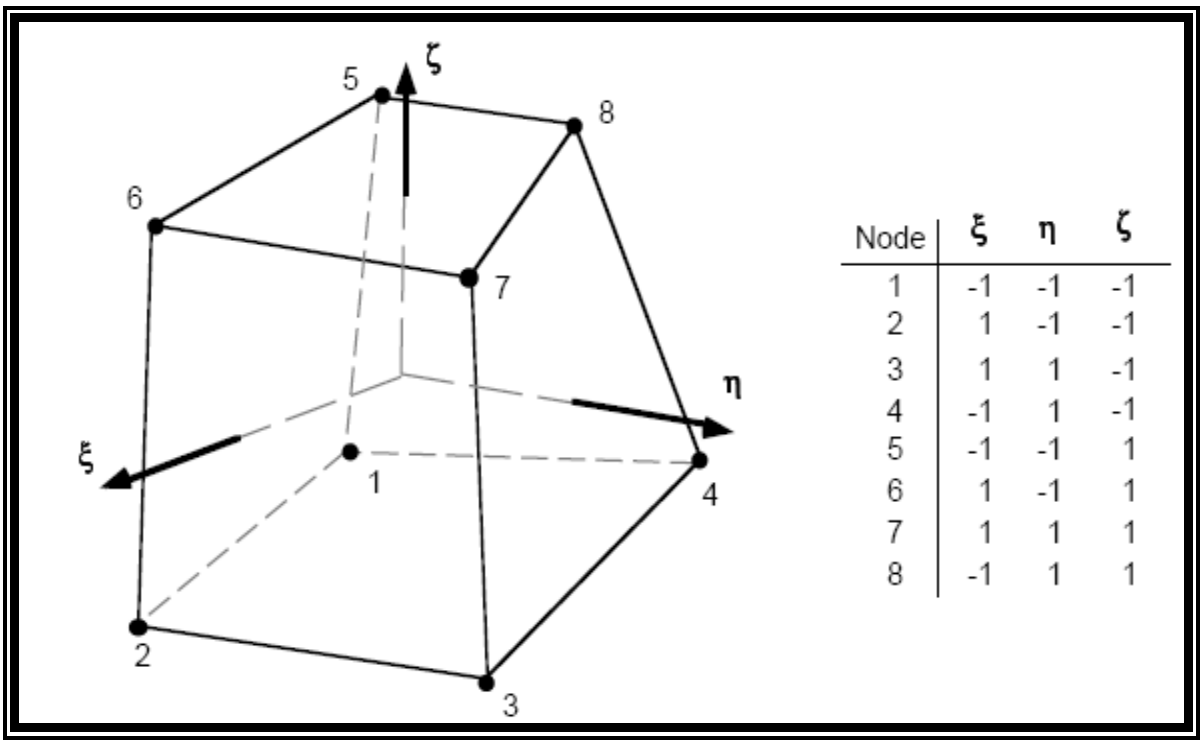

Node	ξ	η	ζ
1	-1	-1	-1
2	1	-1	-1
3	1	1	-1
4	-1	1	-1
5	-1	-1	1
6	1	-1	1
7	1	1	1
8	-1	1	1

Fig. (٣-١): ٨-Node Solid Hexahedron Element *(DYANA, ١٩٩٨)*

٣.٣.١ Shape functions:

The shape functions for the ٨- node brick element are introduced to express the coordinates and displacements of any point within the element in terms of nodal coordinates and displacements. The local coordinates of the ٨-node brick element are placed at the center of the brick and are given in terms of ξ, η, ζ which range from - ١ to +١ as shown in Fig. (٣-١). The isoparametric definition of the brick element is:

$$u(\xi,\eta,\zeta)=\sum_{i=1}^{8} N_i(\xi,\eta,\zeta).u_i$$

$$v(\xi,\eta,\zeta)=\sum_{i=1}^{8} N_i(\xi,\eta,\zeta).v_i \qquad \text{.....(٣.١٩)}$$

$$w(\xi,\eta,\zeta)=\sum_{i=1}^{8} N_i(\xi,\eta,\zeta).w_i$$

Where N_i (ξ, η, ζ) is the shape function at the i-th node and u_i, v_i, w_i are the corresponding nodal displacements. The shape functions for the ٨-node brick element which are adopted to map the element are given in Table ٣.١.

Table (٣-١): Shape Functions for the ٨-Node Hexahedral Element (*Mottoram and Shaw,* ١٩٩٦ and *Muhsen*, ٢٠٠٢)

Location	ξ_i	η_i	ζ_I	$N_I(\xi_i, \eta_I, \zeta_I)$
Corners nodes	±١	±١	±١	٠.١٢٥(١+ξξi)(١+ηηi)(١+ ζζi)

٣.٣.٢ Evaluation of Element Stiffness Matrix:

The function N_i is a function of local coordinates while the strains given in Eq. (٣.٨) are function of global coordinates. Therefore, a relationship between the derivatives in the two coordinate systems must be defined. The total derivatives of a typical shape function N_i are given as:

$$\begin{Bmatrix} \frac{\partial N_i}{\partial \xi} \\ \frac{\partial N_i}{\partial \eta} \\ \frac{\partial N_i}{\partial \zeta} \end{Bmatrix} = \begin{bmatrix} \frac{\partial x}{\partial \xi} & \frac{\partial y}{\partial \xi} & \frac{\partial z}{\partial \xi} \\ \frac{\partial x}{\partial \eta} & \frac{\partial y}{\partial \eta} & \frac{\partial z}{\partial \eta} \\ \frac{\partial x}{\partial \zeta} & \frac{\partial y}{\partial \zeta} & \frac{\partial z}{\partial \zeta} \end{bmatrix} \begin{Bmatrix} \frac{\partial N_i}{\partial x} \\ \frac{\partial N_i}{\partial y} \\ \frac{\partial N_i}{\partial z} \end{Bmatrix} = [J] \begin{Bmatrix} \frac{\partial N_i}{\partial x} \\ \frac{\partial N_i}{\partial y} \\ \frac{\partial N_i}{\partial z} \end{Bmatrix} \qquad \text{..... (٣.٢٠)}$$

Where, [J] is the Jacobian matrix of the global coordinates with respect to the local coordinates. The global coordinates are expressed in terms of the local coordinates (by the same shape functions for displacements) as:

$$x=\sum_{i=1}^{8} N_i x_i \quad ; \quad y=\sum_{i=1}^{8} N_i y_i \quad ; \quad z=\sum_{i=1}^{8} N_i z_i \qquad \text{..... (٣.٢١)}$$

Where: xi, y_i, and z_i, are the nodal coordinates.

By substitution of these relations in Eq.(٣.٢٠) , the Jacobian [J] is constructed in the following form:

$$[J]=\begin{bmatrix} \sum_{i=1}^{8}\frac{\partial Ni}{\partial \xi}.x_i & \sum_{i=1}^{8}\frac{\partial Ni}{\partial \xi}.y_i & \sum_{i=1}^{8}\frac{\partial Ni}{\partial \xi}.z_i \\ \sum_{i=1}^{8}\frac{\partial Ni}{\partial \eta}.x_i & \sum_{i=1}^{8}\frac{\partial Ni}{\partial \eta}.y_i & \sum_{i=1}^{8}\frac{\partial Ni}{\partial \eta}.z_i \\ \sum_{i=1}^{8}\frac{\partial Ni}{\partial \zeta}.x_i & \sum_{i=1}^{8}\frac{\partial Ni}{\partial \zeta}.y_i & \sum_{i=1}^{8}\frac{\partial Ni}{\partial \zeta}.z_i \end{bmatrix} \qquad \text{..... (٣.٢٢)}$$

Then the derivatives of the shape functions with respect to the global coordinates can be found by inverting [J], as:

$$\begin{Bmatrix} \frac{\partial N_i}{\partial x} \\ \frac{\partial N_i}{\partial y} \\ \frac{\partial N_i}{\partial z} \end{Bmatrix} = [J]^{-1} \begin{Bmatrix} \frac{\partial N_i}{\partial \xi} \\ \frac{\partial N_i}{\partial \eta} \\ \frac{\partial N_i}{\partial \zeta} \end{Bmatrix} \qquad \text{..... (٣.٢٣)}$$

The elemental volume in the global coordinates (dx, dy and dz) can be written in terms of local coordinates (dξ, dη, dζ) as

$$dV_e = dx\,dy\,dz = \det[J]\,d\xi\,d\eta\,d\zeta \qquad \text{.....(٣.٢٤)}$$

By substituting Eq (٣.٢٤) into (٣.١٧), the element stiffness matrix may be written in the form

$$[K]^e = \int_{-1}^{+1}\int_{-1}^{+1}\int_{-1}^{+1} [B]^T[D][B]|J|d\xi d\eta d\zeta \qquad \text{..... (٣.٢٥)}$$

The simple integration limits should be noted. These integrals may be evaluated by the numerical integration technique described in Sec. ٣.٦.

٣.٤ Fibre Reinforced Polymer (FRP) Representation:

The ٨-node quadratic-order membrane shell element shown in Fig. (٣-٢) is used in the present work to model the FRP. This element has four corner nodes with three degrees of freedom u, v and w in the X, Y and Z direction respectively at each node.

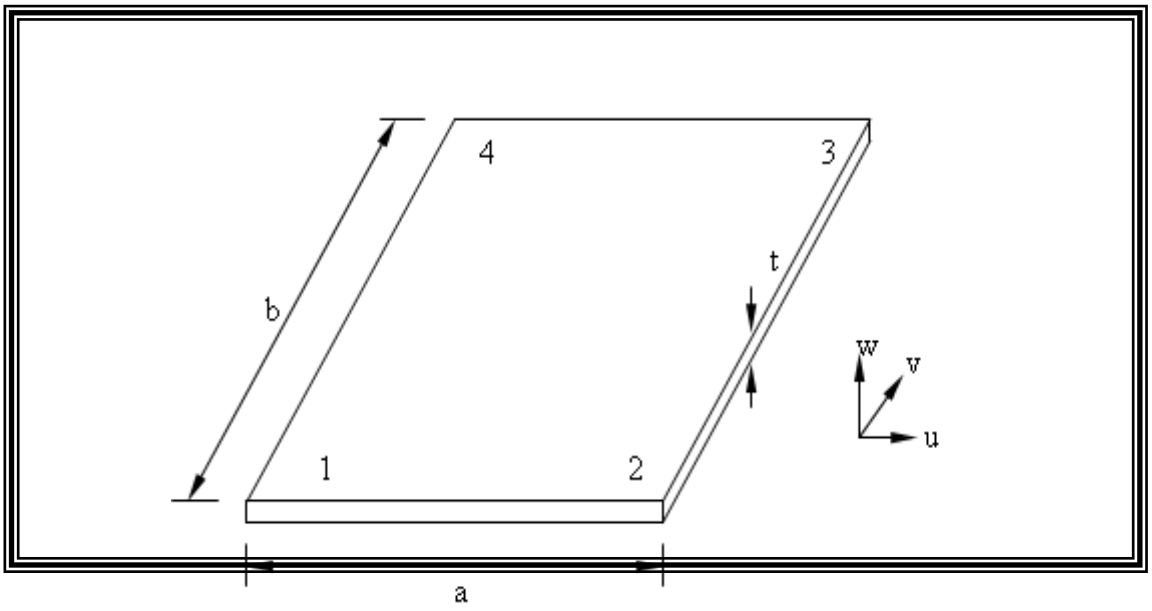

Fig. (٣-٢): Shell Element Geometry and Nodal

٣.٤.١ Shape Function & Evaluation of Stiffness Matrix:

The local coordinates of the ٨-node shell element are placed at the center of the shell and are given in terms of ξ, η, ζ which range from - ١ to + ١ as shown in Fig. (٣-٣). The isoparametric definition of the shell element

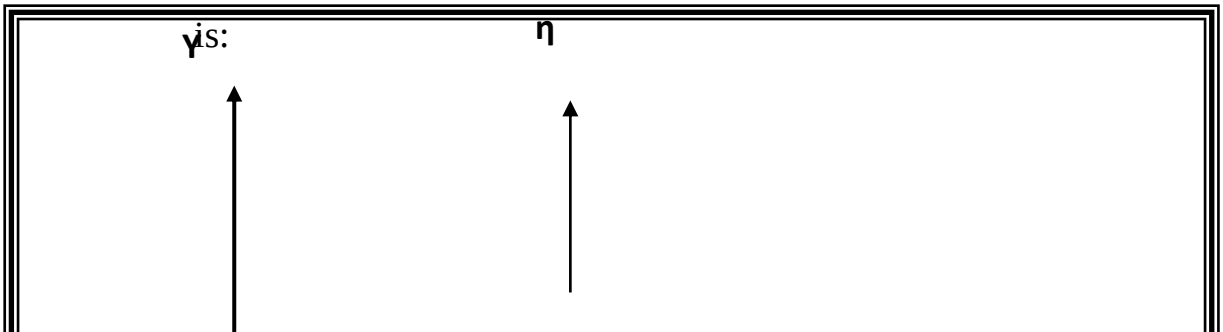

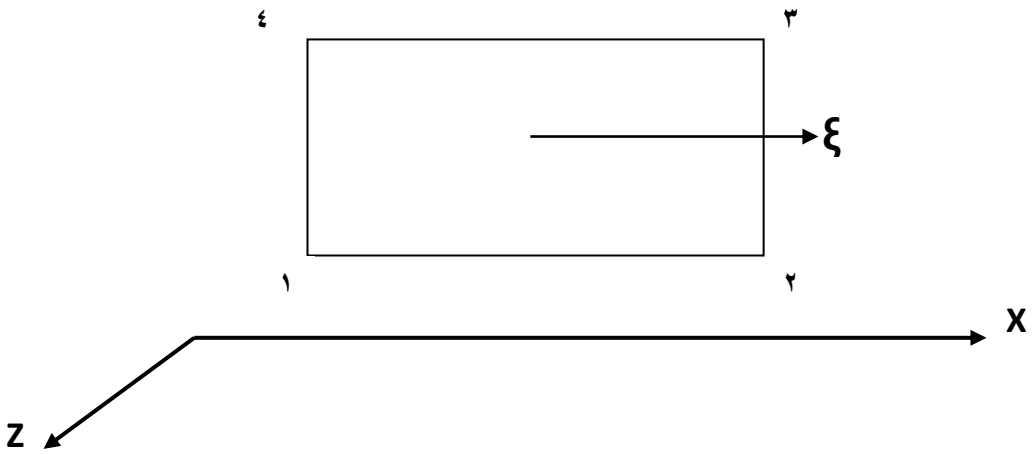

Fig. (٣-٤): Element Local Coordinate System and Node

$$u(\xi,\eta,\zeta)=\sum_{i=1}^{4} N_i(\xi,\eta,\zeta).u_i$$

$$v(\xi,\eta,\zeta)=\sum_{i=1}^{4} N_i(\xi,\eta,\zeta).v_i \qquad \text{..... (٣.٢٦)}$$

$$w(\xi,\eta,\zeta)=\sum_{i=1}^{4} N_i(\xi,\eta,\zeta).w_i$$

The shape functions are the follows:

$$N_1=\frac{1}{4}(1-\eta)(1-\xi)$$

$$N_2=\frac{1}{4}(1+\eta)(1-\xi)$$

$$N_3=\frac{1}{4}(1+\eta)(1+\xi) \qquad \text{..... (٣.٢٧)}$$

$$N_4=\frac{1}{4}(1-\eta)(1+\xi)$$

The global coordinates of any point, within the element, in term of the natural coordinates are:

$$x=\sum_{i=1}^{4} N_i x_i$$

$$y=\sum_{i=1}^{4} N_i y_i \qquad \text{.....}$$

$$z=\sum_{i=1}^{4} N_i z_i$$

(٣.٢٨)

The strain-displacement relationship is as follows:

$$\begin{Bmatrix} \varepsilon_x \\ \varepsilon_y \\ \varepsilon_z \end{Bmatrix} = \begin{Bmatrix} \dfrac{\partial u}{\partial x} \\ \dfrac{\partial v}{\partial y} \\ \dfrac{\partial u}{\partial y} + \dfrac{\partial v}{\partial x} \end{Bmatrix} \qquad \text{..... (٣.٢٩)}$$

The development of the stiffness characteristic of the shell element follows essentially the same procedure as that for the brick element, i. e.

$$[k]^e = \int_{-1}^{+1}\int_{-1}^{+1} [B]^T [D][B]|J|.d\xi.d\eta \qquad \text{.....}$$

(٣.٣٠)

٣.٥ Reinforcement Idealization

In developing a finite element model for reinforced concrete members, at least three alternative representations of reinforcement have been used:

a) Discrete Representation.

b) Distribution Representation.

c) Embedded Representation.

This study adopted the distribution (smeared) representation which is shown in Fig.(٣-٤), the steel is assumed to be distributed in the concrete element with a particular orientation angleθ. In the composite concrete, reinforcement constitutive relation is used in this case [*ASCE (١٩٨١); Chen (١٩٨٢)*]. To derive such a relation, perfect bond is usually assumed between the concrete and steel. In Ansys programme SOLID ٦٥ allows the presence of four different materials within each element; one matrix (e.g. concrete) and a maximum of three independent reinforcing materials. The concrete material is capable of directional integration point cracking and crushing besides

incorporating plastic and creep behaviour. The reinforcement (which also incorporates creep and plasticity) has uniaxial stiffness only and is assumed to be smeared throughout the element. Directional orientation is accomplished through user specified angles. The stress-strain matrix [D]used for this element and anther deformations are found in **Appendix [A]**.

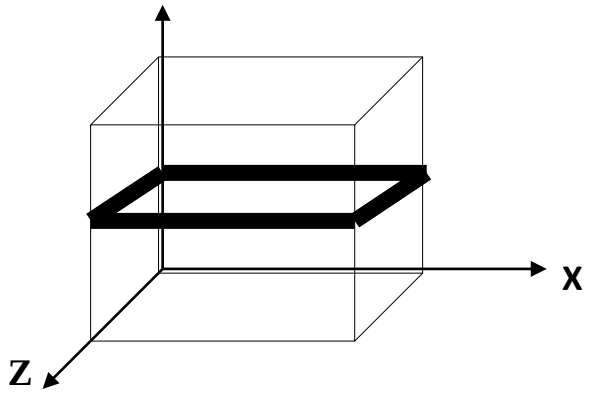

Fig. (٣- ٤): Representation of distributed reinforcement

٣.٦ Numerical integration:

The element stiffness matrix cannot be evaluated analytically and hence the use of numerical integration techniques makes the isoparametric element practical. The Gauss quadrate is a numerical integration method that allows the sampling points to be chosen such that the best possible accuracy may be obtained where the sampling points and weights are based on Gauss-Legender polynomials. However this type of numerical integration is referred to as Gauss- Legender quaderature scheme. In this scheme the summation is used in lieu of the integration in the evaluation process of the function to be integrated.

For isoparametric hexahedral brick element, the element stiffness Eq.(٣.٢٥) can be expressed in the form (**Bath**, ١٩٩٦)

$$\mathbf{I} = \int_{-1}^{+1}\int_{-1}^{+1}\int_{-1}^{+1} \mathbf{f}(\xi,\eta,\zeta)\mathbf{d}\xi\mathbf{d}\eta\mathbf{d}\zeta \qquad \text{..... (٣.٣١)}$$

This can be calculated numerically as:

$$I = \sum_{i=1}^{n}\sum_{j=1}^{n}\sum_{k=1}^{n} W_i W_j W_k F(\xi_i, \eta_j, \zeta_k) \qquad \text{..... (٣.٣٢)}$$

In this study the integration used is the ٨ point (٢x٢x٢) integration rule for concrete, Fig. (٣-٥). The distribution of sampling points over the volume of the ٨-node brick element and their weighting factors are given in Table (٣-٢).

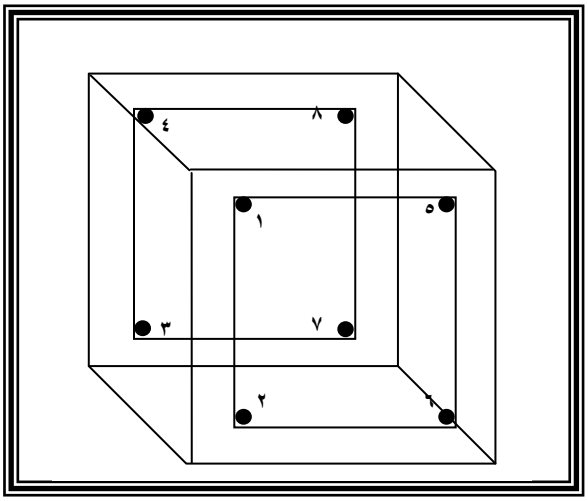

Fig. (٣-٥): Distribution of Integration Point (ANSYS, ١٩٩٨)

Table (٣-٢): Sampling Points and Associated Weights for the (٢x٢x٢) Rule

(Mottoram and Shaw, ١٩٩٦)

Number of Sampling Points	Gauss point			Weight
	ξ	η	ζ	
١,٢,٣,٤,٥,٦,٧,٨	±٠.٥٧٧٣٤	±٠.٥٧٧٣٤	±٠.٥٧٧٣٤	١.٠

In determining the stiffness matrix of a two-dimensional isoparametric quadrilateral, can be concerned with evaluating definite integrals of the form:

$$I = \int_{-1}^{+1}\int_{-1}^{+1} F(\xi,\eta)\,d\xi\,d\eta \qquad \text{..... (٣.٣٣)}$$

The integral of a function F of ξ and η with respect to ξ and η in the rang - ١ to + ١. This can be achieved numerically by first evaluating the inner integral with ξ kept constant and then evaluating the outer integral. Thus:

$$I = \int_{-1}^{+1}\left(\int_{-1}^{+1} F(\xi,\eta)d\xi\right).d\zeta = \int_{-1}^{+1}\left(\sum_{j=1}^{n_j} W_j(\xi,\eta)\right).d\zeta \qquad \text{..... (٣.٣٤)}$$

$$I = \sum_{j=1}^{n_j} W_j\left(\sum W_j F\left(\xi_j,\eta_j\right)\right) = \sum_{j=1}^{n_j}\sum_{j=1}^{n_j} W_i W_j F\left(\xi_j,\eta_j\right)$$

In this expression, it is assumed that there is n_j sampling points in the ξ direction and n_i in the η direction; there are consequently a total of n_ix n_j sampling points. Usually the same number of sampling points are used in each direction, thus n_i= n_j=n. In Fig. (٣- ٦) the position of the Gauss points are shown on the parent element for n= ٢, that is for ٢x ٢ integration rules.

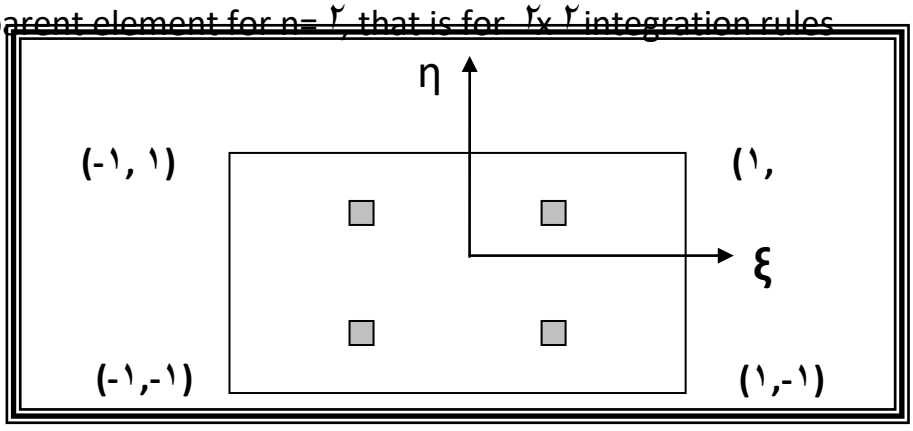

١ ٢

Fig. (٣-٦): Distribution of Integration Point *(ANSYS, ١٩٩٧)* Over the ٤-Node Shell Element

Table (٣-٣): Sampling Points and Associated Weights for the (٢x٢) Rule *(Mottoram, ١٩٩٦)*

Number of	Gauss point	Weight

Sampling Points	ξ	η	
١,٢,٣,٤	±٠.٥٧٧٣٤	±٠.٥٧٧٣٤	١.٠

The standard ١-D numerical integration formulas which are used in the element library are of the form:

$$\int_{-1}^{+1} f(\xi).d\xi = \sum_{j=1}^{n} W_j f(\xi_j) \qquad \text{..... (٣.٣٥)}$$

Table (٣-٤): Sampling Points and Associated Weights *(Mottoram, ١٩٩٦)*

Number of Sampling Points	Gauss point	Weight
	ξ	
١,٢	±٠.٥٧٧٣٤	١.٠

٣.٧ Nonlinear Solution Techniques:

Concrete elements, if loaded beyond their elastic limit, exhibit a nonlinear deformation response. This nonlinearity is caused by material nonlinearities. In other cases, nonlinearity may be due to geometric nonlinearities. In nonlinear problems sophisticated solution strategies have to be employed. For a nonlinear system the equilibrium equations can be written in the form:

$$\{r(\{a\})\} = \{p(\{a\})\} - \{f\} \qquad \text{..... (٣.٣٦)}$$

Where, $\{r(\{a\})\}$, is the out-of-balance residual force vector, $\{a\}$ is the vector of nodal displacements, $\{f\}$ is the external load vector and $\{p(\{a\})\}$ is the internal nodal load vector given by:

$$\{p(\{a\})\} = \int_v [B]^T . \{\sigma\} . dV \qquad \text{..... (٣.٣٧)}$$

Solution of the equilibrium occurs at balance between external and internal loads vector Eq.(٣.٣٦), that is when residual forces are zero. The solution of nonlinear problems is attempted by one of the three techniques. These are:

١. Iterative techniques

٢. Incremental techniques, and

٣. combined incremental-iterative techniques.

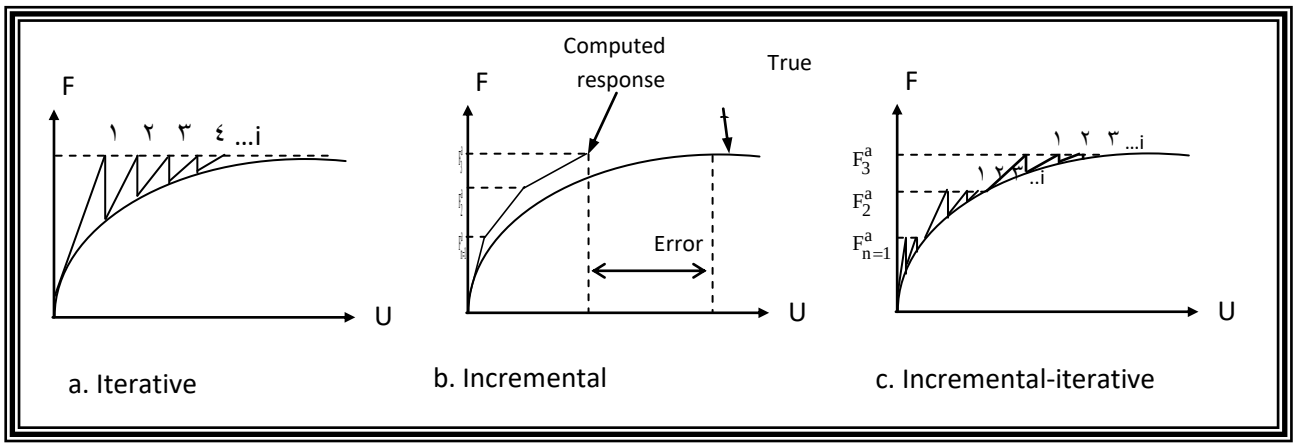

Fig. (٣-٧) Basic Techniques for Solving Nonlinear Equations (Zienkiweicz, ١٩٧٧)

٣.٧.١ Iterative Techniques:

In the iterative techniques, Fig.(٣-٧a), the full load is applied in one increment. An initial estimate of the vector of unknown nodal displacements $\{a\}_i$ is obtained. Iterative corrections are performed in order to get a progressively improved solution $\{a\}_١$, $\{a\}_٢$**.** This can be achieved as follows. The stresses corresponding to the predicted initial solution are calculated using the relevant constitutive relations. These stresses are used to calculate the internal force vector {p({a})}, and then the out of balance forces are successively

applied to the structure. The iteration correction continues until the out of balance forces becomes negligible. The total displacement can be calculated by summing the displacements from each of the iterations. The iterative technique cannot be used to predict the entire response of the structure, since it fails in predicting information about the intermediate stages.

3.7.2 Incremental Techniques:

The basis of the incremental procedure, Fig.(٣.٧b), is the subdivision of the load into small partial loads (increments). One increment of load is applied at a time, whereas during the application of each load increment, the structure is assumed to respond linearly. The basic disadvantage of this method is that a real estimate of the solution accuracy is not possible, since equilibrium is not satisfied at any given load level. So, for stability requirements, it is necessary to use small load increments, which in turns will increase the computation cost if compared with other techniques.

3.7.3 Incremental – Iterative Techniques:

In this type of techniques a combination of the incremental and iterative techniques are utilized, as shown in Fig. (٣.٧c), the load is applied as a series of increments. At each increment, iterative solution is carried out to find the real response of the structure. The Newton-Raphson methods are usually used as incremental-iterative technique for solving nonlinear equations. These methods can be classified as:

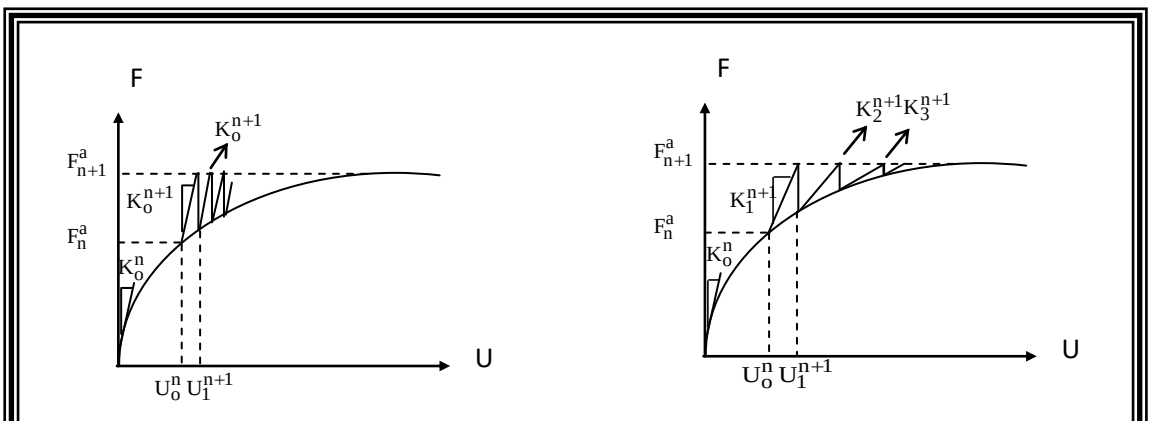

(a) **(b)**

(c)

Fig.(٣-٨): Incremental-IterativePprocedures: (a) Initial Stiffness Method, (b) Standard N-R. Method, (c) Modified N-R. Method.

١. The initial-stiffness method

In which the stiffness matrix is formed and decomposed only once at the beginning of the analysis, Fig.(٣-٨a). For this procedure the computation cost per iteration is significantly reduced. In the case of strong nonlinearities, the method often fails to converge even if an acceleration scheme is used.

٢. Full Newton-Raphson method

In which the stiffness matrix is updated at each iteration and a new system of equations is solved for each iteration. A disadvantage of this procedure is that a large amount of computational effort may be required to form and discompose the stiffness matrix, Fig.(٣-٨b).

٣. The modified Newton-Raphson method, [KT١]

In this method the stiffness matrix is updated only once for each first increment of loading. This method requires more steps for convergence, but each step is done quickly, Fig.(٣-٨c).

٤. The modified Newton-Raphson method, [KT٢]

In this method the stiffness matrix is only formulated at the second iteration of each increment of loading.

These methods ٣, ٤ are generally more economically than the full Newton Raphson method since they involve fewer stiffness matrix reformulations. However, the convergence is slower and a large number of iterations are required to achieve converged solution. This is particularly true for an increment of loading at which a sudden softening may occur due to cracking, yielding or substantial nonlinear behavior of concrete in compression. In order to make the modified methods more effective at loading stages at which slow convergence occurs, the stiffness matrix may be updated more than once within the increment. The ANSYS programme incorporates a modified Newton-Raphson method. The KT٢ is adopted in this study.

٣.٨ Nonlinear Solution for ANSYS:

In nonlinear analysis, the total load applied to a finite element model is divided into a series of load increments called load steps. At the completion of each incremental solution, the stiffness matrix of the model is adjusted to reflect nonlinear changes in structural stiffness before proceeding to the next load increment. The ANSYS program (*ANSYS* ١٩٩٨) uses Newton-Raphson equilibrium iterations for updating the model stiffness.Newton-Raphson equilibrium iterations

provide convergence at the end of each load increment within tolerance limits. Figure (٣-٩) shows the use of the Newton-Raphson approach in a single degree of freedom nonlinear analysis.

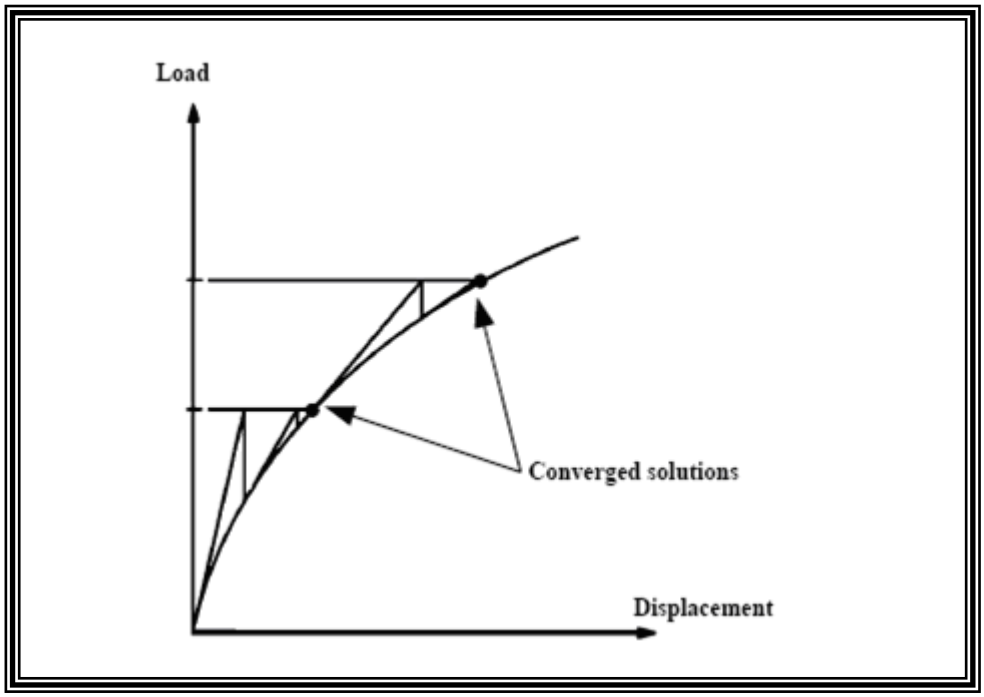

Fig. (٣-٩): Newton-Raphson Iterative Solution (٢ Load Increments) (*ANSYS*, ١٩٩٨)

Prior to each solution, the Newton-Raphson approach assesses the out-of-balance load vector, which is the difference between the restoring forces (the loads corresponding to the element stresses) and the applied loads. Subsequently, the program carries out a linear solution, using the out-of-balance loads, and checks for convergence. If convergence criteria are not satisfied, the out-of-balance load vector is re-evaluated, the stiffness matrix is updated, and a new solution is attained. This iterative procedure continues until the problem converges (***ANSYS,*** ١٩٩٨).

٣.١٠ Convergence Criteria:

For every incremental load the iteration continues until a convergence is achieved. The convergence criteria for the nonlinear analysis of structural problems can be generally classified into:

١. force criteria

٢. displacement criteria

In this study, for the reinforced concrete solid elements, convergence criteria were based on force and displacement, and the convergence tolerance limits were initially selected by the ANSYS program. It was found that convergence of solutions for the models was difficult to achieve due to the nonlinear behavior of reinforced concrete.

In the displacement criterion, the incremental displacements at iteration i and the total displacement are determined. The solution is considered to be converged when the norms of the incremental displacements are within a given tolerance of the norm of the total displacements; the (Euclidean norm) is used and takes the form:

$$\left\|\{\Delta U_i\}\right\| = \left(\sum \Delta U_i^2\right)^{0.5} \le T_n \left(\sum U_i^2\right)^{0.5} \quad \text{..... (٣.٣٨)}$$

Where: U may equal u, v. w

The force criteria the norm of the residual forces at the end of each iteration are checked against the norm of the current applied forces as:

$$\left\|\{R\}\right\| = \left(\sum R_i^2\right)^{0.5} \le T_n \left(\sum F_i^{a\,2}\right)^{0.5} \quad \text{..... (٣.٣٩)}$$

Where: {R} is residual load vector

$$\{R\} = \{F^a\} - \{F^{nr}\} \qquad \text{..... (٣.٤٠)}$$

Where: $\{F^a\}$ =vector of applied loads

$\{F^{nr}\}$ =internal load vector

In this study, the tolerance T_n is taken equal to ٠.١%.

٣.١١ Analysis Termination Criteria:

In the physical test under force control, collapse of a structure takes place when no further loading can be sustained. This is usually indicated in the numerical tests by successively increasing iterative displacements and a continuous growth in the dissipated energy. Hence, the convergence of the iterative process cannot be achieved. A maximum number of iterations for each increment are specified to stop the nonlinear solution if the convergence limit has not been achieved for this study. It has been observed that a maximum number of about ٥٠ iteration is generally sufficient predicted the solution divergence or failure. This maximum number of iterations depends on the type of the problem, extent of nonlinearities, and on the specified tolerance (*Hinto and Owen, ١٩٨٤*). In this study the maximum number of iteration is ٥٠.

٣.١٢ ANSYS Computer Program:

ANSYS (ANalysis SYStem) (version ٥.٤) is a powerful and impressive engineering tool that may be used to solve a variety of problems.

ANSYS is a comprehensive general-purpose finite element computer program that contains over ١٠٠,٠٠٠ lines of codes with about ١٦٥ different elements conducted in the program. ANSYS is capable of performing static

(linear and nonlinear problems), dynamic, heat transfer, and fluid flow and electromagnetism analyses. It has been a leading finite element analyses program for well over ٢٠ years. The current version of ANSYS has a completely new look, with multiple windows incorporating Graphical User Interface (GUI), Pull-down menus, dialog boxes, and a tool bar.

In order to use ANSYS or any other "canned" finite element analyses computer program intelligently, it is imperative that one first fully understands the underlying basic concepts and limitations of the finite element method.

At this point it is worth noting that:

١. There are three processors that have been frequently used: (a) the pre-processor (PREP ٧), (b) the processor (SOLUTION) and (c) the general postprocessor (POSTI).

٢. The commends of the pre-processor (PREP٧) contains that you need to use to build a model:

- define element types and options
- define element real constants
- define material properties
- create model geometry
- define meshing controls
- mesh the object created

٣. The commands of the solution processor (SOLUTION) that allow applying boundary conditions and loads. The solution processor also solves for the nodal solutions and calculates other elemental information.

٤. The commands of the general postprocessor (POST١) contain that allow to list and display results of an analysis:

- read results data from results file
- read element results data
- plot results
- list results

٥. ANSYS writes and reads many files during a typical analysis.

٦. ANSYS program also offers the capability to select information about a portion of the model, such as certain nodes, elements, lines, areas and volumes, for further processing.

٧. ANSYS program provides numerous features that allow enhancing the visual presented information. Some examples of the graphics capabilities of ANSYS are deformed shapes, result contours, sectional views and animation.

The main objective of the program is to analyze reinforced concrete members strengthened with CFRP under general three-dimensional states of loading up to failure.

In the present study, the program has been preceded using a personal computer. The program has been implemented on Pentium IV, ١٧٠٠MHz IBM compatible computer with ٢٥٦ megabyte RAM.

The modified program is suitable for analyzing reinforced concrete beams strengthened with CFRP under general states of loading.

CHAPTER FOUR

MODELING OF MATERIAL PROPERTIES

٤-١: Introduction

The modeling of material properties is one of the most important aspects of any realistic non-linear finite element analysis of reinforced concrete members. Since the concrete, CFRP (Carbon Fiber Reinforced Polymer) plate and the reinforcing steel have very different material properties, the behavior of the composite, reinforced concrete, is usually simulated by considering the constitutive relations of the constituents independently. Full interaction between materials has been assumed to exist throughout the present work. This chapter outlines the constitutive models for the concrete, CFRP plate and the steel reinforcement used in the present study. Several pre-processors of ANSYS are available for this purpose. ANSYS offers various solid and shell elements which can be used to model concrete and CFRP plate respectively. The choice depends on type and geometry of the structure/member. Eight-node (solid ٦٥) and four-node (membrane shell-٤١) elements are used to model concrete and CFRP plate respectively in the present work.

٤-٢: Modeling of concrete

In Fig.(٤-١) a load versus midpoint deflection plot is drawn. Three dotted ellipses encircle A) the concrete cracking load, B) the steel yield load C) Concrete begins to crush *(Nordin, ٢٠٠٣).*

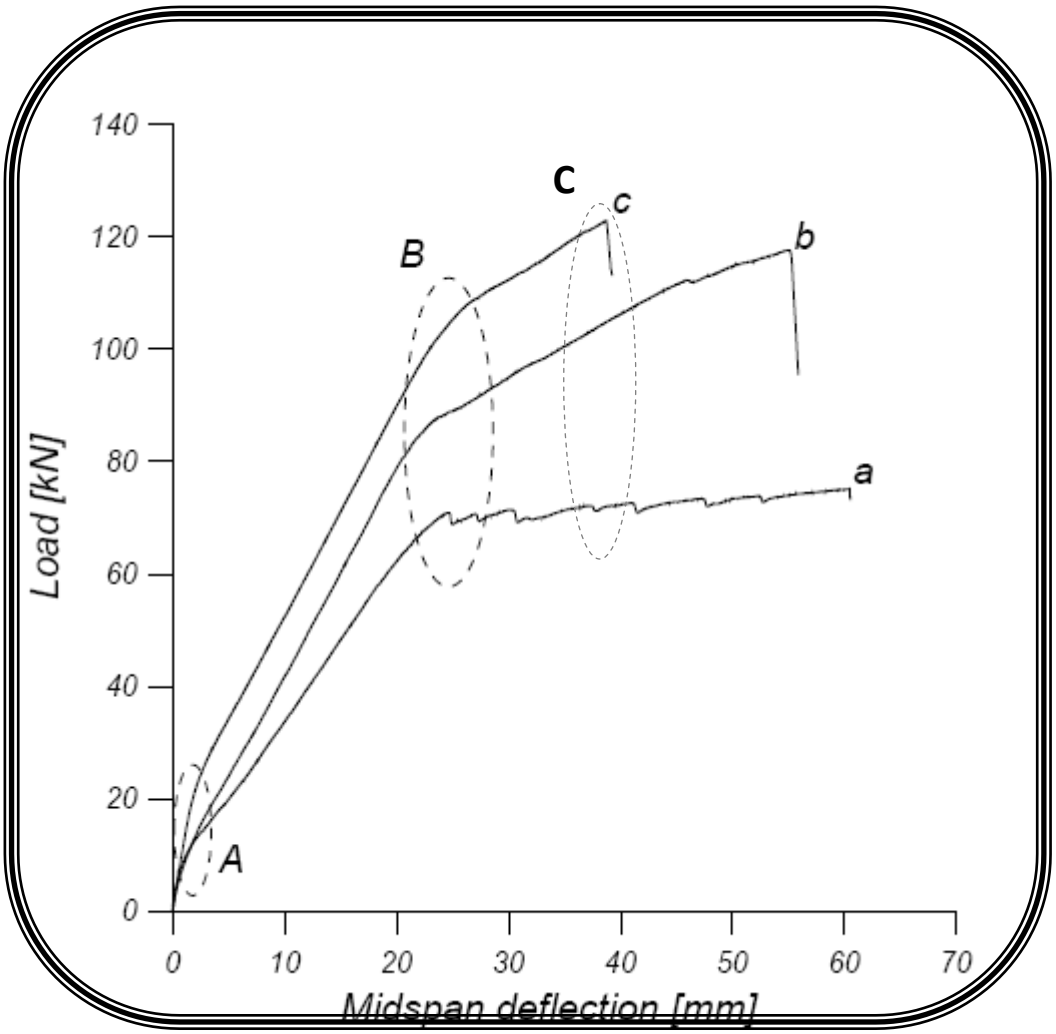

Fig.(٤-١): Beams Strengthened with CFRP, (a)Unstrengthened,

The nonlinear response of load-deflection curve is mainly caused by cracking of concrete, yielding of steel, and the nonlinear stress-strain behavior of concrete in compression. Other time-independent nonlinearities arise from the nonlinear action of the individual constituents of the CFRP (Carbon Fiber Reinforced Polymer)-concrete beam, e.g. bond slip between the CFRP and concrete. Creep, shrinkage and temperature change, the time dependent effects also contribute to the nonlinear response. In this chapter, only the time independent material nonlinearities will be considered in the mathematical modeling of the materials.

The response of concrete under uniaxial and muiltiaxial loading states is described in the following sections.

٤-٣: Mechanical Behavior of Concrete

Concrete is an artificial stone obtained by mixing aggregates, cement and water and allowing the product to cure for hardening. It is mostly used as structural material. The strength of concrete depends upon the ingredients quantities and the manner in which they are mixed, compacted and cured. It can produce concrete of different grades for various purposes by suitably adjusting the proportion of cement, aggregate and water.

Concrete after hardening contains a large number of microcracks at interface between aggregate and mortar, even before any loads have been applied *(Chen, ١٩٨٢).* The gradual growth of these microcracks under additional load contributes to the nonlinear behavior of concrete. Many of these microcracks are caused by segregation, shrinkage or thermal expansion in the mortar. Some microcracks may develop during loading due to the difference in stiffness between aggregate and mortar *(Chen, ١٩٨٢).* Concrete may be subjected to uniaxial, biaxial and traixial stresses. The behavior of concrete under these states of stresses is described below.

٤-٣-١: Uniaxial Stress Behavior of Concrete

٤-٣-١-١: Uniaxial Compression Behavior

A typical uniaxial compression stress-strain curve is shown in Fig.(٤-٢). Up to a stress level of about ٣٠ percent of its uniaxial compressive strength, (f_c'), concrete behaves as a linear elastic material *(Chen, ١٩٨٢).* For stress levels ranging between (٠.٣ f_c') and (٠.٥ f_c') the stress- strain start to show a

slight non-linearity. A gradual increase in the curvature of the stress-strain curve occurs up to about (٠.٧٥ f_c'). For compressive stresses above this value, the rate of crack propagation increases rapidly and the stress-strain curve bends sharply until the peck stress level is reached. Beyond the peck stress, concrete exhibits a strain-softening response, which is expressed by the descending portion of the curve *(Chen, ١٩٨٢).*

The modulus of elasticity of concrete depends on its compressive strength. The modulus of elasticity of concrete E_c, may be estimated from the ACI / Building Code ٣١٨ M-٠٢ as:

$$E_c = W_c^{1.5} (0.043) f_c'^{0.5} \quad \text{(MPa)} \qquad \text{...(٤-١)}$$

where W_c is the unit weight of concrete in kg/m^3. For normal concrete, equation (٤- ١) will be reduced to

$$E_c = 4700 \sqrt{f_c'} \quad \text{(MPa)} \qquad \text{...(٤-٢)}$$

Poisson ratio (υ), which is defined as the ratio of lateral strain to the principal compressive strain has been observed in experiments to be constant up to a stress level of ($0.8 f_c'$) and ranges between ٠.١٥ and ٠.٢٢ *(Chen, ١٩٨٢).*

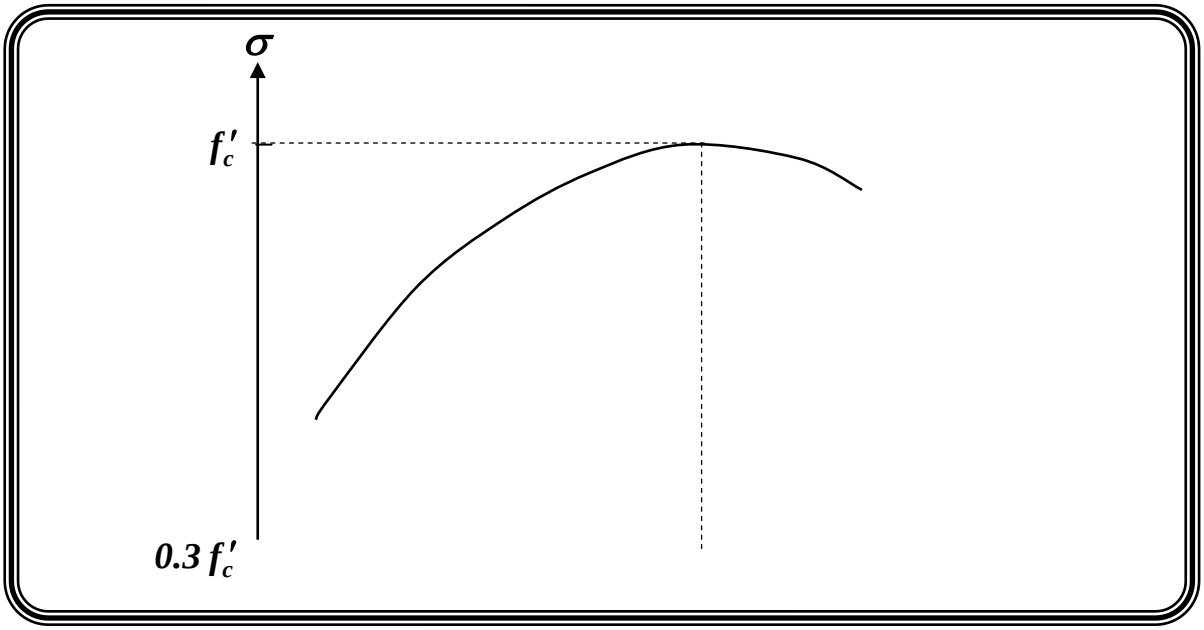

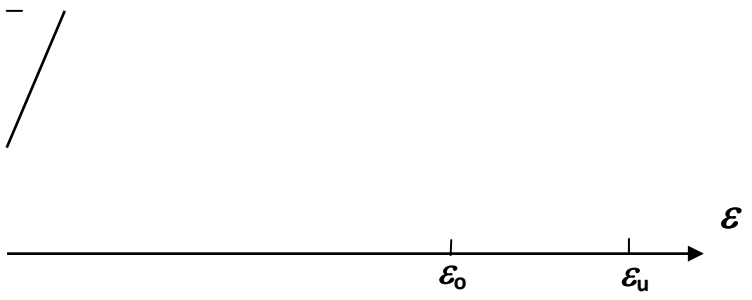

Fig.(٤-٢):Typical Uniaxial Stress-Strain Curve for Concrete in Compression.

٤-٣-١-٢: Uniaxial Tensile Behavior

The stress-strain curve for concrete under uniaxial tension is as shown in Fig.(٤-٣) *(Chen, ١٩٨٢).* It is nearly linear up to about ٠.٦ f_t (cracking stress). Beyond this level, bond micro-cracks start to grow and non-linearity of the curve is started to increase as the stress level increases until peak stress is reached.

As a result of the difficulties in implementing the direct testing of concrete in pure axial tension, indirect tests are alternatively used to determine the concrete cracking strength. These tests are the modulus of rupture f_r, which is determined from bending test, and the splitting strength f_{sp}, which is determined by splitting a concrete cylinder with a line load. Also the double punching test is another indirect test method for determining concrete cracking strength *(Chen, ١٩٨٢).*

The splitting tensile strength and modulus of rupture of concrete are determined by using the following equations respectively.

$$f_{sp} = 0.65 \sqrt{f'_c} \quad \textbf{(MPa)} \qquad \text{...(٤-٣)}$$

$$f_r = 0.7\sqrt{f'_c} \quad \text{(MPa)} \qquad \ldots(٤\text{-}٤)$$

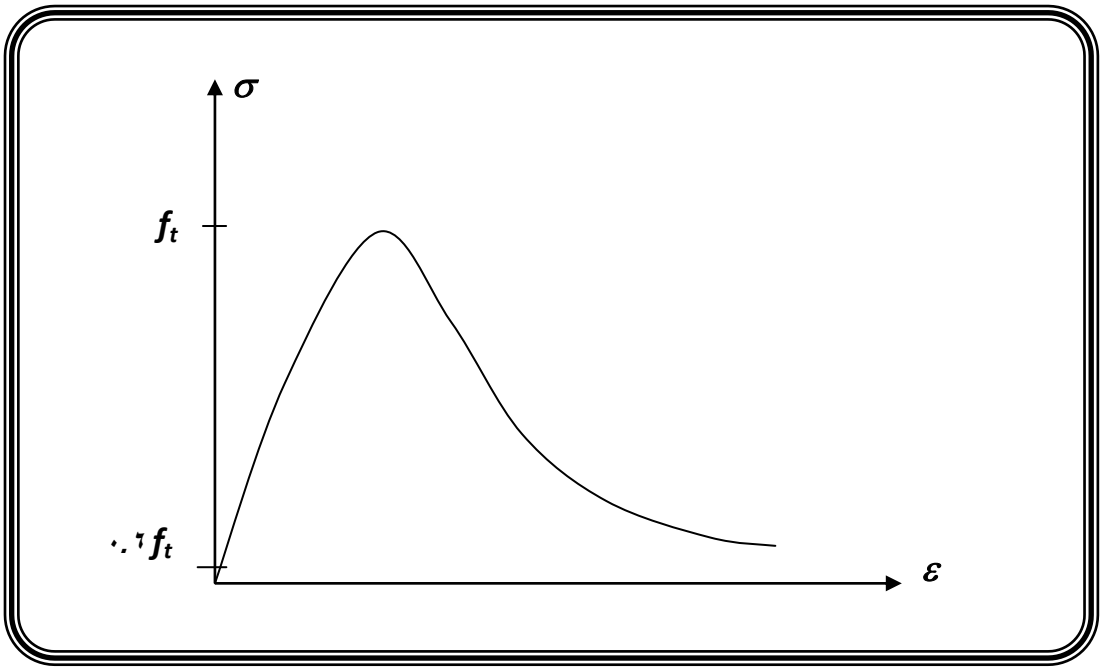

Fig.(٤-٣): Typical Uniaxial Stress-Strain Curve for Concrete in Tension

٤-٣-١-٣: Multiaxial Behavior of Concrete

The behavior of concrete under multiaxial stress condition is very complex if compared with that under uniaxial stress condition. A typical biaxial strength envelope is shown in Fig.(٤-٤.a). When subjected to biaxial compressive, concrete has an increased up to about ($1.25\,f_c'$) for a principal stress ratio of ٠.٥ and up to about ($1.16\,f_c'$) for principal stress ratio of ١.٠. Under biaxial tension-compression, the tensile strength decrease almost linearly as applied compression

increase. For biaxial tension states, concrete exhibits nearly constant tensile strength *(Kupfer et al., ١٩٦٩).*

Under triaxial compressive stress, concrete exhibits strength which increases with the increasing confining pressures. Experimental studies indicate that the three-dimensional failure envelope is a function of the three principal stresses, Fig.(٤-٤.b). This failure surface can be represented by three-stress invariants. These invariants are the first invariant of the stress tensor (I_1), and the second and the third invariant of the stress deviatoric tensor (J_2) and (J_3) *(Chen, ١٩٨٢).*

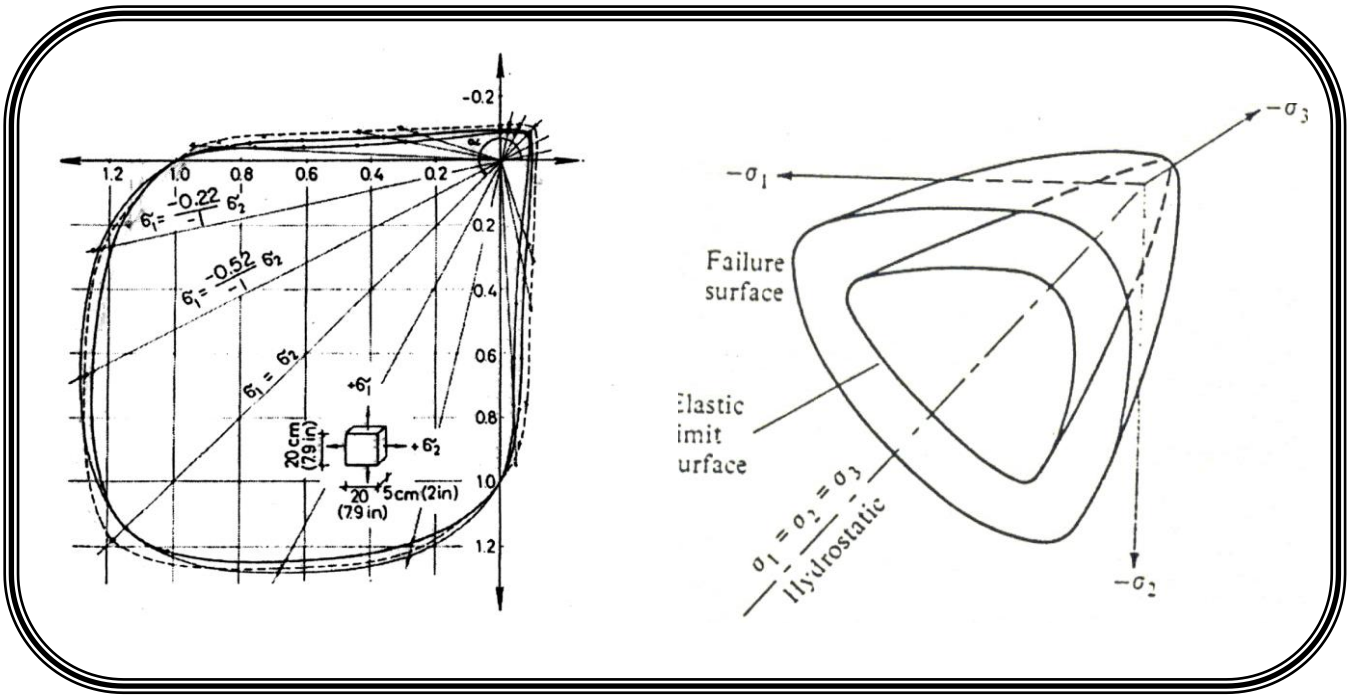

a. biaxial b. triaxial

Fig.(٤-٤): Typical Multiaxial Stress-Strain Curves for Concrete *(Kupfer, ١٩٦٩* and *Chen, ١٩٨٢)*

٤-٤: Concrete Material Modeling

There are many constitutive models which have been developed to predict the response of reinforced concrete under various stress states. Some of the main constitutive models are the elasticity based and plasticity based models.

The elasticity-based models can simulate the concrete as a linear elastic or nonlinear elastic material. The linear elasticity model has been used to study the nonlinear response of reinforced concrete beams, panels, and shells in which the main nonlinearity is introduced by the cracking of the concrete *(Chen, ١٩٨٢).*

The linear elastic models for concrete in compression can be significantly improved by assuming a nonlinear elastic stress-strain relationship. In recent years, there have been a large number of nonlinear elastic stress-strain relationships proposed for concrete materials *(Yasuhiro and Chen, ١٩٨٧).* They can be generally classified in to:

١. The total stress-strain formulation in the form of secant stiffness relation.

٢. The incremental stress-strain formulation in the form of tangential stiffness formulation (hypo elastic model).

Since concrete is an irreversible and load path dependent material, it is not appropriate to use the elasticity based models (except the hypo elastic model) for structural analysis involving un loading behavior. The hypo elastic model can incorporate the loading history effect including the unloading behavior of the structure *(William and Warnke, ١٩٧٥).*

In the plasticity based models, concrete can be described as an elastic perfectly plastic material or elastic-work hardening material. When a material under compression load does admit changes of permanent strain under constant stress, this material is called perfect plastic. If does not, this material is called a work-hardening material *(Chen, ١٩٨٢).* These models have been used extensively in recent years to describe the behavior of concrete. On the other side, an important characteristic of concrete that cannot be adequately treated by the classical theory of plasticity is the full stress- softening effect *(Chen, ١٩٨٢).*

Arnesen et al., ١٩٨٠ have stated that classical elasticity and plasticity theories can be sufficiently accurate for many applications; this is particularly true when the concrete structure fails in cracking of concrete and yielding of reinforcement bars. Plasticity theory for concrete is sufficiently accurate for uniaxial stress state and two-dimensional state of stress with proportional loading. But for complex loading histories and three-dimensional state of stress, it has been shown that these theories are inadequate.

In the present study, concrete behavior is considered to be elasto-plastic followed by perfect plastic brittle fracture model. This model should include the following:

١. Stress-strain relationship.

٢. Failure criterion to simulate cracking and crushing types of fractures.

٣. Cracking modeling.

٤. Crushing modeling.

٤-٤-١: Stress-Strain Relationship

Development of a model for the behavior of concrete is a challenging task. Concrete is a quasi brittle material and has different behavior in

compression and tension. Fig.(٤-٥)shows a typical stress-strain curve for normal weight concrete (*Bangash,* ١٩٨٩).

In compression, the stress-strain curve for concrete is linearly elastic up to about ٣٠ percent of the maximum compressive strength. Above this point, the stress increases gradually up to the maximum compressive strength. After it reaches the maximum compressive strength σ_{cu}, the curve descends into a softening region, and eventually crushing failure occurs at an ultimate strain ε_{cu}. In tension, the stress-strain curve for concrete is approximately linearly elastic up to the maximum tensile strength. After this point, the concrete cracks and the strength decreases gradually to zero (*Bangash,* ١٩٨٩).

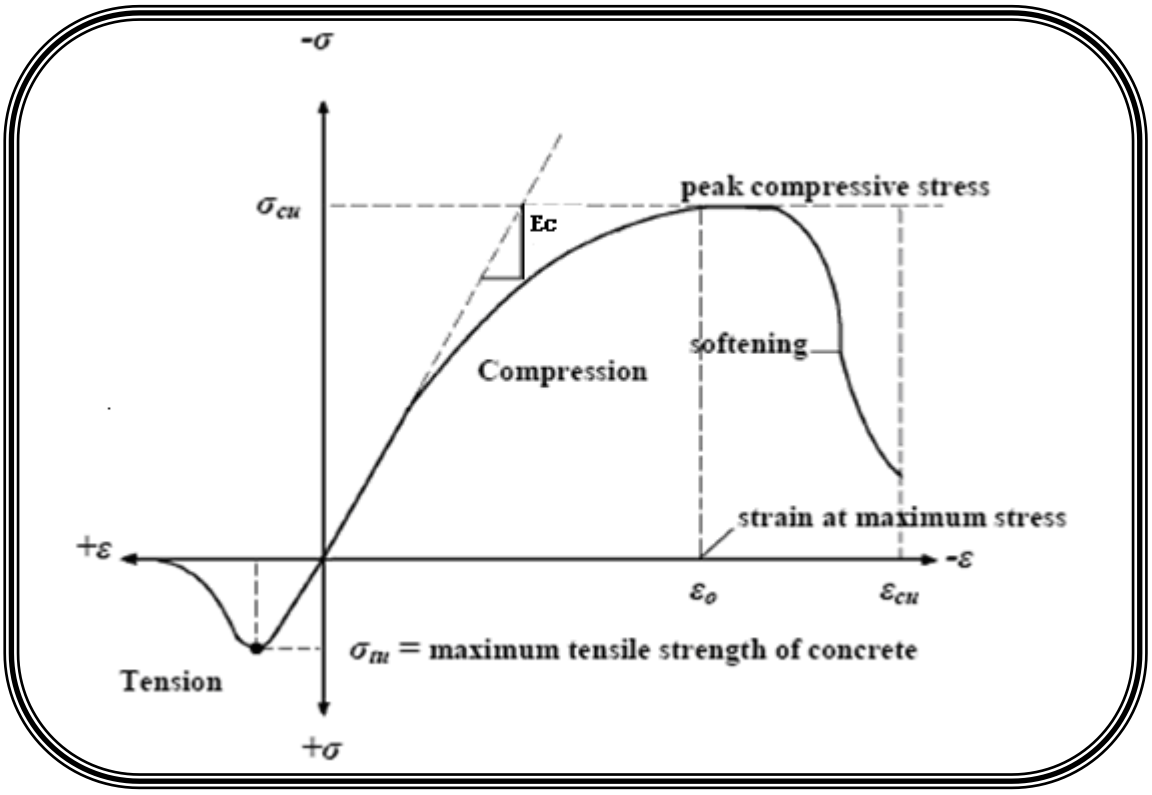

Fig.(٤-٥): Typical uniaxial compressive and tensile stress-strain curve for concrete (*Bangash* ١٩٨٩)

The ANSYS program requires the uniaxial stress-strain relationship for concrete in compression in Fig.(٤-٦). Numerical expressions, Equations (٤-٥)

and (٤-٦), were used along with Equation (٤-٧) (*Gere and Timoshenko,* ١٩٩٧) to construct the uniaxial compressive stress-strain curve for concrete in this study.

$$f = \frac{E_c \varepsilon}{1 + \left(\frac{\varepsilon}{\varepsilon_o}\right)^2} \qquad \ldots(٤\text{-}٥)$$

$$\varepsilon_o = \frac{2f'c}{E_c} \qquad \ldots(٤\text{-}٦)$$

$$E_c = \frac{f}{\varepsilon} \qquad \ldots(٤\text{-}٧)$$

Where:

f = Stress at any strain ϵ.

ϵ = Strain at stress f.

ϵ_o = Strain at the ultimate compressive strength f'c.

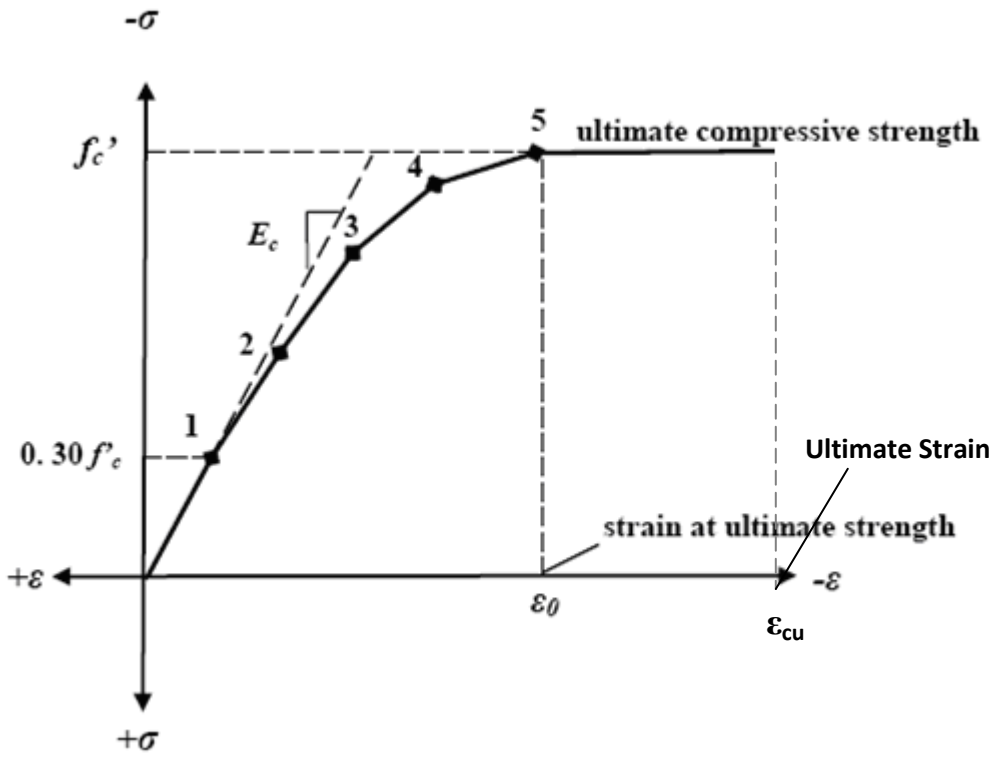

Fig.(٤-٦): Simplified compressive uniaxial stress-strain curve for concrete *(Kachlakev et al., ٢٠٠١).*

The simplified stress-strain curve for each beam model is constructed from six points connected by straight lines. The curve starts at zero stress and strain. Point No. ١, at ٠.٣٠*f'*c, is calculated for the stress-strain relationship of the concrete in the linear range (Equation (٤-٧)). Point Nos. ٢, ٣, and ٤ are obtained from Equation (٤-٥), in which ε_o is calculated from equation (٤-٦). Point No. ٥ is at ε_o and *f'*c. In this study, an assumption was made of perfectly plastic behavior after Point No. ٥ *(Kachlakev et al., ٢٠٠١).*

For uncracked concrete the stress-strain matrix for concrete can be defined by *(ANSYS, ١٩٩٨).* The matrix $[\mathbf{D}^c]$ is derived by specializing the orthotropic stress-strain relations to the case of an isotropic material.

$$[D^c] = \frac{E}{(1+\nu)(1-2\nu)} \begin{bmatrix} (1-\nu) & \nu & \nu & 0 & 0 & 0 \\ \nu & (1-\nu) & \nu & 0 & 0 & 0 \\ \nu & \nu & (1-\nu) & 0 & 0 & 0 \\ 0 & 0 & 0 & \frac{(1-2\nu)}{2} & 0 & 0 \\ 0 & 0 & 0 & 0 & \frac{(1-2\nu)}{2} & 0 \\ 0 & 0 & 0 & 0 & 0 & \frac{(1-2\nu)}{2} \end{bmatrix} \quad \text{...(٤-٨)}$$

The stress-strain relationship can be written in a matrix form as:

$$\{\sigma\} = [D_c]\{\epsilon\} \quad \text{...(٤-٩)}$$

Where: **E** = Young's modulus for concrete.

ν = Poisson's ratio for concrete.

$[D_c]$ = Constitutive matrix for concrete.

{Є} = The strain vector

٤-٤-٢ Failure Criteria for Concrete

When the state of stress reaches a certain critical value, concrete fails by fracturing. Fracture of concrete can be classified as cracking type of fracture and crushing type of fracture *(Chen, ١٩٨٢).*

To determine the fracture of concrete under a multiaxial state of stress, a failure criterion that specifies the limit value is needed *(Chen, ١٩٨٢).* The fives parameter failure criterion developed by *(Willam and Wornke, ١٩٧٥)* are used Fig.(٤-٧), and it can be expressed in the form *(ANSYS, ١٩٩٨).*

$$\frac{F}{f'c} - S \geq 0 \quad \text{...(٤-١٠)}$$

A total of input strength parameters are needed to define equation (٤-١٠), the failure surface as well as an ambient hydrostatic stress state.

Table (٤-١): Concrete Material

LABEL	DESCRIPTION
F	A function of the principal stress state (σ_1 , σ_2 , σ_3)
S	Failure surface expressed in terms of principal stresses and five input parameters f 'c, f_t, f_{cb}, f_1 and f_2
$\mathbf{f_t}$	Ultimate uniaxial tensile strength
f'c	Ultimate uniaxial compressive strength
$\mathbf{f_{cb}}$	Ultimate biaxial compressive strength
$\mathbf{f_1}$	Ultimate compressive strength for a state of biaxial compression superimposed on hydrostatic stress state (σ_h^a)
$\mathbf{f_2}$	Ultimate compressive strength for a state of uniaxial compression superimposed on hydrostatic stress state (σ_h^a)
σ_h^a	Ambient hydrostatic stress state

If this equation is not satisfied, there is no attendant cracking or crushing. Other wise the material will crack if any principle stress is tensile while crushing will occur if all principle stressed are compressive (ANSYS, ١٩٩٨).

However, the failure surface can be specified with a minimum of two constant, f_t, f'c. The other three constant defaults to *(William and Warnke, ١٩٧٥):*

$$f_{cb} = ١.٢\ f'_c \qquad \text{...(٤-١١)}$$

$$f_1 = ١.٤٥\ f'_c \qquad \text{...(٤-١٢)}$$

$$f_2 = ١.٧٢٥\ f'_c \qquad \text{...(٤-١٣)}$$

However, these default values are valid only for stress states where the condition is satisfied.

$$\left|\sigma_h\right| \subseteq \sqrt{3} f'c \qquad \text{...(٤-١٤)}$$

(σ_h = hydrostatic stress state = $\frac{1}{3}\left(\sigma_{xp} + \sigma_{yp} + \sigma_{zp}\right)$) ...(٤-١٥)

Thus condition (٤-١٤) applies to stress situations with a low hydrostatic stress component. Both the function F and the failure surface S are expressed in terms of principal stresses denoted as σ_1,σ_2 and σ_3 where:

$\sigma_1 = \max(\sigma_{xp}, \sigma_{yp}, \sigma_{zp})$ ...(٤-١٦)

$\sigma_2 = \min(\sigma_{xp}, \sigma_{yp}, \sigma_{zp})$ ...(٤-١٧)

and $\sigma_1 \geq \sigma_2 \geq \sigma_3$. The failure of concrete is categorized into four domains:

١. $0 \geq \sigma_1 \geq \sigma_2 \geq \sigma_3$ **(compression - compression – compression)**

٢. $\sigma_1 \geq 0 \geq \sigma_2 \geq \sigma_3$ **(tensile - compression – compression)**

٣. $\sigma_1 \geq \sigma_2 \geq 0 \geq \sigma_3$ **(tensile - tensile – compression)**

٤. $\sigma_1 \geq \sigma_2 \geq \sigma_3 \geq 0$ **(tensile- tensile – tensile)**

In each domain, independent functions describe F and the failure surface S. The four functions describing the general function F are denoted as F_1, F_2, F_3 and F_4 while the functions describing S are denoted as S_1, S_2, S_3 and S_4. The functions S_i (i=١,٤) have the properties that the surface they describe is continuous while the surface gradients are not continuous when any one of the principal stresses changes sign. The surface will be shown in Fig.(٤-٧) and Fig. (٤-٩) these functions are discussed in detail below for each domain.

٤-٤-٢-١: Compression – Compression – Compression Regime

In the $0 \geq \sigma_1 \geq \sigma_2 \geq \sigma_3$ domain the failure criterion of *(William and Wranke, ١٩٧٥)* is implemented. In this case, F takes the form:

$$F = F_1 = \frac{1}{\sqrt{15}}\left[(\sigma_1 - \sigma_2)^2 + (\sigma_2 - \sigma_3)^2 + (\sigma_3 - \sigma_1)^2\right]^{\frac{1}{2}} \quad \text{...(٤-١٨)}$$

and S is defined as

$$S = S_1 = \frac{2r_2(r_2^2 - r_1^2)\cos\eta + r_2(2r_1 - r_2)\left[4(r_2^2 - r_1^2)\cos^2\eta + 5r_1^2 - 4r_1r_2\right]^{\frac{1}{2}}}{4(r_2^2 - r_1^2)\cos^2\eta + (r_2 - 2r_1)^2} \quad \text{...(٤-١٩)}$$

Terms used to define S are:

$$\cos\eta = \frac{2\sigma_1 - \sigma_2 - \sigma_3}{\sqrt{2}\left[(\sigma_1 - \sigma_2)^2 + (\sigma_2 - \sigma_3)^2 + (\sigma_3 - \sigma_1)^2\right]^{\frac{1}{2}}} \quad \text{...(٤-٢٠)}$$

$$r_1 = a_0 + a_1\xi + a_2\xi^2 \quad \text{...(٤-٢١)}$$

$$r_2 = b_0 + b_1\xi + b_2\xi^2$$

$$\xi = \frac{\sigma_h}{f'c}$$

σ_h is defined by equation (٤-١٥) undetermined coefficients a., a١, a٢, b., b١and b٢ are discussed below.

This failure surface is shown as Fig.(٤-٧). The angle of similarity η describes the relative magnitudes of the principal stresses. Form equation (٤-٢٠), η=٠ ˚ refers to any stress state such that σ٣ = σ٢ > σ١ (e. g. uniaxial tension, biaxial tension) while ξ= ٦٠ ˚ for any stress state where σ٣ > σ٢ = σ١ (e. g. uniaxial tension, biaxial compression). All other multiaxial stress state have angles of similarity such that ٠ ˚ ≤ η ≤ ٦٠ ˚. When η = ٠ ˚, S١ (equation (٤-١٩) equals r١ while if η = ٦٠ ˚, S١ equals r٢. Therefore, the function r١ represents the failure surface of all stress stases with η = ٠ ˚. The functions r١,r٢ and the angle η are depicted on Fig.(٤-٧).

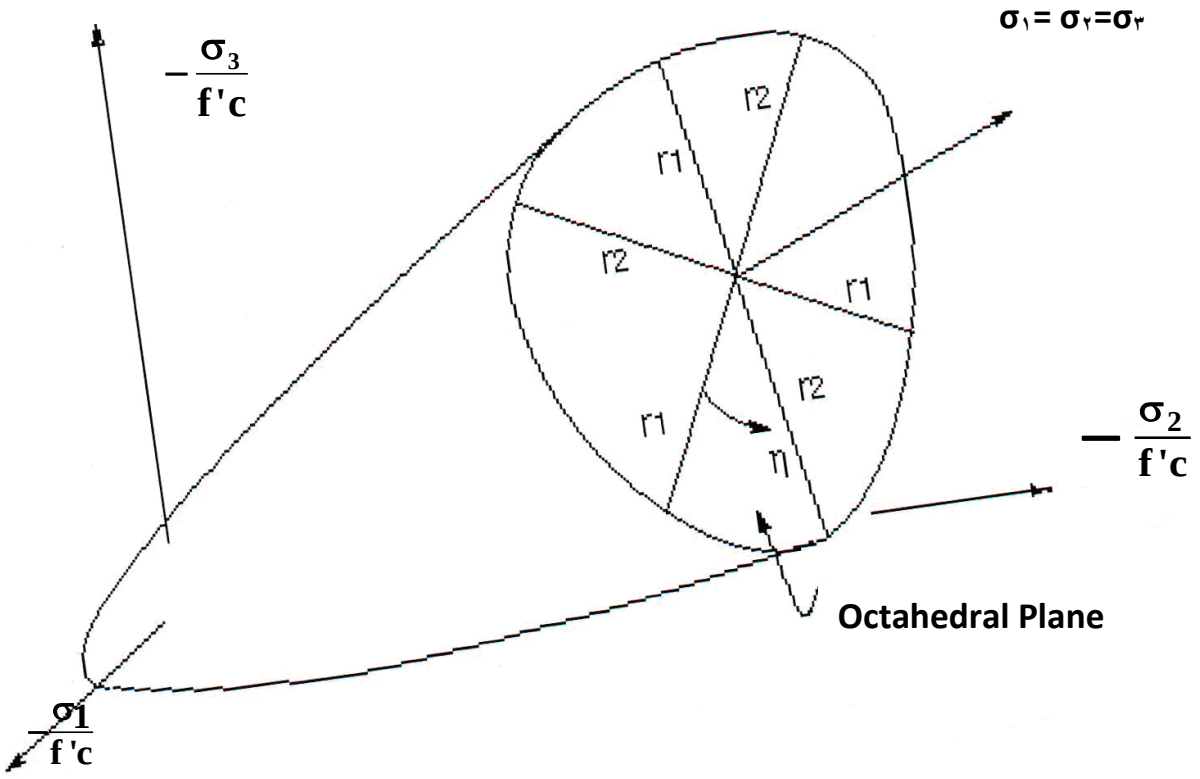

Fig.(٤-٧): ٣-D Failure Surface in Principal Stress Space (ANSYS, ١٩٩٨)

It may be seen that the cross-section of the failure plane has cyclic symmetry about each ١٢٠° sector of the octahedral plane due to the range ٠° ≤ η ≤ ٦٠° of the angle of similitude. The function r_1 is determined by adjusting a_0, a_1 and a_2 such that f_t, f_{cb} and f_1 all lie on the failure surface. The proper values for these coefficients are determined through solution of the simultaneous equations:

$$\begin{Bmatrix} \frac{F_1}{f'c}(\sigma_1 = f_t, \sigma_2 = \sigma_3 = 0) \\ \frac{F_1}{f'c}(\sigma_1 = 0, \sigma_2 = \sigma_3 = -f_{cb} \\ \frac{F_1}{f'c}(\sigma_1 = -\sigma_h^a, \sigma_2 = \sigma_3 = -\sigma_h^a - f_1 \end{Bmatrix} = \begin{bmatrix} 1 & \xi_t & \xi_t^2 \\ 1 & \xi_{cb} & \xi_{cb}^2 \\ 1 & \xi_1 & \xi_1^2 \end{bmatrix} \begin{Bmatrix} a_0 \\ a_1 \\ a_2 \end{Bmatrix} \quad \text{...(٤-٢٣)}$$

With

$$\xi_t = \frac{f_t}{3f'c}, \xi_{cb} = -\frac{2f_{cb}}{3f'c}, \xi_1 = -\frac{\sigma_h^a}{f'c} - \frac{2f_1}{3f'c} \qquad \text{...(٤-٢٤)}$$

The function r_2 is calculated by adjusting b_0, b_1 and b_2 to satisfy the conditions:

$$\begin{Bmatrix} \frac{F_1}{f'c}(\sigma_1 = \sigma_2 = 0, \sigma_3 = -f) \\ \frac{F_1}{f'c}(\sigma_1 = \sigma_2 = -\sigma_h^a, \sigma_3 = -\sigma_h^a - \frac{f_2}{f'c}) \\ 0 \end{Bmatrix} = \begin{bmatrix} 1 & -\frac{1}{3} & \frac{1}{9} \\ 1 & \xi_2 & \xi_2^2 \\ 1 & \xi_0 & \xi_0^2 \end{bmatrix} \begin{Bmatrix} b_0 \\ b_1 \\ b_2 \end{Bmatrix} \qquad \text{...(٤-٢٥)}$$

ξ_2 is defined by :

$$\xi_2 = -\frac{\sigma_h^a}{f'c} - \frac{f_2}{3f'c} \qquad \text{...(٤-٢٦)}$$

And ξ_0 is the positive root of the equation

$$r_2(\xi_0) = a_0 + a_1\xi_0 + a_2\xi_0^2 = 0 \qquad \text{...(٤-٢٧)}$$

Where: a_0, a_1 and a_2 are evaluated by equation (٤-٢٣).

Since the failure surface must remain convex, the ratio r_1 / r_2 is restricted to the range.

$$0.5 < r_1 / r_2 < 1.25 \qquad \text{...(٤-٢٨)}$$

Although the upper bound is not considered to be restrictive since $r_1 / r_2 < 1$ for most materials *(ANSYS, ١٩٩٨).* Also, the coefficients a_0, a_1, a_2, b_0, $b_1$and b_2 must satisfy the conditions *(William and Warnke, ١٩٧٥):*

$$a_0 > 0 , a_1 \leq 0 , a_2 \leq 0 \qquad \text{...(٤-٢٩)}$$

$$b_0 > 0 , b_1 \leq 0 , b_2 \leq 0 \qquad \text{...(٤-٣٠)}$$

Therefore, the failure surface is closed and predicts failure under high hydrostatic pressure ($\xi > \xi_2$). This closure of the failure surface has not been verified experimentally and it has been suggested that a von Misses type cylinder is a more valid failure surface for large compressive σ_h values *(ANSYS, ١٩٩٨).* Consequently, it is recommended that values of f_1 and f_2 are selected at a hydrostatic stress level (σ_h^a) in the vicinity of or above the expected maximum hydrostatic stress encountered in the structure.

Equation (٤-٢٧) expresses the condition that failure surface has an apex at $\xi = \xi_0$.. A profile of r_1 and r_2 as a function of ξ is shown in Fig.(٤-٨).

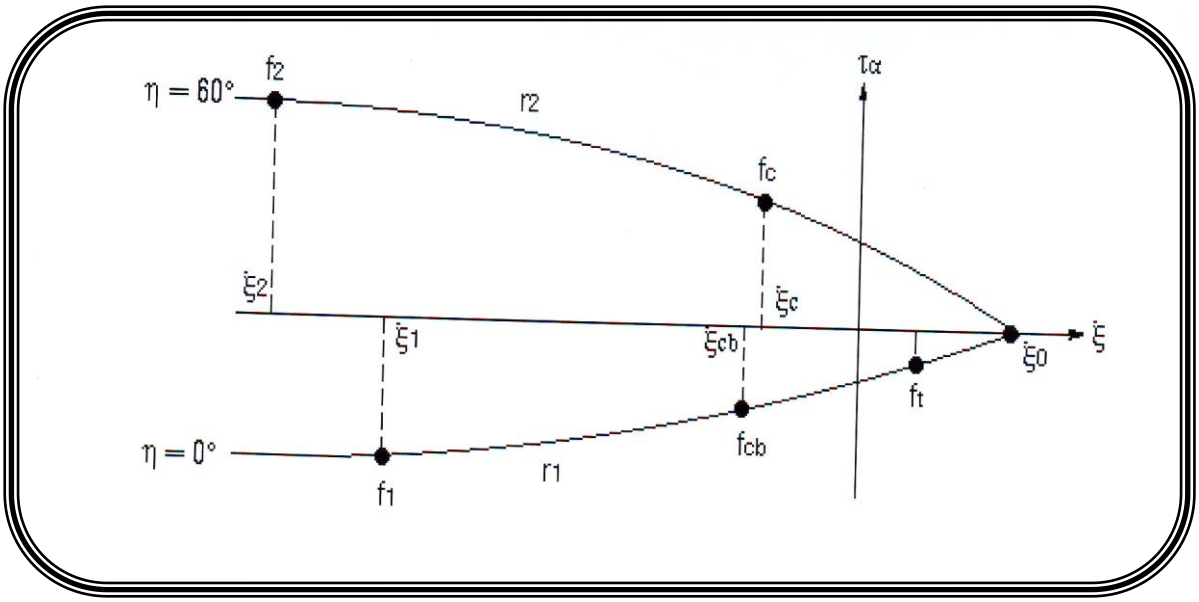

Fig.(٤-٨): A profile of the Failure Surface as a Function of ξ_α*(ANSYS ١٩٩٨).*

The lower curve represents all stress states such that η=٠ ° while the upper curve represents stress states such that η=٦٠ °. If the failure criterion is satisfied, the material is assumed to crush.

٤-٤-٢-٢: Tensile – Compression – Compression Regime

In the domain $\sigma_1 \geq 0 \geq \sigma_2 \geq \sigma_3$, F takes the form:

$$F = F_2 = \frac{1}{\sqrt{15}}\left[(\sigma_1 - \sigma_3)^2 + \sigma_2^2 - \sigma_3^2\right]^{0.5} \quad \text{...(٤-٣١)}$$

And S is defined as

$$S = S_2 = \left(1 - \frac{\sigma_1}{f_t}\right)\frac{2p_2\left(p_2^2 - p_1^2\right)\cos\eta + p_2(2p_1 - p_2)\left[4\left(p_2^2 - p_1^2\right)\cos^2\eta + 5p_1^2 - 4p_1p_2\right]^{\frac{1}{2}}}{4\left(p_2^2 - p_1^2\right)\cos^2\eta + (p_2 - 2p_1)^2} \quad \text{...(٤-٣٢)}$$

Where cos η is defined by equation (٤-٢٠) and

$$p_1 = a_0 + a_1\chi + a_2\chi^2 \quad \text{...(٤-٣٣)}$$

$$p_2 = b_0 + b_1\chi + b_2\chi^2 \quad \text{...(٤-٣٤)}$$

The coefficient a., a١, a٢, b. , b١,b٢ are defined by equations (٤-٢٣) and (٤-٢٥) while

$$\chi = \frac{1}{3}(\sigma_2 + \sigma_3) \quad \text{...(٤-٣٥)}$$

If the failure criterion is satisfied, cracking occurs in the plane perpendicular to principal stress σ١, Fig.(٤-٩).

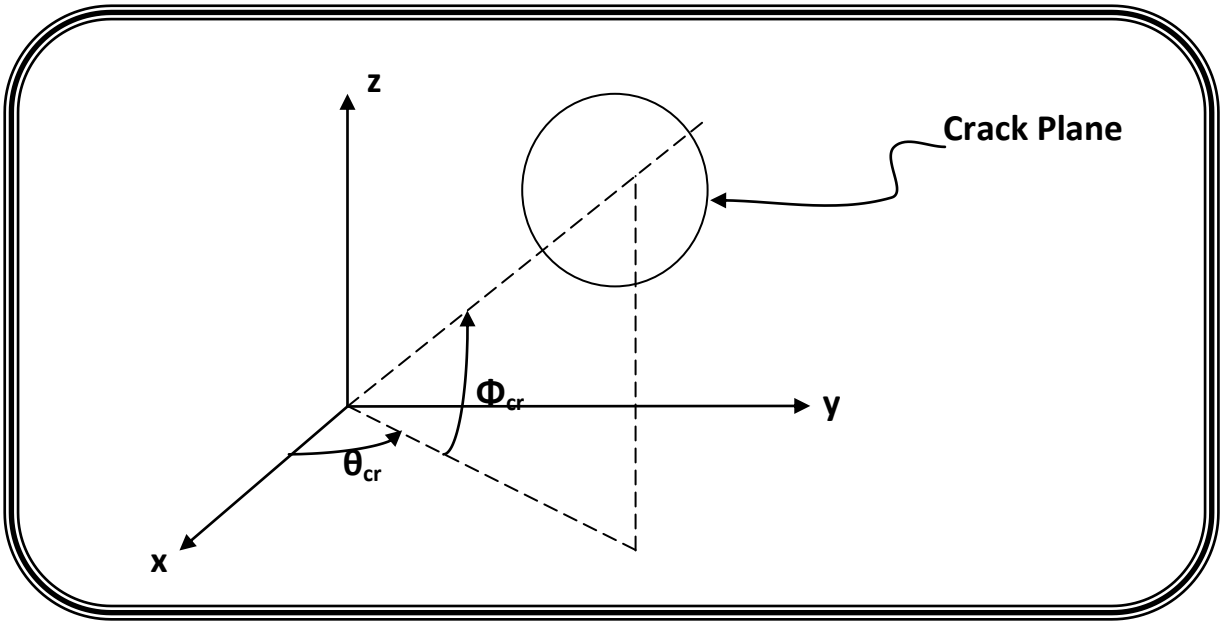

Fig.(٤-٩): Cracks Formation in One Direction (ANSYS, ١٩٩٨).

٤-٤-٢-٣: Tension – Tension – Compression Regime

In the domain $\sigma_1 \geq \sigma_2 \geq 0 \geq \sigma_3$, F takes the form:

$$F = F_3 = \sigma_i \quad ; \quad i = 1,2 \qquad \text{...(٤-٣٦)}$$

and S is defined as

$$S = S_3 = \frac{f_t}{f'c}\left(1 + \frac{\sigma_3}{S_2(\sigma_i, 0, \sigma_3)}\right) \quad ; \quad i = 1,2 \qquad \text{...(٤-٣٧)}$$

If the failure criterion for both i=١,٢ is satisfied, cracking occurs in the planes perpendicular to principal stress σ_1 and σ_2. If the failure criterion is satisfied only for i=١, cracking occurs in the plane perpendicular to principal stress σ_1.

٤-٤-٢-٤: Tension – Tension – Tension – Regime

In the domain $\sigma_1 \geq \sigma_2 \geq \sigma_3 \geq 0$,F takes the form:

$$F = F_4 = \sigma_i \quad ; \quad i = 1,2,3 \qquad \text{...(٤-٣٨)}$$

and S is defined as

$$S = S_4 = \frac{f_t}{f'c} \qquad \text{...(٤-٣٩)}$$

If the failure criterion is satisfied in direction ١,٢ and ٣, cracking occurs in

the planes perpendicular to principal stresses σ_1, σ_2 and σ_3.If the failure criterion is satisfied in directions ١ and ٢, cracking occurs in the plane perpendicular to principal stresses σ_1 and σ_2.If the failure criterion is satisfied in directions ١, cracking occurs in the plane perpendicular to principal stress σ_1.

A three-dimensional failure surface for concrete is shown in Fig.(٤-١٠). The most significant nonzero principal stresses are in the x and y directions, represented by *σxp* and *σyp,* respectively. Three failure surfaces are shown as projections on the *σxp*-*σyp* plane. The mode of failure is a function of the sign of *σzp* (principal stress in the z direction).For example, if *σxp* and *σyp* are both negative (compressive) and *σzp* is slightly positive (tensile), cracking would be predicted in a direction perpendicular to *σzp*. However, if *σzp* is zero or slightly negative, the material is assumed to crush (*ANSYS* ١٩٩٨).

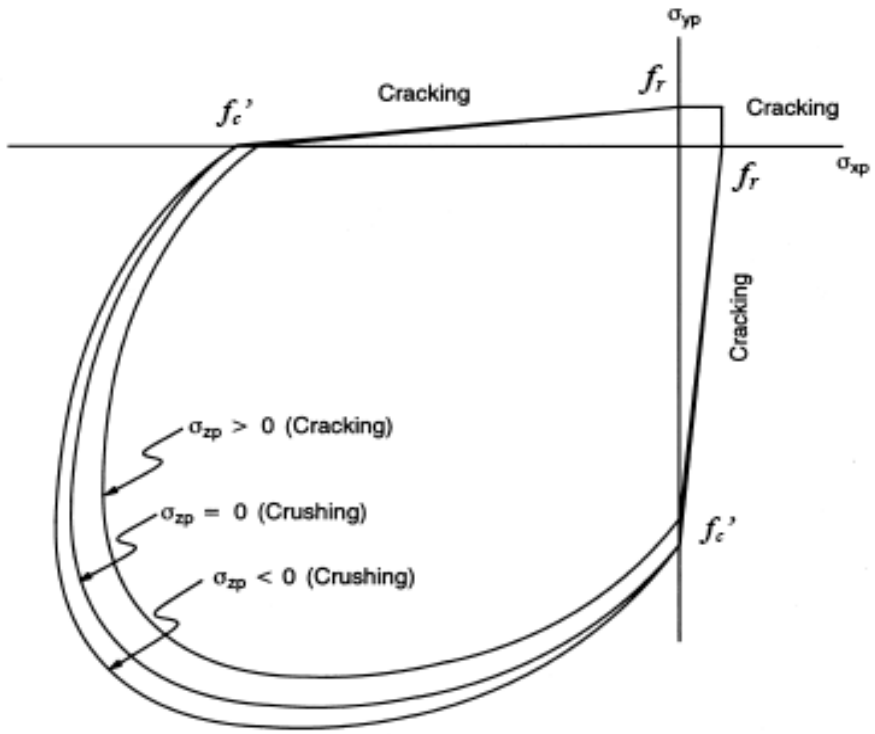

Fig.(٤-١٠): Failure Surface in Principal Stress Space σ_{zp} Close to Zero (ANSYS, ١٩٩٨)

In a concrete element, cracking occurs when the principal tensile stress in any direction lies outside the failure surface. After cracking, the elastic modulus of the concrete element is set to zero in the direction parallel to the principal tensile stress direction. Crushing occurs when all principal stresses are compressive and lie outside the failure surface; subsequently, the elastic modulus is set to zero in all directions (*ANSYS,* ١٩٩٨), and the element effectively disappears. Crushing of the concrete started to develop in elements located directly under the loads. Subsequently, adjacent concrete elements crushed within several load steps as well, significantly reducing the local stiffness. Finally, the model showed a large displacement, and the solution diverged. A pure “compression” failure of concrete is unlikely. In a compression test, the specimen is subjected to a uniaxial compressive load. Secondary tensile strains induced by Poisson’s effect occur perpendicular to

the load. Because concrete is relatively weak in tension, these actually cause cracking and the eventual failure (*Mindess and Young, ١٩٨١; Shah, et al. ١٩٩٥*).

٤-٤-٣: Cracking Modeling

The internal stresses and deflections of reinforced concrete structures are affected by cracking. This phenomenon can be modeled in finite element schemes as smeared cracking approach.

The smeared crack model introduced by *(Rashid, ١٩٦٨)* represents cracks as a change in the material property of the element over which the cracks are assumed to be smeared and offers an automatic generation of cracks without the redefinition of the finite element topology. It assumes that the concrete becomes orthotropic after the cracking has occurred with zero modulus of elasticity in the direction normal to the crack. A crack is represented by an infinite element, Fig.(٤-١١). Poisson's effect is neglected due to lack of interaction between the two orthogonal directions after cracking.

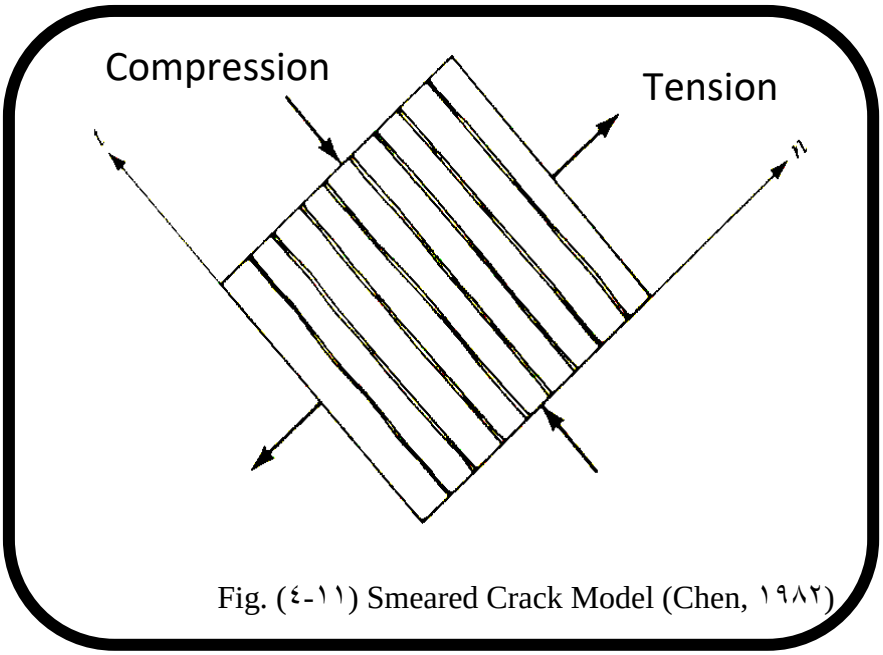

Fig. (٤-١١) Smeared Crack Model (Chen, ١٩٨٢)

The smeared crack approach can be divided to fixed and rotating crack categories. In the fixed crack category, concrete in tension is assumed to crack along the direction normal to the principal tensile stress direction, when the tensile stress at that point satisfies the failure criterion. This direction is assumed fixed during the entire computational process *(Channakeshava and Sudara, ١٩٨٨).* In the rotating crack model, the crack direction is always aligned normal to the direction of maximum principal strain, and the principal stress and strain directions are assumed to coincide.

Since the overall load-deflection behavior is desired, the cracking of concrete in the present study is considered through an adjustment of material properties which effectively treats the cracking as a smeared band of cracks with fixed crack orientation *(ANSYS, ١٩٩٨).* This model is terms of shear transfer model and closing and reopening of cracks.

٤-٤-٣-١: Shear Transfer Model

Concrete is assumed to behave linearly in tension up to the onset of cracking. When concrete cracks, its shear stiffness is reduced. However, cracked concrete can partially transmit shear across the crack due to aggregate interlock and dowel action of the reinforcement. The shear transfer mechanism depends on the reinforcement ratio, bar size, bar arrangement, the amount of concrete cover, the type of concrete and aggregate size *(Fenwick and Paulay, ١٩٦٨).* To estimate such an effect, a shear coefficient β is introduced which represents a shear strength reduction factor for concrete across the crack face *(ANSYS, ١٩٩٨).* When the crack is formed, only a constant

value of a shear transfer coefficient β_o for the opened crack is introduced, and if the crack is closed, the shear transfer coefficient β_c is used. The values of β_o and β_c are always in the range $1 > \beta_o > \beta_c > 0$. These values depend on the texture of the cracked surface.

The shear transfer coefficient, β, represents conditions of the crack face. The value of β ranges from ٠.٠ to ١.٠, with ٠.٠ representing a smooth crack (complete loss of shear transfer) and ١.٠ representing a rough crack (no loss of shear transfer) (*ANSYS* ١٩٩٨).The value of β_o used in many studies of reinforced concrete structures, however, varied between ٠.٠٥ and ٠.٢٥ (*Kachlakev* ٢٠٠١*; Santhakumar and Chandrasekaran* ٢٠٠٤). A number of preliminary analyses were attempted in this study with various values for the shear transfer coefficient within this range, but convergence problems were encountered at low loads with β_o less than ٠.٢. Therefore, the shear transfer coefficient with open crack and with close crack used in this study was equal to ٠.٢ and ٠.٨٥ respectively.

٤-٤-٣-٢: Closing and Reopening of Cracks

The unloading and reopening of a cracked integration point may occur as a result of stress redistribution at neighboring points. Cracks are assumed to open perpendicular to the highest principal tensile stress direction, when the failure surface has been reached. The stress-strain relation for a material that has cracked in one direction only becomes *(ANSYS,* ١٩٩٨*):*

$$\left[D_c^{ck}\right]=\frac{E}{(1+\nu)}\begin{bmatrix}0 & 0 & 0 & 0 & 0 & 0\\ 0 & \frac{1}{(1-\nu)} & \frac{\nu}{(1-\nu)} & 0 & 0 & 0\\ 0 & \frac{\nu}{(1-\nu)} & \frac{1}{(1-\nu)} & 0 & 0 & 0\\ 0 & 0 & 0 & \frac{\beta_o}{2} & 0 & 0\\ 0 & 0 & 0 & 0 & \frac{1}{2} & 0\\ 0 & 0 & 0 & 0 & 0 & \frac{\beta_o}{2}\end{bmatrix} \qquad \ldots(٤-٤٠)$$

Where the superscript **ck** signifies that the stress strain relation refer to coordinate system parallel to principal stress directions with the x^{ck} axis perpendicular to the cracking face.

If the crack closes, then all compressive stress normal to the crack plane are transmitted a cross the crack. Then $[D_c^{ck}]$ can be expressed as:

$$\left[D_c^{ck}\right]=\frac{E}{(1+\nu)(1-2\nu)}\begin{bmatrix}(1-\nu) & \nu & \nu & 0 & 0 & 0\\ \nu & (1-\nu) & \nu & 0 & 0 & 0\\ \nu & \nu & (1-\nu) & 0 & 0 & 0\\ 0 & 0 & 0 & \beta_c\frac{(1-2\nu)}{2} & 0 & 0\\ 0 & 0 & 0 & 0 & \frac{(1-2\nu)}{2} & 0\\ 0 & 0 & 0 & 0 & 0 & \beta_c\frac{(1-2\nu)}{2}\end{bmatrix} \ldots(٤-٤١)$$

The stress-strain relations for concrete has cracked in two directions are:

$$\left[D_c^{ck}\right] = E\begin{bmatrix} 0 & 0 & 0 & 0 & 0 & 0 \\ 0 & 0 & 0 & 0 & 0 & 0 \\ 0 & 0 & 1 & 0 & 0 & 0 \\ 0 & 0 & 0 & \frac{\beta_o}{2(1+\nu)} & 0 & 0 \\ 0 & 0 & 0 & 0 & \frac{\beta_o}{2(1+\nu)} & 0 \\ 0 & 0 & 0 & 0 & 0 & \frac{\beta_o}{2(1+\nu)} \end{bmatrix} \qquad \ldots(٤-٤٢)$$

If both directions reclose:

$$\left[D_c^{ck}\right] = \frac{E}{(1+\nu)(1-2\nu)}\begin{bmatrix} (1-\nu) & \nu & \nu & 0 & 0 & 0 \\ \nu & (1-\nu) & \nu & 0 & 0 & 0 \\ \nu & \nu & (1-\nu) & 0 & 0 & 0 \\ 0 & 0 & 0 & \beta_c\frac{(1-2\nu)}{2} & 0 & 0 \\ 0 & 0 & 0 & 0 & \beta_c\frac{(1-2\nu)}{2} & 0 \\ 0 & 0 & 0 & 0 & 0 & \beta_c\frac{(1-2\nu)}{2} \end{bmatrix} \qquad \ldots(٤-٤٣)$$

The stress-strain relation for concrete that has cracked in all three directions are:

$$\left[D_c^{ck}\right] = E\begin{bmatrix} 0 & 0 & 0 & 0 & 0 & 0 \\ 0 & 0 & 0 & 0 & 0 & 0 \\ 0 & 0 & 0 & 0 & 0 & 0 \\ 0 & 0 & 0 & \frac{\beta_o}{2(1+\nu)} & 0 & 0 \\ 0 & 0 & 0 & 0 & \frac{\beta_o}{2(1+\nu)} & 0 \\ 0 & 0 & 0 & 0 & 0 & \frac{\beta_o}{2(1+\nu)} \end{bmatrix} \qquad \ldots(٤-٤٤)$$

If all three cracks reclose, equation (٤-٤٣) is followed. There are ١٦ possible combinations of crack arrangement and appropriate changes in stress-strain relationships incorporated in the analysis *(ANSYS, ١٩٩٨).*

The transformation of $[D_c^{ck}]$ to element coordinates has the form:

$$[D_c] = [T^{ck}]^T [D_c^{ck}][T^{ck}] \quad \text{...(٤-٤٥)}$$

Where:

$[T^{ck}]$ has a form identical to equation (A-٥)and three columns of [A] in equation (A-٦) are now the principal direction vectors *(ANSYS, ١٩٩٨).*

The open or closed status of cracked integration point cracking is based on a strain value $[\varepsilon_c^{ck}]$ called the crack strain. For the case of possible crack in the X direction, this is evaluated as:

$$\varepsilon_c^{ck} = \begin{cases} \varepsilon_x^{ck} + \dfrac{\nu}{1-\nu}(\varepsilon_y^{ck} + \varepsilon_z^{ck}) & \text{If no cracking has occurred} \\ \varepsilon_x^{ck} + \nu\varepsilon_z^{ck} & \text{If y direction has cracked} \\ \varepsilon_x^{ck} & \text{If y and z direction have cracked} \end{cases} \quad \text{...(٤-٤٦)}$$

Where:

$\varepsilon_x^{ck}, \varepsilon_y^{ck}, \text{and}, \varepsilon_z^{ck}$ =three normal component strains in crack orientation.

The vector $\{\epsilon^{ck}\}$ is computed by:

$$\{\varepsilon^{ck}\} = [T^{ck}]\{\varepsilon'\} \quad \text{...(٤-٤٧)}$$

Where: {ϵ'} = Modified total strain (in element coordinates)

{ϵ'}, in turn, is defined as:

$$\{\varepsilon'_n\} = \{\varepsilon_{n-1}^{el}\} + \{\Delta\varepsilon_n\} - \{\Delta\varepsilon_n^{th}\} - \{\Delta\varepsilon_n^{pl}\} \quad \text{...(٤-٤٨)}$$

Where:

n = substep number.

$\{\varepsilon_{n-1}^{el}\}$ = Elastic strain from previous substep

$\{\Delta\varepsilon_n\}$ = Total stain increment (based on $\{\Delta_{un}\}$, the displacement increment over the substep)

$\{\Delta\varepsilon_n^{th}\}$ = Thermal strain increment

$\{\Delta\varepsilon_n^{pl}\}$ = Plastic strain increment

If ε_c^{ck} is less than zero, the associated crack is assumed to be close. If ε_c^{ck} is greater than zero, the associated crack is assumed to be open. When cracking first occurs at an integration point, the crack is assumed to be open for the next iteration *(ANSYS, ١٩٩٨).*

٤-٤-٤: Crushing Modeling

If the material at an integration point fails in uniaxial, biaxial, or triaxial compression, the material is assumed to crush at that point. In brick elements, crushing is defined as the complete deterioration of the structural integrity of material (e.g. material spalling).Under this conditions where crushing has occurred, material strength is assumed to have degraded to an extent such that the contribution to the stiffness of an element at the integration point in question can be ignored *(ANSYS, ١٩٩٨).*

٤-٥: Steel Reinforcement Modeling

The steel reinforcement for the finite element models was assumed to be an elastic-perfectly plastic material and identical in tension and compression.

Poisson's ratio of ٠.٣ was used for the steel reinforcement in this study (*Gere and Timoshenko, ١٩٩٧*). Fig.(٤-١٢) shows the stress-strain relationship used in this study.

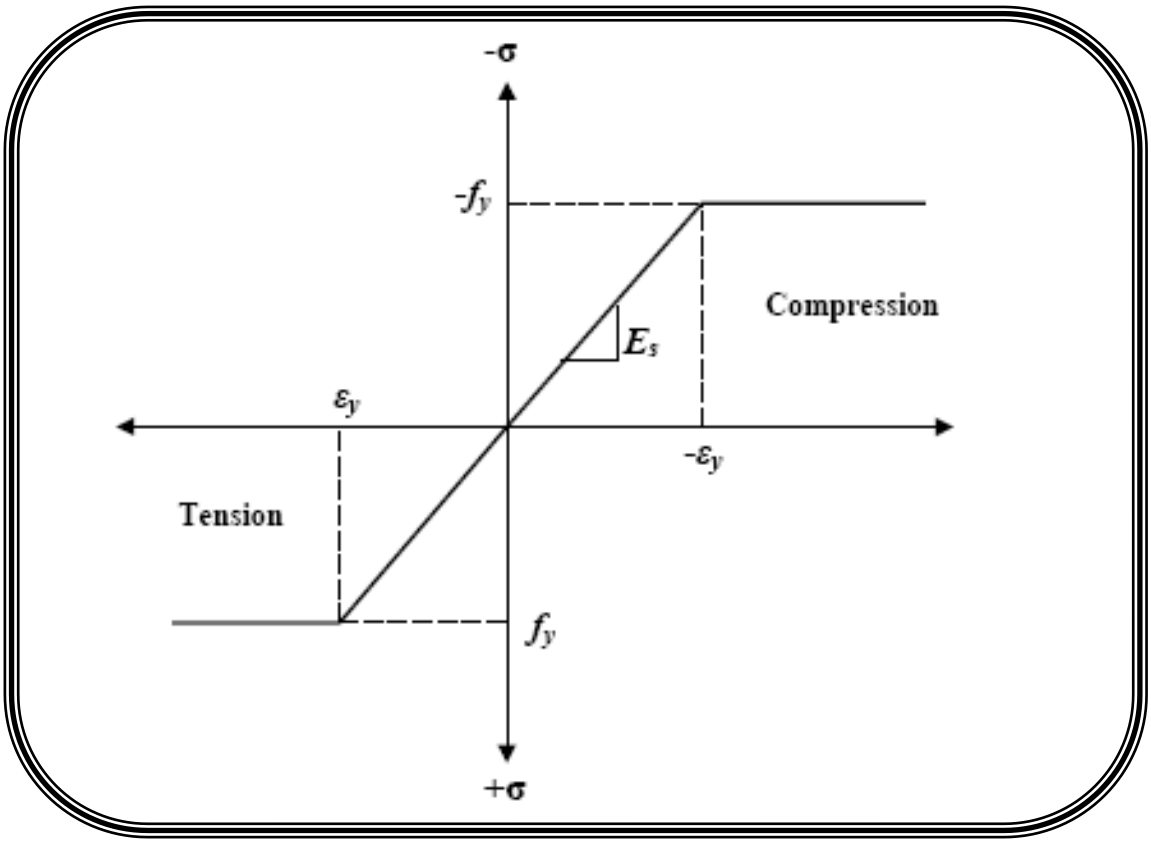

Fig.(٤-١٢): Stress-Strain Curve for Steel Reinforcement

٤-٦: FRP Composites Modeling

FRP composites are materials that consist of two constituents. The constituents are combined at a macroscopic level and are not soluble in each other. One constituent is the reinforcement, which is embedded in the second constituent, a continuous polymer called the matrix (*Kaw, ١٩٩٧*). The reinforcing material is in the form of fibers, i.e., carbon and glass, which are typically stiffer and stronger than the matrix. The FRP composites are anisotropic materials; that is, their properties are not the same in all directions. Fig.(٤-١٣) shows a schematic of FRP composites.

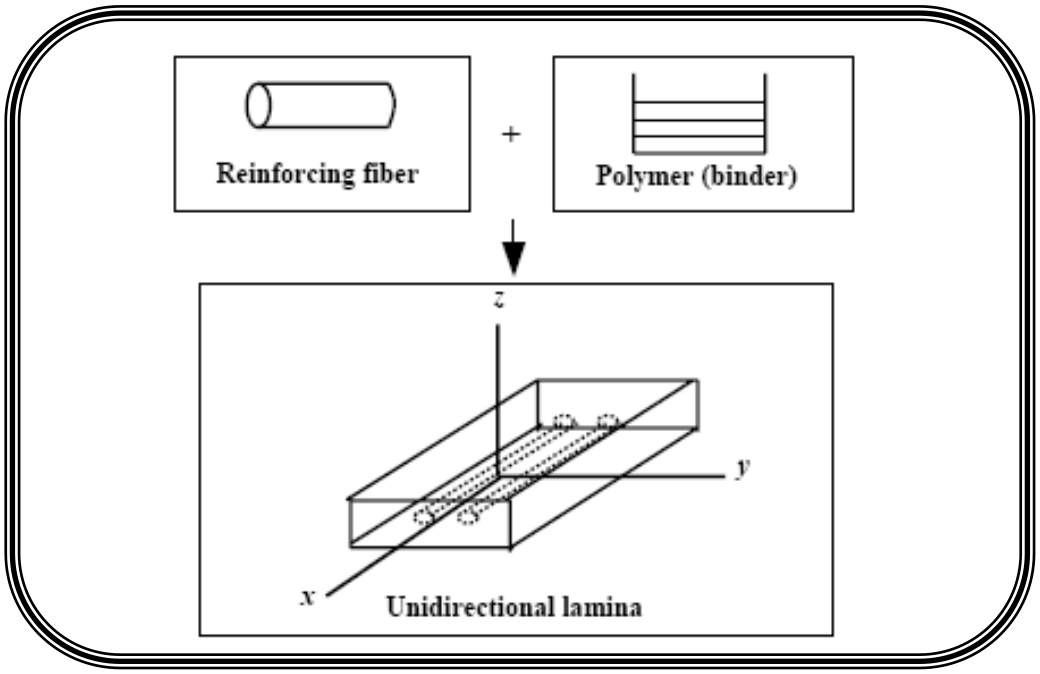

Fig.(٤-١٣): Schematic of FRP Composites (*Kaw, ١٩٩٧*)

Carbon fiber reinforced polymer was used for flexural reinforcement because of its high tensile strength. Linear elastic properties of the FRP composites were assumed throughout this study. Fig.(٤-١٤) shows the stress-strain curves used in this study for the FRP composites in the direction of the fiber. The properties of CFRP are assumed isotropic materials, such as elastic modulus and Poisson's ratio, are identical in all directions

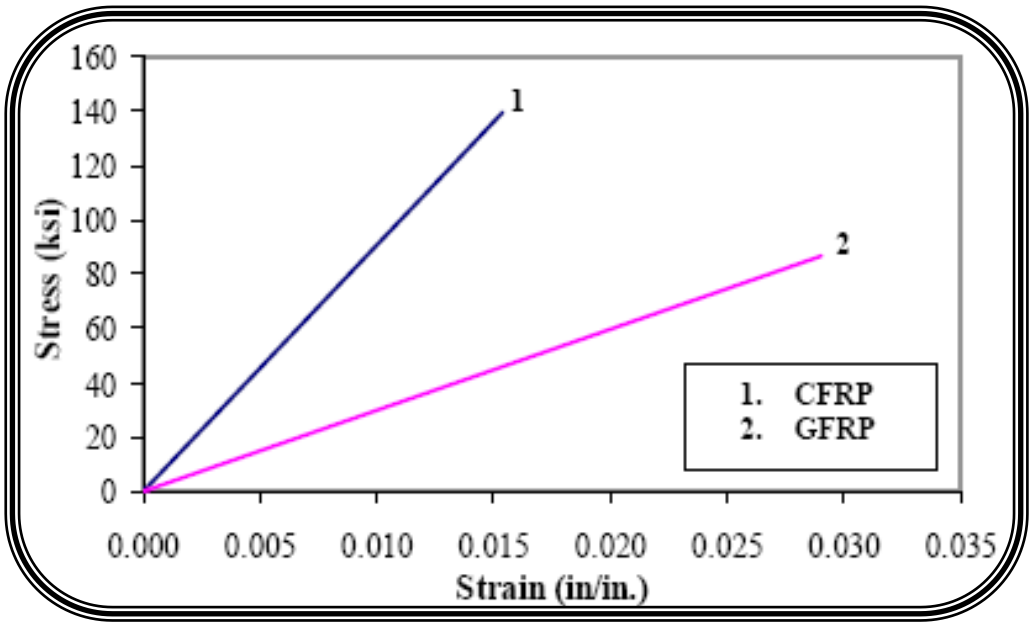

Fig.(٤-١٤): Stress-Strain Curves for the FRP Composites in the Direction of the Fibers *(Kachlakev et al., ٢٠٠١).*